Import of proteins along the presequence pathway

Dissertation

in partial fulfillment of the requirements
for the degree "*Doctor rerum naturalium*"
in the Molecular Biology Program
at the Georg-August-University Göttingen,
Faculty of Biology

Submitted by

Alexander Schendzielorz

born in
Papenburg, Germany

Göttingen, September 2017

Members of the Thesis Committee

Prof. Dr. Peter Rehling (Supervisor and first referee)	Institute of Cellular Biochemistry Univeristy Medical Center Göttingen, Germany
Prof. Dr. Marina Rodnina (Second referee)	Department of Physical Biochemistry Max Planck Institute for Biophysical Chemistry Göttingen, Germany
Prof. Dr. Dirk Görlich	Department of Cellular Logistics Max Planck Institute for Biophysical Chemistry Göttingen, Germany

Additional Members of the Examination Board

Dr. Alexander Stein	Membrane Protein Biochemistry Max Planck Institute for Biophysical Chemistry Göttingen, Germany
PD Dr. Wilfried Kramer	Institute for Microbiology and Genetics Department Molecular Genetics Georg-August-University Göttingen, Germany
Prof. Dr. Stefan Jakobs	Structure and Dynamics of Mitochondria Max Planck Institute for Biophysical Chemistry Göttingen, Germany

Date of oral examination: 15.11.2017

Affidavit

I hereby declare that I prepared the PhD thesis “Import of proteins along the presequence pathway” on my own and with no other sources and aids than quoted.

Göttingen, September 30th, 2017

_____

Alexander Schendzielorz

Acknowledgments

First of all, I would like to thank Prof. Peter Rehling for giving me the opportunity to work in the lab on different exiting projects. I really enjoyed the last four years and I am grateful for all the inspiring discussions and the support I received.

Moreover I would like to thank Prof. Marina Rodnina and Prof. Dirk Görlich for all the fruitful discussions during my Thesis Committee Meetings and for readily sharing lab equipment and knowledge.

A special thanks goes to my supervisor Dr. Christian Schulz who has been an inspiring mentor and never got tired to help me whenever I struggled with my projects.
In addition I would like to thank all current and past members of the Institute for Cellular Biochemistry for creating a very nice and supportive work atmosphere. Special thanks goes to Dr. David Pacheu-Grau, Dr. Natallia Naumenko and Ridhima Gomkale not only for valuable discussions throughout my PhD time but also for being good friends.

Furthermore, I am grateful for all the small collaborations that I had. Thanks to Frank Löhr for NMR analysis, Marina Rodnina for FRET experiments, Achim Dickmanns for crystallization experiments and Klaus Neifer for help with recombinant protein purification.

I would like to thank the IMPRS Molecular Biology and GGNB for their support and advice during my PhD time.

Last and most important I would like to thank my family and Klara for their constant and unlimited support.

Contents

List of Publications

Schulz, C., Schendzielorz, A. & Rehling, P. Unlocking the presequence import pathway. *Trends Cell Biol* **25,** 265–275 (2015).*

Melin, J. *et al.* A presequence-binding groove in Tom70 supports import of Mdl1 into mitochondria. *Biochim Biophys Acta* **1853,** 1850–1859 (2015).*

Richter-Dennerlein, R. *et al.* Mitochondrial Protein Synthesis Adapts to Influx of Nuclear-Encoded Protein. *Cell* **167,** 471–483.e10 (2016).*

Schendzielorz, A. B. *et al.* Two distinct membrane potential-dependent steps drive mitochondrial matrix protein translocation. *The Journal of Cell Biology* **216,** 83–92 (2017).

Denkert N[#], Schendzielorz AB[#], Barbot M, Versemann L, Richter F, Rehling P, Meinecke M (2017) Cation selectivity of the presequence translocase Tim23 is crucial for efficient protein import. *Elife* **6**, e28324 (2017).

# these authors contributed equally to the work

---

*results of this publication are not discussed here

List of Figures

Abbreviations

5-FOA	5-Fluoroorotic acid
AAC	ATP/ADP carrier
ALDH	Aldehyde dehydrogenase
AVO	Antimycin A, valinomycin, and oligomycin
BSA	Bovine Serum albumin
Cdk1	Cell division cycle 1
CK2	Cytosolic kinase 2
CTD	C-terminal domain
DHFR	dihydrofolate reductase
DMSO	Dimethyl sulfoxide
DTT	Dithiothreitol
Dy	Membrane potential
ER	Endoplasmic reticulum
ERMES	ER-mitochondria encounter structure
EDTA	Ethylenediaminetetraacetic acid
IBM	Inner boundary membrane
IM	Inner membrane
IMP	Inner membrane peptidase
IMS	Intermembrane space
MIA	Mitochondrial intermembrane space assembly machinery
MICOS	mitochondrial contact site and cristae organizing system
MIM	Mitochondrial Import
MOPS	3-(N-morpholino)propanesulfonic acid
MPP	Matrix processing peptidase
mtHsp70	Mitochondrial matrix Hsp70, Ssc1
NBD	Nucleotide binding domain
Ni-NTA	Nickel-nitriloacetic acid
NTD	N-terminal domain
OM	Outer membrane
OXA	Cytochrome oxidase activity
OXPHOS	Oxidative phosphorylation
PAM	Presequence translocase-associated motor
PBD	Presequence binding domain
PEX	Peroxin
PK	Proteinase K
PMSF	Phenylmethylsulfonyl fluoride
ROS	Reactive oxygen species
SAM	Sorting and assembly machinery
SBD	Substrate binding domain
SDS	Sodium dodecyl sulfate
SEM	Sucrose EDTA MOPS
SRP	Signal recognition particle
SPR	Surface plasmon resonance spectroscopy
TIC	translocon of the inner envelope membrane
TIM	Translocase of the inner mitochondrial membrane
TM	Transmembrane
TMS	Transmembrane segment
TOB	topogenesis of outer-membrane β-barrel

TOC	translocon of the outer envelope membrane
TOM	Translocase of the outer mitochondrial membrane
UPRam	unfolded protein response activated by mistargeting of proteins
YPD	Yeast Extract, peptone, glucose
YPG	Yeast Extract, peptone, glycerol

Joint authors contribution to the 2nd manuscript

(Cation selectivity of the presequence translocase Tim23 is crucial for efficient protein import)

Name: Niels Denkert

Individual contribution:

Design of project and experiments. Initial selection of mutations in Tim23 that were addressed in the project. In general all experiments related to electrophysiology. Generation and purification of recombinant Tim23 protein, electrophysiological basic characterization of channel properties of Tim23 mutants (Fig 1 D, E). Characterization of Tim23 N150A gating (Fig 3 A-C), reverse potential (Fig 3 D) and open probabilities of Tim23 channel in presence of Tim50 IMS domain (Fig 3 E-F). Effect of signal peptides on wild type and mutant Tim23 on gating frequency (Fig 5). Electrophysiological screening of Tim23 mutants (Fig 1 S1 B-D). Niels prepared all figures and was involved in writing the paper.

Name: Alexander Schendzielorz

Individual contribution:

All yeast work in the paper. Generation of yeast strains with mutant *tim23 (*Fig 1 B), screening of strains that fulfill the requirements for the study (growth test, steady state analysis, TIM23 complex isolation, membrane potential assessment, Fig 1 C, Fig 2 A-E, Fig 2 S2 A-C). Import analysis with different precursors into isolated mitochondria (Fig 4, Fig 4 S1) to confirm physiological relevance of *in vitro* experiments done by Niels Denkert. Proofreading the paper.

Abstract

The aim of this study was to investigate the mechanism of protein transport by the presequence translocase (TIM23) in the inner mitochondrial membrane. Presequence-containing proteins are imported through the translocase of the outer membrane (TOM) complex and handed over to the receptor Tim50 in the inner membrane. The membrane potential ($\Delta\psi$) acts on positive charges within the presequence, which drives initial translocation through the Tim23 channel.

I found that matrix targeted proteins display surprisingly different dependencies on $\Delta\psi$. Interestingly, the precursor´s hypersensitivity to a reduction in $\Delta\psi$ was not linked to the presequence but to the mature part of the protein. The small membrane protein Pam17 is selectively recruited to the translocase by the presequence receptor Tim50 to promote transport of hypersensitive proteins. Pam17 dissociates from the import channel once the Hsp70 based import motor takes over driving the precursor in an ATP-dependent manner. I have therefore identified a second $\Delta\psi$-dependent step, which acts on the mature part of the import substrate and takes place after $\Delta\psi$-driven translocation of the presequence but prior to ATP-mediated import motor action.

In the second part of the thesis, the molecular function of the channel forming protein Tim23 was investigated. Conserved residues in the second transmembrane segment that face the water filled pore were analyzed. Different mutations of these residues led to reduced cation selectivity and response to presequences of the Tim23 protein and renders the channel insensitive to substrates. One of these mutations, a N150A substitution, caused a growth and import defect in yeast. Since stability and assembly of the mutant Tim23 protein were not compromised, it was concluded that highly conserved residues in the channel are crucial for substrate affinity *in vitro* and for protein import *in vivo*.

1. Introduction

1.1 Compartmentalization of the eukaryotic cell

A hallmark feature of eukaryotic cells, which distinguishes them from prokaryotes, is the presence of membrane-enclosed organelles (Palade, 1964). As the first example, the nucleus was described in 1719 and later mitochondria were identified in the 1840s. While the nucleus plays a major role in gene expression by storing genetic material and separating it from the translation machinery, mitochondria are well known for their role in energy production. Although it is not known when the first organisms acquired organelles, it is generally accepted that they are of endosymbiotic origin (de Duve, 2007).

By creating cellular compartments, cells are able to separate opposing biochemical reactions, for instance glycolysis and gluconeogenesis, from each other. Moreover, the fragile genetic material stored in the nucleus is protected from most chemical damage. Additionally, transcription and translation are separated from each other by the nucleus in eukaryotes. Reactive oxygen producing reactions are located in mitochondria and therefore separated from the nuclear genome by mitochondrial and nuclear membranes.

Furthermore, biological membranes can be used to establish ion gradients to store energy, which can be used for the generation of adenosine triphosphate (ATP) in mitochondria, action potentials in nerve cells, or cell motility in bacterial cells. Also, mitochondria and the endoplasmic reticulum (ER) can store Ca^{2+} ions and release them in response to external signals. Organelles massively increase the total membrane surface in a cell favoring the above-mentioned processes.

The appearance of chloroplast, which led to the presence of molecular oxygen in the atmosphere, has changed life on earth tremendously. Oxygen can in turn be used by mitochondria as a terminal electron acceptor to produce ATP and H_2O. Even though mitochondria are best known for their role in energy production, they play crucial roles in many other cellular processes. Besides their function in Ca^{2+} signaling, they are essential for apoptosis. During this process, mitochondria release soluble cytochrome *c* from the intermembrane space into the cytosol, which triggers downstream events that finally lead to the formation of the apoptosome, a key

checkpoint during programmed cell death (Wang and Youle, 2009). Mitochondria are also involved in key metabolic processes such as the urea cycle, the TCA cycle, β-oxidation and amino acid synthesis. However, mitochondria are essential, even in non-respiring organisms, because of their role in iron sulfur biogenesis (Lill, 2009).

The ER forms a membrane network within most eukaryotic cells and is involved in the secretion of proteins and the metabolism of lipids and carbohydrates. Its membrane is continuous with the outer membrane of the nucleus and can be divided into smooth and rough ER. While the rough ER is covered with ribosomes, the smooth ER is the site of lipid metabolism and detoxification.

Even though organelles have added significantly to the complexity of life, this also comes with new challenges that eukaryotic organisms have to overcome. Despite the fact that mitochondria and chloroplasts have retained their own genome, most genes were transferred to the nucleus (Daley et al., 2002). Therefore, most proteins are synthesized on cytoplasmic ribosomes and have to be targeted and imported to their respective destinations, which involves transport across one or more membranes. In yeast and higher eukaryotes, secreted proteins are mainly translated on ribosomes associated with the ER. The Sec61 complex imports these proteins into the ER in a co-translational manner, from where they can be targeted to different compartments. This often involves extensive modification like oxidation, protease cleavage and glycosylation in the ER and Golgi apparatus. The Sec61 system is of prokaryotic origin, whereby it's bacterial counterpart, the SecYEG machinery, is responsible for protein secretion (Park and Rapoport, 2012). In chloroplasts, the transport of unfolded protein chains is mediated mainly by the translocon of the outer/inner envelope membrane (TOC/TIC) (Andrès et al., 2010; Kovács-Bogdán et al., 2010). The PEX machinery in peroxisomes is even able to import folded proteins and assembled protein complexes, most likely by forming a dynamic import pore that assembles with the substrates prior to import (Platta et al., 2014).

These basic principles highlight that many different mechanisms have evolved to facilitate protein transport. Mitochondria harbor different types of proteins including soluble proteins, α-helical and β-barrel membrane proteins in different compartments, which require dedicated machineries for import.

1.1.2 Mitochondrial structure and dynamics

Two membranes surround mitochondria (Figure 1). Due to their endosymbiotic origin, both membranes are of different nature. The outer membrane (OM) corresponds to the host cell, whereas the inner membrane is of α-proteobacterial origin (Gray et al., 1999). The outer membrane forms an envelop around the mitochondrion. Due to the presence of β-barrel pores (Por1 in yeast, VDAC in higher eukaryotes), the outer membrane is permeable to ions and small metabolites (Benz, 1994). In contrast, the inner membrane (IM) forms a diffusion barrier for ions or metabolites and is one of the most protein rich membranes known (Simbeni et al., 1991). Cardiolipin is the signature lipid of mitochondrial membranes and is essential for membrane organization and for the assembly and function of macromolecular complexes, like the respiratory chain complexes (Ikon and Ryan, 2017). Consequently, mutations in the cardiolipin biosynthesis pathway are associated with diseases like Barth syndrome (Dudek and Maack, 2017).

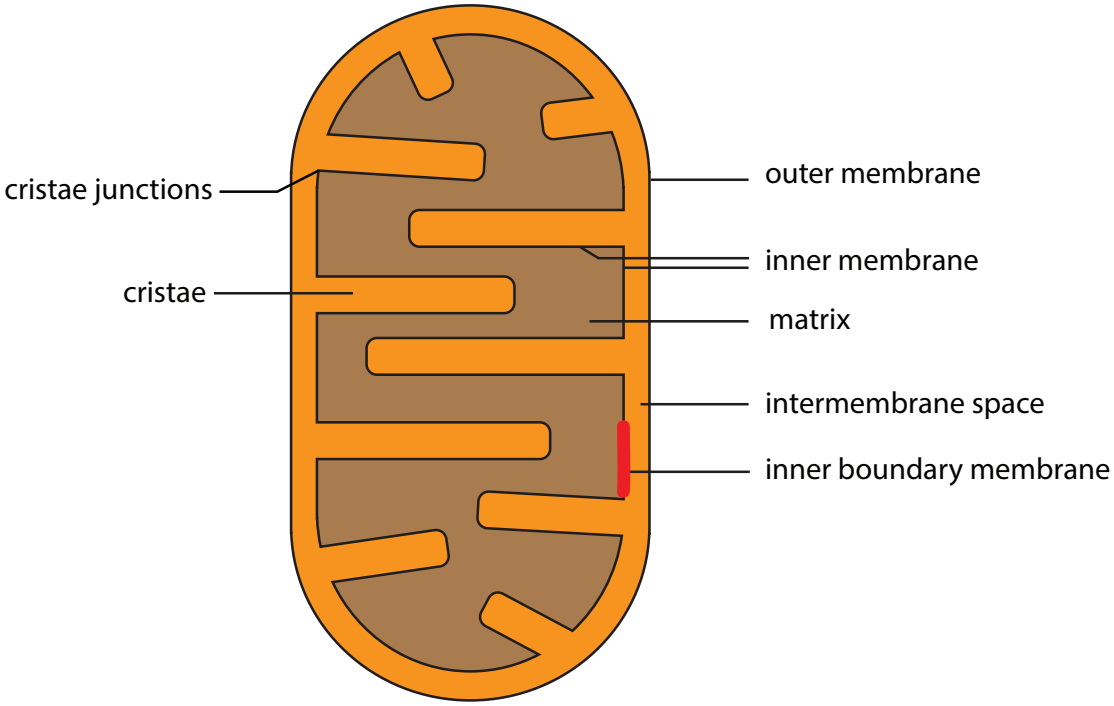

Figure 1: Mitochondrial structure. The mitochondrial outer and inner membranes confine the intermembrane space. The inner boundary membrane (red) is in close contact to the outer membrane and is the site of protein import. Invaginations of the inner membrane, termed cristae, are defined by cristae junctions and cristae tips.

The inner membrane forms different sub-compartments. The inner boundary membrane (IBM) is in close contact to the outer membrane and is the main site for protein import (Vogel et al., 2006). Large invaginations of the inner membrane are called cristae and are formed essentially by two protein complexes. A membrane complex termed mitochondrial contact site and cristae organizing system (MICOS) is crucial for cristae junction formation by inducing membrane curvature at the proximal end (Barbot et al., 2015; van der Laan et al., 2012), while dimerization of the ATP synthase is required for cristae tip formation (Paumard et al., 2002).

The ATP synthase (also called complex V) is the final enzyme of respiratory chain, which is composed of three to four additional enzyme complexes that generate a proton gradient across the inner membrane by oxidative phosphorylation. Theses complexes are mainly located in the membranes of the cristae (Gilkerson et al., 2003). The proton gradient is used by the F_1F_0-ATP synthase to generate ATP from ADP and inorganic phosphate. Moreover, protein transport across the inner membrane requires the $\Delta\psi$ (Martin et al., 1991).

Proteins also regulate the overall shape of mitochondria. Despite their depiction in textbooks as rod-shaped structures, it has become apparent that mitochondria form a reticulum-like network in the cell (Friedman and Nunnari, 2014). This network is highly dynamic and undergoes constant fusion and fission to respond to changes in metabolic demand and to separate damaged parts from the network (Müller et al., 2015).

In conclusion, mitochondria undergo constant turnover and mitochondrial biogenesis is crucial to maintain functional organelles. Mitochondria still contain their own transcription and translation machinery, however, the mitochondrial genome encodes only for eight proteins in yeast and thirteen in mammals. All other proteins are imported by dedicated translocation machineries.

1.2 Targeting signals for mitochondrial precursors and import machineries

Proteins that are synthesized in the cytosol have to find their destination, which can be the cell membrane, or organelles like the nucleus, mitochondria or peroxisomes. In 1975, Blobel and Dobberstein found that some newly synthesized proteins contain

ER-targeting signal sequences that are cleaved off once the protein has reached its destination (Blobel and Dobberstein, 1975). This signal hypothesis was later expanded from the ER to other organelles, including mitochondria (Neupert and Schatz, 1981). Even though the most common targeting signal for mitochondria is a positively charged amphipathic N-terminal cleavable α-helix, called the presequence (Vögtle et al., 2009), the set of motifs that guide proteins to different mitochondrial compartments has increased significantly. Some targeting signals are non-cleavable and internal, even though the exact motif often remains to be elucidated (Chacinska et al., 2009).

Different protein complexes mediate the import of mitochondrial proteins (Figure 2). The translocase of the outer membrane (TOM) complex is the main entry gate for almost all proteins. Some single-spanning or polytopic outer membrane proteins are imported with the help of the mitochondrial import (MIM) complex. β-Barrel proteins are first imported through the TOM complex and subsequently inserted into the outer membrane by the sorting and assembly machinery (SAM). Small, cysteine rich, soluble intermembrane space proteins are trapped by oxidative folding via the mitochondrial intermembrane space import and assembly (MIA) pathway. Hydrophobic polytopic carrier proteins are inserted by the translocase of the inner membrane (TIM22) complex, whereas mitochondrial encoded proteins require the OXA machinery for insertion into the inner mitochondrial membrane. Finally, presequence proteins are inserted by the translocase of the inner membrane (TIM23) complex into the inner membrane and, with the help of the presequence translocase associated motor (PAM) complex, further driven into the matrix. The different import signals and the respective translocases that mediate their import will be discussed in the following section with a focus on results obtained in the budding yeast *Saccharomyces cerevisiae.*

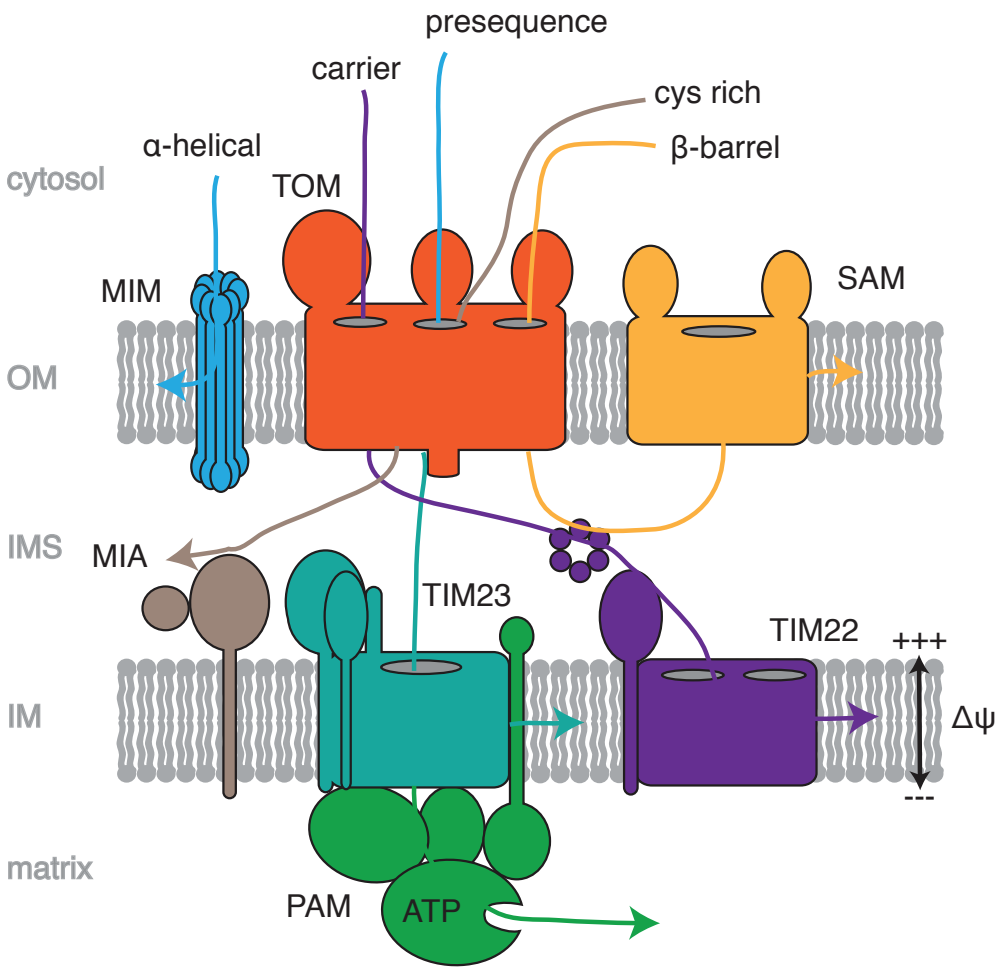

Figure 2: Import pathways into mitochondria. Almost all proteins enter mitochondria through the TOM complex. β-Barrel proteins are shielded by small Tim chaperones on the intermembrane space side and inserted into the outer membrane (OM) by the SAM complex. Hydrophobic multi-spanning inner membrane proteins are also shielded by small Tim chaperones and inserted into the inner membrane in a membrane potential dependent manner by the TIM22 complex. Cysteine rich proteins are trapped in the intermembrane space (IMS) by the MIA pathway. Presequence proteins are imported through the TOM complex and handed over to the TIM23 complex, from where they can be inserted into the inner membrane or transported into the matrix, which requires the presequence translocase associated motor (PAM).

1.2.1 Translocation across the outer mitochondrial membrane: The TOM complex

The outer mitochondrial membrane contains two types of proteins: α-helical proteins, which can be anchored by their N- or C-terminus and possess one or many membrane spans, and β-barrel proteins, which originated from the Gram-negative bacterial ancestor of mitochondria. Even though only a few β-barrel proteins have been identified so far, they perform crucial functions in mitochondria. Proteins of the

voltage-dependent anion channel (VDAC)-porin superfamily allow ions and metabolites to freely diffuse through the outer membrane (Benz, 1994). The SAM complex, also termed TOB (topogenesis of outer-membrane β-barrel), with its core subunit Sam50 imports and assembles β-barrel proteins in the outer membrane. Tom40 is the channel forming subunit of the TOM complex (Wiedemann and Pfanner, 2017) (Figure 3). Each TOM complex contains three copies of Tom40 that form the protein-conducting channel (Model et al., 2008; Shiota et al., 2015). However, Tom40 not only serves as a passive channel but can also bind to hydrophobic stretches of the precursor, thereby preventing aggregation (Esaki et al., 2003). Tom22 is positioned at the center of the Tom40 trimer, which contains an N-terminal receptor domain exposed to the cytosol, a hydrophobic transmembrane segment in the middle of the protein and a C-terminal receptor domain in the IMS (Lithgow et al., 1994; Shiota et al., 2011). Recent cryo-electron microscopy data from *Neurospora crassa* confirmed the central position of Tom22 connecting Tom40 molecules, however, the TOM complex seems only to consist of two instead of three copies of Tom40 in this fungus (Bausenwein et al., 2017). Besides its receptor function, Tom22 is also involved in the assembly and stability of the TOM complex (van Wilpe et al., 1999). The cytosolic kinase, CK2, phosphorylates the precursor of Tom22 at Ser44/46 in the cytosol, thereby promoting Tom22 import and TOM biogenesis (Schmidt et al., 2011). Consequently, Tom22 not only acts as a signal receptor but also as an assembly platform for the TOM complex, which is regulated by cytosolic kinases. Tom20 is another receptor of the TOM complex that, by crosslinking experiments, was shown to be positioned at the periphery of the TOM complex (Shiota et al., 2015). Like Tom22, Tom20 is not essential for mitochondrial function, but deletion of Tom20 leads to a reduction in the import of presequence-containing substrates (Söllner et al., 1989; Yamano et al., 2008b). Phosphorylation of Tom22 increases the interaction with Tom20, which enhances Tom22 import and assembly. The third import receptor of the TOM complex, Tom70, and its less abundant paralog, Tom71, mediate the import of hydrophobic carrier proteins, which contain internal targeting signals. Tom70 exposes a large receptor domain to the cytosol, which contains 11 tetratricopeptide repeats (TPR). TRP 1-3 associate with Hsp70/Hsp90 chaperones that bind carrier proteins in the cytosol, thereby shielding them from the aqueous environment. Structural studies suggest that a hydrophobic pocket formed by TRP 4-11 binds to carrier proteins (Li et al., 2009; Wu and Sha,

2006). The release of chaperones from the carrier proteins requires ATP hydrolysis and is Tom70 dependent (Ryan et al., 1999).

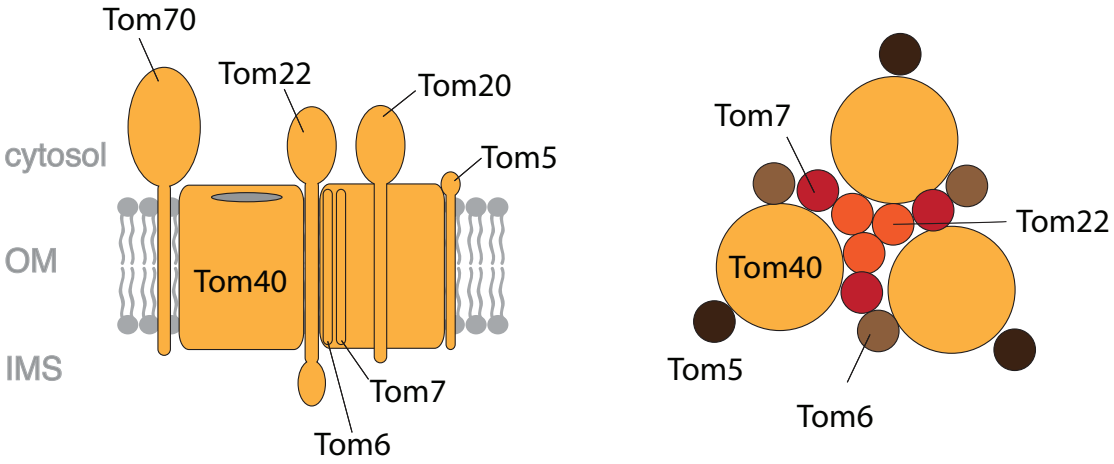

Figure 3: TOM complex composition and architecture. Left: Tom40 forms the channel of the TOM complex while Tom70, Tom22 and Tom22 are primary receptors. Tom5 is involved in handing over substrates from Tom22 to the channel. Tom6 and Tom7 regulate TOM assembly. Right: Top view of the TOM complex. The central presequence receptor Tom22 sits in the middle of the TOM complex and serves as an assembly platform. Three copies of Tom40 assemble around Tom22 to form the channels. Tom6 and Tom7 connect, together with Tom22, the β-barrels of Tom40. Tom5 sits at the periphery of the complex.

In addition to the channel protein and the three receptors described, the TOM complex contains three small Tom proteins that have a regulatory role: Tom5, Tom6 and Tom7. Tom5 is involved in transferring precursor proteins from Tom22 to Tom40 and is also required for Tom40 biogenesis (Becker et al., 2010; Dietmeier et al., 1997; Schmitt et al., 2005). Tom6 and Tom7 seem to act in an antagonistic manner. Whereas Tom6 promotes TOM biogenesis, Tom7 destabilizes the complex. Interestingly, Tom6 gets phosphorylated in a cell-cycle dependent manner by Cdk1, promoting its import and thereby TOM assembly (Harbauer et al., 2014). Tom7, on the other hand, not only binds to the TOM complex, but also to Mitochondrial Distribution and Morphology 10 (Mdm10), another β-barrel protein that has a dual localization in mitochondria, whereby it associates with both SAM and the ER-Mitochondria Encounter Structure (ERMES) (Ellenrieder et al., 2016). Binding of Mdm10 to the SAM complex promotes TOM biogenesis by releasing TOM from the SAM complex. In contrast, binding of Tom7 to Mdm10 prevents binding to SAM and therefore reduces TOM biogenesis.

Even though most proteins are imported through the TOM complex, some α-helical proteins utilize the MIM complex. These proteins are typically targeted to mitochondria by their hydrophobic membrane segment and positive charged residues

at the flanking C-terminus. The MIM complex is composed of the α-helical proteins Mim1 and Mim2 and forms a 200 kDa complex (Dimmer et al., 2012; Popov-Celeketić et al., 2008b). Mim1 oligomerizes with the help of GXXXG/A motifs and directly binds to substrates with its transmembrane segment (Popov-Celeketić et al., 2008b). Typical substrates of the MIM complex are Tom20, Tom70 and the polytopic outer membrane protein Ugo1 (Hulett et al., 2008; Papić et al., 2011). Notably, MIM inserts proteins without a protein-aqueous pore.

1.2.2 Biogenesis of β-barrel proteins: The SAM complex

A hallmark of the mitochondrial outer membrane is the presence of β-barrel proteins, derived from the ancestral Gram-negative bacteria. The SAM complex is chiefly responsible for mediating the import of β-barrel proteins. β-Barrel proteins are targeted to mitochondria by a β-hairpin element which is located at the last β-strand and consists of a polar amino acid (lysine or glutamine), an invariant glycine and two hydrophobic residues and is recognized by Tom20 (Jores et al., 2016; Kutik et al., 2008). After their passage through the TOM complex, β-barrel proteins are chaperoned by two small Tim proteins, namely Tim9-Tim10, which prevent the aggregation of β-barrel proteins (Curran et al., 2002; Wiedemann et al., 2004). Sam50, a β-barrel protein that is derived from bacterial BamA, forms the import pore (Paschen et al., 2003). The peripheral membrane protein, Sam35, binds together with Sam50 the β-signal which directs membrane insertion, probably by opening a proposed lateral gate in the Sam50 pore (Kutik et al., 2008; Wiedemann and Pfanner, 2017). Sam37 promotes the formation of a SAM-TOM complex by interacting with Tom22 (Qiu et al., 2013; Wenz et al., 2015). This is important because the initial import of β-barrel proteins depends on the TOM complex, from which they are handed over to the SAM complex in the IMS.

1.2.3 The MIA pathway couples oxidative folding with import

Small soluble intermembrane space proteins are often cysteine rich and contain CX_3C or CX_9C motifs that serve as a targeting signal. These cysteines are kept in a reduced

state in the cytosol but are oxidized after import into the IMS (Fischer and Riemer, 2013). In addition, the MIA import signal involves hydrophobic residues, which are recognized by a hydrophobic binding pocket in the mitochondrial intermembrane space import and assembly (MIA) 40 protein (Milenkovic et al., 2009; Sideris et al., 2009). MIA substrates are imported through the TOM complex independently of Tom20 or Tom22. Instead, Mia40 acts as the *trans* receptor in the IMS, which traps the substrates on the IMS site (Gornicka et al., 2014; Peleh et al., 2016). Moreover, Mia40 acts a thiol oxidase, which promotes disulfide bond formation in substrates, which includes transient intermolecular disulfides with the precursor (Chacinska et al., 2004). Reduced Mia40 is recycled by the sulfhydryl oxidase Erv1, which accepts electrons from Mia40 and transfers them to cytochrome *c* (Allen et al., 2005).

Recently, the set of substrates for MIA has been extended to include inner membrane proteins like Tim17 or Tim22, which contain intramolecular disulfide bonds. For Tim22, the Mia40 hydrophobic binding pocket interacts with the Tim22 protein and directly induces disulfide bond formation, essential for proper membrane integration and for the assembly of Tim22 with other components of the Tim22 complex (Wrobel et al., 2013). For Tim17, Mia40 binding is crucial for import, however, Erv1 can directly oxidize Tim17 (Ramesh et al., 2016).

Intermembrane space proteins that are not targeted and folded properly can be retrotranslocated back to the cytosol. Their accumulation in the cytosol induces the Unfolded Protein Response activated by mistargeting of proteins (UPRam), which includes upregulation of the proteasome and modulation of translation (Wrobel et al., 2015).

1.2.4 Import of hydrophobic carrier proteins: The TIM22 pathway

Carrier proteins comprise of a large family of mitochondrial inner membrane proteins, including metabolite carriers like the ATP/ADP carrier (AAC), or phosphate carrier (PiC). Members of this family typically contain six α-helical membrane-spanning segments, which are shielded by cytosolic chaperones to prevent misfolding (Young et al., 2003). Internal targeting signals guide the precursor protein to Tom70, where chaperones are removed in an ATP-dependent manner (Brix et al., 1999; Young et al., 2003). Unlike presequence substrates, which are imported as a linear polypeptide,

carrier proteins are threaded through the TOM complex as a loop (Curran et al., 2002; Wiedemann et al., 2001). Interestingly, the cytosolic N-terminus of Tom40 reaches through the TOM complex to recruit small Tim proteins in the IMS (Shiota et al., 2015). Once the carrier proteins emerge on the *trans* side of the TOM complex, small Tim proteins bind to hydrophobic segments. In most cases, the heterohexamer formed by Tim9-Tim10 guides the substrate to the TIM22 complex in the inner membrane (Davis et al., 2007). Not only carrier proteins, but also core proteins of inner membrane translocases, including Tim23, Tim17 and Tim22, are imported via the TIM22 pathway (Curran et al., 2002). For Tim23, the nonessential Tim8-Tim13 hexamer guides the protein to the TIM22 complex (Beverly et al., 2008). Another small TIM protein, called Tim12, binds the Tim9-Tim10 hexamer and transfers the complex to the TIM22 complex (Gebert et al., 2008). Tim54, a transmembrane protein that exposes a large domain to the IMS binds the Tim9-Tim10-Tim12 complex, which initiates protein import (Kerscher et al., 1997). Tim22 has four transmembrane segments and forms the translocation pore. Protein translocation through the TIM22 complex requires $\Delta\psi$, which most likely acts on positively charged residues in the matrix loops of transmembrane segments (Rehling et al., 2003).

Additional components of the TIM22 complex are Tim18 and Sdh3, which support assembly of the translocase. Sdh3, together with Sdh4, is part of complex II of the respiratory chain, but also assembles with Tim18 into the TIM22 complex to support Tim54 association with the complex (Gebert et al., 2011; Sun et al., 2005).

1.2.5 Insertion of proteins from the matrix in the inner membrane is mediated by the oxidase assembly translocase Oxa1

In yeast, the mitochondrial genome encodes eight proteins, seven of them are membrane proteins of complex III, IV and the ATP synthase of the oxidative phosphorylation complexes. The core component of the translocase that mediates export of mitochondrial-encoded proteins is Oxa1 (ortholog of the bacterial YidC), or its paralog Oxa2 (Cox18). However, Oxa2 plays only a minor role in protein export. The C-terminus of Oxa1 binds, together with Mba1, the mitochondrial ribosome to

insert proteins in a co-translational manner (Hell et al., 2001; Herrmann et al., 1997; Pfeffer et al., 2015).

In addition, the OXA complex can insert matrix proteins into the inner membrane that have been translocated by a TOM-TIM23 pathway referred to as conservative sorting (Hartl et al., 1986). However, in most cases the TIM23 complex inserts presequence proteins directly into the inner membrane by a process called lateral sorting (see below for details). Interestingly, some proteins like Mdl1 can use a combination of both pathways. Mdl1 contains six α-helical transmembrane domains. The third and fourth helices are transported into the matrix by the PAM complex and then reinserted into the membrane by OXA. All other transmembrane helices are laterally released by the TIM23 complex in a stop-transfer mechanism (Bohnert et al., 2010). Recently, the substrate spectrum of the OXA translocase was substantially extended (Stiller et al., 2016). This now includes the TIM22 components Sdh3 and Tim18, which is why transport along the carrier pathway is affected in Oxa1 mutants (Stiller et al., 2016).

1.3 Import of cleavable precursors: The presequence pathway

About 70% of mitochondrial proteins contain N-terminal targeting signals called presequences (Vögtle et al., 2009). A presequence is an amphipathic α-helix with a net positive charge, it is 15-50 amino acid in length and is usually cleaved off after import by the matrix processing peptidase (MPP) (Hawlitschek et al., 1988). The presequence is recognized by receptors of the TOM complex. Even though recent reports indicate that Tom70 might bind presequences, the well-established receptors for presequences are Tom20 and Tom22 (Abe et al., 2000; Lithgow et al., 1994; Melin et al., 2015). Tom20 binds to the hydrophobic side of the presequence, while Tom22 binds the positively charged surface (Abe et al., 2000; Brix et al., 1997). Due to this observation, it was speculated that Tom20 and Tom22 bind at the same time to the presequence, forming a composed receptor. In the yeast *Saccharomyces castellii*, the acidic N-terminus of Tom22 is fused to Tom20, which was called domain stealing, supporting the concept of a composed receptor (Hulett et al., 2007). However, attempts to reconstitute both receptors with a presequence *in vitro* have failed so far.

Tom5 helps to hand over the substrate from Tom22 to the Tom40 channel (Dietmeier et al., 1997). Tom40 seems to bind to presequences and keeps the linear polypeptide in an unfolded state (Esaki et al., 2003; Melin et al., 2014). Crosslinking data suggests that soluble matrix-targeted proteins and hydrophilic inner membrane proteins use different pathways in the channel (Shiota et al., 2015). Once the presequence emerges on the *trans* side of the channel, it is bound by the IMS domain of Tom22 from where it is handed over to the TIM23 complex (Komiya et al., 1998).

Despite the extensive knowledge of the TOM complex, the driving force that drives protein translocation is not known. However, the "acid chain" hypothesis suggests an increase in affinity for substrates from the *cis* to the *trans* side of the TOM complex (Komiya et al., 1998).

1.3.1 Import of preproteins by the TIM23 complex

The translocase of the inner membrane (TIM23) complex is in close proximity to the TOM complex, which is facilitated by interactions between the IMS domain of Tom22 with $Tim21^{IMS}$ and probably $Tim50^{IMS}$ and $Tim23^{IMS}$ of the TIM23 complex (Bajaj et al., 2014a; Chacinska et al., 2005; Shiota et al., 2011; Waegemann et al., 2014) (Figure 4).

The TIM23 complex exists in different forms. The core complex is composed of the essential polytopic proteins Tim23 and Tim17 that contain four α-helical membrane spans, as well as the single membrane-spanning Tim50 protein and Mgr2. Tim23 forms a voltage sensitive protein conducting channel in the inner membrane (Truscott et al., 2001). Changes in $\Delta\psi$ across the inner membrane, or the presence of presequences, triggers conformational changes of the Tim23 protein (Alder et al., 2008a; Bauer et al., 1996; Malhotra et al., 2013).

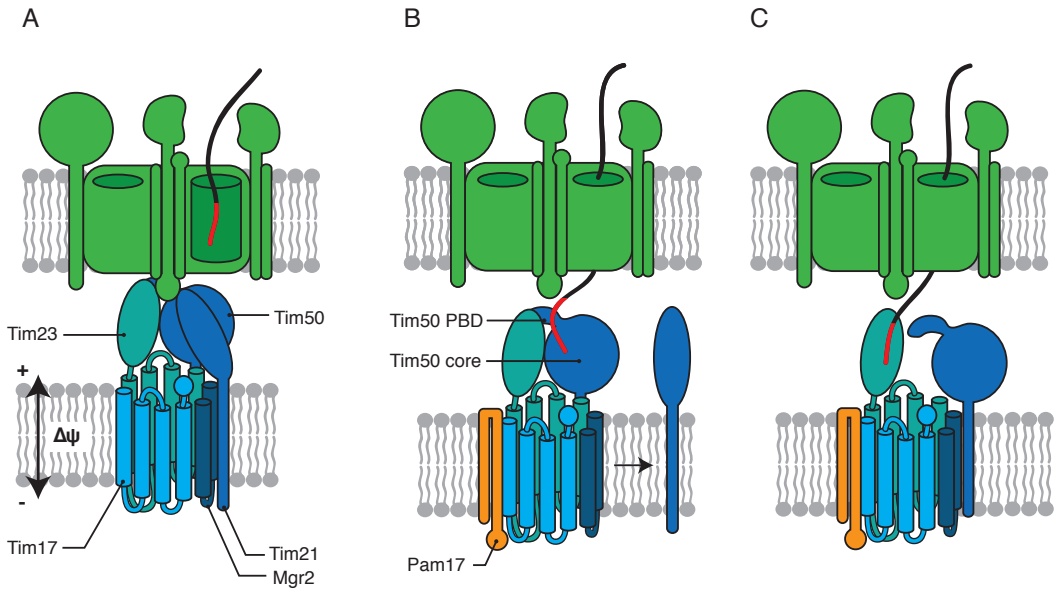

Figure 4: Presequence handover from TOM to TIM23. A: The IMS domains of Tom22, Tim23, Tim50 and Tim21 form connection sites between TOM (green) and TIM23 (blue). B: A presequence substrate is handed over from Tom22 IMS to Tim50 IMS, which leads to Tim21 dissociation and Pam17 recruitment. C: The substrate is handed over from Tim50 to Tim23 from where in can enter the import channel. (Schulz et al., 2015)

The second transmembrane segment (TMS2) of Tim23 was shown to be part of the protein-conducting channel, which is in close proximity to precursor proteins *in transit* (Alder et al., 2008a; Malhotra et al., 2013). Upon reduction of Δψ, the C-terminus of TMS2 becomes more exposed to a hydrophilic environment and a kink in the α-helix is introduced, which might help to prevent ion leakage (Malhotra et al., 2013). A 100 amino acid, hydrophilic IMS domain at the N-terminus of Tim23 serves as a presequence receptor and docking platform for Tim50 and Tim21 (Bajaj et al., 2014a; Bauer et al., 1996; Geissler et al., 2002; la Cruz et al., 2010). The domain was reported to protrude into the outer membrane, even though the physiological relevance is not clear (Bajaj et al., 2014b; Donzeau et al., 2000).

Binding of $Tim50^{IMS}$ to the IMS domain of Tim23 seals the pore during resting state, therefore preventing harmful ion leakage (Meinecke, 2006). Reduced Δψ leads not only to a rearrangement of TMS2 of Tim23, but also to an increased binding of $Tim50^{IMS}$ to TMS1 of Tim23 (Alder et al., 2008b).

Even though Tim23 alone is sufficient to form a channel in reconstitution experiments using lipid bilayers, the mitochondrial translocation pore is most likely formed by Tim17 as well. Tim17 is a homolog of Tim23 that lacks an N-terminal IMS domain,

but also contains four α-helical TMS which possess GxxxG motifs that are essential for structural integrity (Demishtein-Zohary et al., 2015). TMS1 of Tim23 is in close proximity to TMS4 of at least one Tim17 molecule. However, in *tim23-2* mutants, Tim23 can form a pore without Tim17 (Alder et al., 2008b; Truscott et al., 2001). Tim17 seems to exert a regulatory role in protein import. It affects both sorting of membrane proteins and the gating activity of the channel, which requires a disulfide bond between TMS1 and TMS2 on the IMS side (Chacinska et al., 2005; Martinez-Caballero et al., 2007; Ramesh et al., 2016). Moreover, Tim17 is involved in import motor recruitment (Demishtein-Zohary et al., 2017). However, the exact function of Tim17 still remains to be solved.

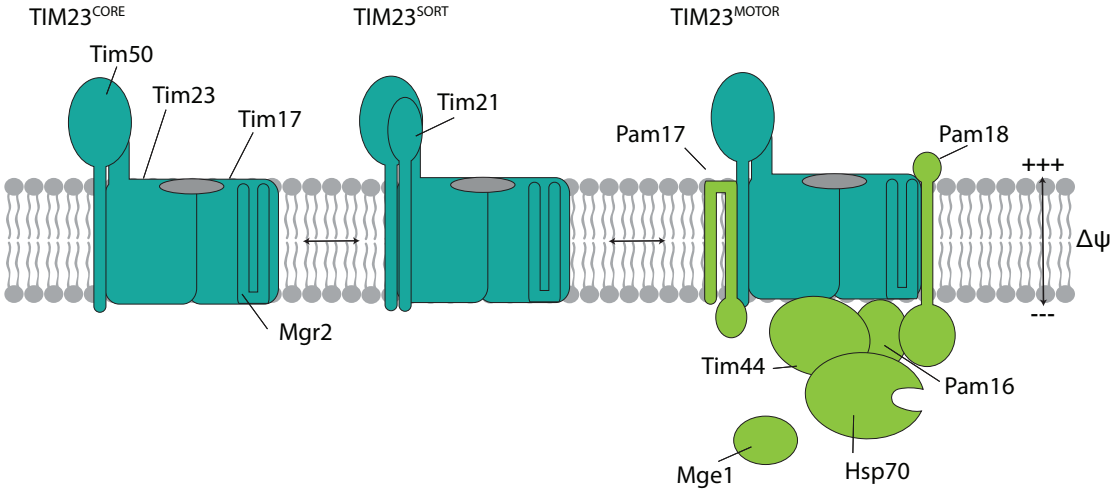

Figure 5: Different forms of the TIM23 complex. Left: The TIM23^{CORE} complex contains the two multi-spanning membrane proteins, Tim23 and Tim17, as well as the presequence receptor Tim50 and the lateral gate-keeper Mgr2. Middle: The TIM23^{SORT} contains Tim21, which links the complex to the respiratory chain. Right: For import of matrix-targeted proteins, the presequence associated motor (PAM) complex binds to the TIM23 complex

The newest identified component of the TIM23 complex is Mgr2, a small protein that has two membrane-spanning segments connected by a matrix loop and, after removal of the C-terminus by Imp1, no soluble domain (Gebert et al., 2012; Ieva et al., 2013). Early studies suggested that Mgr2 couples Tim21 to the translocase (Gebert et al., 2012). More importantly, Mgr2 binds to the hydrophobic stop-transfer signal of membrane proteins and controls the release of precursors into the lipid bilayer (Ieva et al., 2014). Overexpression of Mgr2 leads to a delay in lateral release, whereas deletion of Mgr2 increases sorting events (Ieva et al., 2014). Moreover, artificial fusion proteins of cytochrome b_2 and mouse dihydrofolate reductase (DHFR), with mutated sorting signals that are usually mistargeted into the matrix, are released into

the membrane in an *mgr2*Δ strain (Ieva et al., 2014). This led to the proposal that Mgr2 serves as a lateral gatekeeper, mediating quality control. In addition, Mgr2 seems to regulate the dynamic exchange of motor subunits in the active motor (see below) (Schulz and Rehling, 2014).

Association of Tim21 with the $TIM23^{CORE}$ complex leads to the generation of the $TIM23^{SORT}$ complex (Figure 5). This complex is competent to insert membrane proteins into the membrane of liposomes which only have an artificial $\Delta\psi$ as the driving force (van der Laan et al., 2007). Tim21 contains a single transmembrane domain and exposes a soluble domain to the IMS that interacts with $Tim50^{IMS}$ and $Tom22^{IMS}$, thereby coupling the TOM and TIM23 complex (Albrecht et al., 2006; Chacinska et al., 2005; Shiota et al., 2011). Moreover, Tim21 connects the TIM23 complex to the respiratory chain III-IV supercomplex and supports membrane protein insertion, especially under low $\Delta\psi$ conditions (van der Laan et al., 2006). It is assumed that the proton gradient is stronger in the close vicinity of respiratory chain complexes, which are enriched in the cristae membranes but also exist in the inner boundary membrane. Not surprisingly, active TOM-TIM23 complexes have been found at cristae junctions, enabling both proximity to the outer membrane and to the respiratory chain (Gold et al., 2014). Interestingly, the TIM23 complex also associates with the ADP/ATP carrier, which might support protein import when respiratory chain activity is low (Mehnert et al., 2014).

Even though the Tim23 IMS domain can bind presequences, the central presequence receptor of the Tim23 complex is Tim50 (Geissler et al., 2002; Lytovchenko et al., 2013; Schulz et al., 2011; Yamamoto et al., 2002). Tim50 binds to the IMS domain of Tim23 and induces channel closure. Binding of a presequence to Tim50 triggers the release of Tim21 from Tim50, resulting in channel opening (Lytovchenko et al., 2013; Meinecke, 2006). Tim50 possesses two presequence binding domains, one in the conserved core domain, for which structural data exists, and the other one in a fungi-specific C-terminal presequence binding domain (PBD) (Lytovchenko et al., 2013; Qian et al., 2011; Schulz et al., 2011). Since the PBD also binds to Tom22 to mediate TOM-TIM23 coupling, and the PBD binding site for $Tim50^{CORE}$ overlaps with its presequence binding site, one could envision that the presequence is handed over from Tom22 to $Tim50^{PBD}$ (probably with the support of Tim21) and from there to $Tim50^{CORE}$ (Rahman et al., 2014; Shiota et al., 2011; Waegemann et al., 2014). This

mechanism allows for the handover of preproteins from TOM to TIM23 and their subsequent translocation through the inner membrane, while the C-terminus of the preprotein still spans the TOM complex (Schülke et al., 1997).

Interestingly, recent data shows that the TIM23 complex is also involved in the insertion of proteins into the outer membrane (Song et al., 2014; Wenz et al., 2014). The outer membrane protein Om45 initially follows the presequence pathway using TOM and TIM23. Om45 import depends on Tim50, Tim23 and $\Delta\psi$ across the inner membrane. However, Om45 does not contain a classical presequence and the targeting signal has not been identified. After release from TIM23, Om45 gets inserted into the outer membrane with the help of the MIM complex (Wenz et al., 2014).

1.3.2 Membrane insertion of single spanning membrane proteins by the TIM23 complex

The TIM23 complex can import two different classes of substrates: inner membrane proteins and soluble matrix proteins. The first class requires only the $\Delta\psi$, whereas the latter additionally depends on an ATP-driven motor complex (Schulz et al., 2015). For the import of inner membrane proteins, two basic models have been proposed. In the "conservative sorting" model, membrane proteins are imported into the matrix using the TIM23 complex and then re-exported by the OXA machinery. In the alternative "stop-transfer" mechanism, hydrophobic TMSs in the preprotein lead to a stalling of the protein in the Tim23 channel and subsequent lateral release into the membrane. Even though both scenarios occur in the cell, the more common one seems to be the "stop-transfer" (Glick et al., 1992). Lateral release of membrane proteins into the membrane, also called "sorting", requires a hydrophobic stop-transfer signal in the unfolded protein chain, which overlaps with the membrane segment. The $TIM23^{SORT}$ form is capable of inserting membrane proteins without large matrix domains into the mitochondrial inner membrane without the need for ATP hydrolysis and chaperone activity (van der Laan et al., 2007). Interestingly, association of Tim21 with the TIM23 complex seems to shift the equilibrium away from the $TIM23^{MOTOR}$ form to the sorting form (Chacinska et al., 2010). Consequently, overexpression of Tim21 leads to decreased amounts of motor components at the translocase. While Tim21 has no known direct effect on sorting

events, Mgr2 interacts with the sorting signal and modulates lateral release. Interestingly, the motor component, Pam18, was found in close proximity to sorted precursors and deletion of the Pam18 IMS domain, which affects binding to Tim17, increases the lateral release of precursors (Popov-Celeketić et al., 2011). In contrast to the "stop-transfer", some proteins follow the "conservative sorting" pathway and some proteins even use a combination of both pathways (Hartl et al., 1986; Park et al., 2014). The pathway utilized mainly depends on the hydrophobicity of the membrane segment, whereby stop-transfer signals are more hydrophobic. Moreover, stop-transfer signals have charged amino acids adjacent to the signal and lack prolines (Meier et al., 2005).

1.3.3 Import of matrix proteins requires the activity of the PAM complex

Many translocation machineries require chaperones that provide a driving force for vectorial movement of the unfolded polypeptide chains across membranes (Flores-Pérez and Jarvis, 2013; Kang et al., 1990; Park and Rapoport, 2012). In mitochondria, heat shock proteins are involved in both protein folding and import. MtHsp70 (Ssc1 in yeast) is the core component of the PAM complex and hydrolyses ATP to maintain unidirectional movement into the mitochondrial matrix (Kang et al., 1990). Like its bacterial counterpart, DnaK, mtHsp70 contains a nucleotide binding domain (NBD) and a substrate binding domain (SBD) that are separated by a linker region. In the ATP-bound state, the lid of the SBD is open and the SBD and NBD are docked on each other (Mapa et al., 2010; Mayer, 2013). This renders Hsp70 competent to bind to substrates with a high on and off rate (Liu et al., 2003; Takeda and McKay, 1996). In contrast, in the ADP bound form, SBD and NBD are not docked and the lid of the SBD is closed, which leads to binding of the chaperone to its substrate. Release of ADP and binding of another ATP molecule then triggers the subsequent release of the substrate (Kampinga and Craig, 2010; Liu et al., 2003; Mayer, 2013).

However, chaperones usually don´t perform their cellular function alone but are tightly regulated by other proteins. To prevent futile cycles, the intrinsic ATPase activity of chaperones is often low and they depend on J-domain proteins for ATP hydrolysis (Laufen et al., 1999). All J-proteins contain a conserved histidine-proline-aspartate (HPD) motif in the loop between helix II and helix III, which is essential for

ATPase stimulation (Bukau and Horwich, 1998). However, J-proteins are not only involved in ATPase stimulation, but frequently also in substrate recognition. J-proteins directly bind potential substrates, recruiting co-factors and Hsp70, therefore ensuring substrate specificity (Craig and Marszalek, 2017; Kampinga and Craig, 2010). Cells often contain many more J-proteins than chaperones (Craig and Marszalek, 2017). In yeast mitochondria, the soluble Mdj1 protein supports Hsp70 function for protein folding, while Pam18 is a membrane protein that acts in the import motor (Rowley et al., 1994; D´Silva et al., 2003; Truscott et al., 2003).

Successful release of a substrate bound to Hsp70 requires the release of ADP. This is stimulated by nucleotide exchange factors, which trigger dissociation of ADP from the Hsp70 molecule, allowing for another round of ATP binding and substrate release (Kampinga and Craig, 2010; Mapa et al., 2010). In mitochondria, Mge1 (mitochondrial GrpE) performs this job (Laloraya et al., 1994; Miao et al., 1997).

Hsp70 itself has to be imported PAM-dependent into mitochondria. Interestingly, Hsp70 cannot fold by itself but depends on Hep1, which is located in the mitochondrial matrix (Sichting et al., 2005). Hep1 is a zinc finger protein that is required for folding of the NBD but not the SBD (Blamowska et al., 2012). This mechanism could ensure that Hsp70 only folds and functions properly in mitochondria after import and not in the cytoplasm after translation from cytosolic ribosomes.

1.3.4 The PAM complex drives import into the matrix

MtHsp70 performs essential functions in protein folding and import. For protein import, it is recruited to the translocase by the membrane associated protein Tim44, which acts as a scaffold protein (Kronidou et al., 1994; Schneider et al., 1994; Slutsky-Leiderman et al., 2007). For many years it was thought that the interaction between Tim44 and Hsp70 depends on the nucleotide bound to Hsp70, with ATP dissipating the interaction and ADP favoring the binding (Kronidou et al., 1994; Schneider et al., 1994; Slutsky-Leiderman et al., 2007). However, these conclusions were mainly drawn based on pull-down experiments from mitochondrial lysates in the presence of either ATP or EDTA to chelate Mg^{2+}, which is needed for ATP binding. Liu and colleagues could show that the nucleotide state of Hsp70 does not matter but

instead, the loading of a substrate on Hsp70 dictates the interaction with Tim44 (Liu et al., 2003). Lysing mitochondria with detergent might provide Hsp70 with unfolded protein domains that it could bind in the presence of ATP, which would trigger Tim44 release. However, crosslinking experiments with purified components challenged this view some years ago (Slutsky-Leiderman et al., 2007).

Tim44 associates with the inner mitochondrial membrane, most likely with the help of α-helix A1 and A2 of the crystallized C-terminal domain (CTD, residues 210-431) (Marom et al., 2009; Weiss et al., 1999). This association is increased in the presence of cardiolipin, a signature lipid of the inner membrane (Weiss et al., 1999). Moreover, the CTD binds to the translocase, most likely by interacting with the matrix loop of Tim17, which connects TMS3 and TMS4 (Demishtein-Zohary et al., 2017). Also, the C-terminus was found in close proximity to translocation intermediates (Banerjee et al., 2015). The N-terminal domain (NTD, residues 43-209), however, binds directly to Hsp70 (Schiller et al., 2008). Genetic analysis also indicates an interaction between the NTD of Tim44 and the N-terminus of Pam16 and probably Pam17 (Schilke et al., 2012).

Interestingly, a direct interaction of presequence peptides with recombinant Tim44 was observed using surface plasmon resonance (SPR) measurements, but the physiological implications for this interaction are not clear (Marom et al., 2011). Crosslinking experiments suggest a binding site at residues 160-180 in the NTD, which are also involved in Hsp70 binding (Schilke et al., 2012; Ting et al., 2017). Also, the NTD might bind to Tim17 and Tim23, although only crosslinking data exist and no direct interaction has been reported (Ting et al., 2014; 2017). Taking all interactions into account, Tim44 binds to both the membrane and the core components of the channel, Tim23 and Tim17, and provides a docking platform for Hsp70 and the regulatory proteins, Pam16 and Pam18.

Pam18 is a member of the J-domain protein family that can stimulate Hsp70 activity and is essential for protein import (Mokranjac et al., 2003; Truscott et al., 2003). The N-terminus is located in the IMS, while the HPD motif containing C-terminus is in the matrix. The N-terminus interacts with Tim17 and the C-terminus with Pam16 (Mokranjac et al., 2007; Schilke et al., 2012). Recruitment of Pam18 to the translocase not only depends on Tim17 but also on Pam16. In the cell, Pam16 is in a tight complex with Pam18 and, by binding to Tim44, recruits Pam18 to the complex

(Frazier et al., 2004; Schilke et al., 2012). Even though Pam18 and Pam16 share similarities, Pam16 does not contain a HPD motif and is not able to stimulate Hsp70 activity (Frazier et al., 2004; Kozany et al., 2004; Mokranjac et al., 2006). Instead, Pam16 represses the stimulating activity of Pam18 (Li et al., 2004). Indeed, in the reported crystal structure of the Pam18-Pam16 dimer, the HPD motif is blocked by Pam16 and cannot interact with a Hsp70 molecule (Mokranjac et al., 2006). Therefore, one could envision that Pam16 inhibits Pam18 function in the absence of the translocase and only upon binding of Pam16 to Tim44 at the translocase (or possibly a substrate), structural rearrangement can occur, thereby enabling Hsp70 activation (Mokranjac et al., 2006; Pais et al., 2011; Schulz et al., 2015). However, a study which mainly employed genetic assays questions the inhibitory role of Pam16 on Pam18 and states that Pam16 is mainly important for recruiting and properly positioning Pam18 at the translocase (Pais et al., 2011). Nevertheless, the study mainly relies on growth tests on non-fermentable medium and lacks detailed biochemical data. In addition, a structure of Pam16 and Pam18, in complex with Hsp70 (and Tim44), would help to answer this question.

The Pam16-Pam18 module is recruited to the translocase via interactions between Tim17 with $Pam18^{IMS}$ on the one hand and Tim44 with Pam16 on the other hand. Another factor that might be involved in motor recruitment is the membrane protein Pam17. Pam17 has two membrane spans connected by an IMS loop and a small soluble matrix domain (van der Laan et al., 2005). Early results suggested that Pam17 is involved in recruiting Pam16 and Pam18 to the translocase and the lack of Pam17 leads to a selective defect in the import of motor dependent substrates (van der Laan et al., 2005). Moreover, Pam17 and Tim21 seem to exist in different complexes, with Tim21 being present in the $TIM23^{SORT}$ form and Pam17 in the $TIM23^{MOTOR}$ form. Despite this, the role of Pam17 in the recruitment of motor components remains controversial (Chacinska et al., 2010; Popov-Celeketić et al., 2008a; van der Laan et al., 2005). Interestingly, Pam17 seems to act at a very early stage of protein import, since already the presequence translocation across the inner membrane is affected in a *pam17*Δ strain, which is not the case for other motor subunits (Schiller, 2009). Since the addition of presequence peptides to isolated mitochondria triggers dissociation of Tim21 and association of Pam17, it was proposed that Pam17 mediates the conversion of $TIM23^{SORT}$ to $TIM23^{MOTOR}$ by recruiting the motor module (Lytovchenko et al., 2013).

1.3.5 Vectorial precursor movement facilitated by Hsp70

How does the import motor transport substrates across the inner membrane? Two different models have been discussed over the last decades: In the power-stroke model, Hsp70 binds to the incoming precursor and undergoes conformational changes, driven by ATP hydrolysis, which leads to unidirectional translocation (Glick, 1995; Voisine et al., 1999). In the Brownian Ratchet model, however, spontaneous unfolding of the protein and random movement of the precursor in the TOM and TIM23 channel are translated into protein transport. In the second case, Hsp70 binding traps the precursor and prevents backsliding, but does not generate a pulling force (Neupert and Brunner, 2002; Okamoto et al., 2002; Yamano et al., 2008a). Experiments with fusion proteins containing Hsp70 binding sites, and stretches that cannot engage with Hsp70, in combination with different spacer lengths between them, fused to tightly and loosely folded domains, are mostly in favor of the Brownian Ratchet model (Okamoto et al., 2002; Yamano et al., 2008a). A third model, the entropic pulling model, brings both views together. In this model, binding of Hsp70 to a substrate decreases the diffusion space for Hsp70 near the membrane, which leads to an entropic pulling away from the channel (De Los Rios et al., 2006).
In summary, the following mode of import motor action is the most widely accepted (Chacinska et al., 2009; Mokranjac and Neupert, 2010; Schulz et al., 2015): A precursor is transported through the TOM complex and engages with Tim50 and Tim23 in the IMS. $\Delta\psi$ acts on the positively charged amino acids in the presequence and provides the driving force for the translocation across the TIM23 channel. Then, Hsp70, in its ATP form in complex with Tim44, binds to the precursor. This leads to Pam18-supported ATP hydrolysis and lid closure of Hsp70. The $Hsp70^{ADP}$-substrate complex therefore diffuses away (or actively pushes itself) from the complex, which allows for another $Hsp70^{ATP}$ molecule to bind to Tim44 at the translocase.

1.4 Aim of this work

The presequence pathway is the most common and probably best-described import route into mitochondria. The TIM23 complex can transport preproteins into the inner membrane and mitochondrial matrix. For both, the TOM and the TIM23 complex, the general function of all components has been identified, including signal receptors, channel forming subunits and proteins involved in assembly of the complexes. The TOM complex seems to form a stable unit, however, the TIM23 is a very dynamic complex that readily exchanges subunits based on the nature of transported precursor. While the driving force for protein translocation through the TOM complex is not understood, translocation across the TIM23 complex requires $\Delta\psi$ and ATP hydrolysis by Hsp70. $\Delta\psi$ is considered to act on the positively charged amino acids in the presequence.
However, to what extend $\Delta\psi$ acts on the mature portion of the preprotein or the TIM23 channel and how this drives protein translocation is poorly understood.

In the first part, the role of the inner membrane protein Pam17 was dissected. Only few reports on Pam17 existed to date and its function remained controversial. While in a first study, Pam17 was characterized as a motor protein, other studies and our unpublished data questioned this view. Moreover, the connection between the presequence receptor Tim50 and Pam17 was studied, which seems to play a role in early steps of protein import. Due to results obtained with these experiments, $\Delta\psi$ dependences of different matrix targeted proteins was analyzed with an emphasis on the role of the presequence. Finally, a link between the $\Delta\psi$ and Pam17 dependences of precursor import was investigated.

Tim23 is the pore forming subunit of the TIM23 complex and possesses an N-terminal presequence binding domain exposed to the IMS. The Tim23 channel has a significant preference for cations over anions, which was speculated to be important for presequence transport. Pore-lining, highly conserved residues of Tim23 TM2 were mutagenized and their role in ion selectivity analyzed by electrophysiology experiments. Moreover, the same mutations were introduced in yeast to test the physiological role and the contribution of these residues to protein import.

2. Results

2.1 Manuscript 1: Two distinct membrane potential-dependent steps drive mitochondrial matrix protein translocation

Published December 23, 2016

Two distinct membrane potential–dependent steps drive mitochondrial matrix protein translocation

Alexander Benjamin Schendzielorz,[1] Christian Schulz,[1] Oleksandr Lytovchenko,[1] Anne Clancy,[2] Bernard Guiard,[3] Raffaele Ieva,[4,5] Martin van der Laan,[5,6] and Peter Rehling[1,7]

[1]Department of Cellular Biochemistry and [2]Department of Molecular Biology, University Medical Center Göttingen, Georg-August-Universität Göttingen, 37073 Göttingen, Germany
[3]Centre de Génétique Moléculaire, Centre National de la Recherche Scientifique, 91190 Gif-sur-Yvette, France
[4]Laboratoire de Microbiologie et Génétique Moléculaire, Centre de Biologie Intégrative, Université de Toulouse, Centre National de la Recherche Scientifique, Unité Propre de Service, 31062 Toulouse, France
[5]Institute of Biochemistry and Molecular Biology, Center for Biochemistry and Molecular Cell Research, Faculty of Medicine, University of Freiburg, 79104 Freiburg, Germany
[6]Medical Biochemistry and Molecular Biology, Saarland University, 66421 Homburg, Germany
[7]Max Planck Institute for Biophysical Chemistry, 37077 Göttingen, Germany

Two driving forces energize precursor translocation across the inner mitochondrial membrane. Although the membrane potential ($\Delta\psi$) is considered to drive translocation of positively charged presequences through the TIM23 complex (presequence translocase), the activity of the Hsp70-powered import motor is crucial for the translocation of the mature protein portion into the matrix. In this study, we show that mitochondrial matrix proteins display surprisingly different dependencies on the $\Delta\psi$. However, a precursor's hypersensitivity to a reduction of the $\Delta\psi$ is not linked to the respective presequence, but rather to the mature portion of the polypeptide chain. The presequence translocase constituent Pam17 is specifically recruited by the receptor Tim50 to promote the transport of hypersensitive precursors into the matrix. Our analyses show that two distinct $\Delta\psi$-driven translocation steps energize precursor passage across the inner mitochondrial membrane. The $\Delta\psi$- and Pam17-dependent import step identified in this study is positioned between the two known energy-dependent steps: $\Delta\psi$-driven presequence translocation and adenosine triphosphate–driven import motor activity.

Introduction

About two thirds of mitochondrial precursor proteins use N-terminal presequences as targeting signals (Vögtle et al., 2009). The presequence translocase (TIM23 complex) mediates transport of these precursors across the inner membrane (Neupert and Herrmann, 2007; Schulz et al., 2015). Initially, precursors are transported from the cytosol into the intermembrane space by the TOM complex in the outer membrane and are passed to the TIM23 complex (Chacinska et al., 2009; Endo and Yamano, 2010). Presequence-containing precursors can be subdivided into two classes: (1) precursors fully translocated across the inner membrane into the matrix and (2) precursors released from the translocase into the lipid phase of the inner membrane (inner membrane sorting). Precursor transport across the inner membrane is initially driven by the mitochondrial membrane potential ($\Delta\psi$) that acts on the positively charged presequences (Schleyer et al., 1982; Roise and Schatz, 1988; Martin et al., 1991; Chacinska et al., 2009; Endo and Yamano, 2010; Schulz et al., 2015; Turakhiya et al., 2016). The $\Delta\psi$ draws the presequence of the polypeptide chain through the protein-conducting channel by electrophoretic force. This energy suffices to direct laterally sorted precursors into the inner membrane (van der Laan et al., 2007). However, translocation into the matrix requires ATP hydrolysis by the presequence translocase-associated motor (PAM), in addition to the $\Delta\psi$ (Neupert and Brunner, 2002; Schulz et al., 2015).

The presequence translocase consists of a channel-forming module formed by Tim23 and Tim17. Tim50 acts as the receptor for presequences (Meinecke et al., 2006; Qian et al., 2011; Schulz et al., 2011). In addition to these essential proteins, Tim21 and Mgr2 are also constituents of the TIM23 complex. Tim21 is specific to the "motor-free" state of the translocase and enables its association with proton-pumping respiratory chain complexes (van der Laan et al., 2006). Mgr2 is positioned at the lateral gate of the translocase to regulate inner membrane sorting (Gebert et al., 2012; Ieva et al., 2014) and participates in the dynamics of the mitochondrial import motor (Schulz and Rehling, 2014). For transport of matrix proteins, the import motor is recruited to the TIM23 complex. Its central force-generating constituent is mtHsp70 (Ungermann et al., 1994; Mapa et al., 2010). Whereas Tim44 positions mtHsp70 at the channel exit for precursor engagement (Liu et al., 2003), the Pam16/18 complex regulates its ATPase activity (D'Silva et al., 2003; Truscott et al., 2003; Kozany et al., 2004). In addition, Pam17 was

Correspondence to Peter Rehling: Peter.Rehling@medizin.uni-goettingen.de

Abbreviations used: CCCP, carbonyl cyanide m-chlorophenyl hydrazone; DHFR, dihydrofolate reductase; MTX, methotrexate; PK, proteinase K; WT, wild type.

© 2017 Schendzielorz et al. This article is distributed under the terms of an Attribution–Noncommercial–Share Alike–No Mirror Sites license for the first six months after the publication date (see http://www.rupress.org/terms/). After six months it is available under a Creative Commons License (Attribution–Noncommercial–Share Alike 4.0 International license, as described at https://creativecommons.org/licenses/by-nc-sa/4.0/).

Supplemental Material can be found at:
/content/suppl/2016/12/22/jcb.201607066.DC1.html

The Rockefeller University Press $30.00
J. Cell Biol. Vol. 216 No. 1 83–92
https://doi.org/10.1083/jcb.201607066

Check for updates

THE JOURNAL OF CELL BIOLOGY

Downloaded from on January 8, 2017

Published December 23, 2016

suggested as a subunit or assembly factor of the import motor (van der Laan et al., 2005; Hutu et al., 2008). However, its molecular function has remained enigmatic.

In this study, we demonstrate that mitochondrial precursors differ significantly with regard to their $\Delta\psi$ requirement for import. In contrast to the current view of how $\Delta\psi$ energizes the translocation process, we find that a precursor's hypersensitivity to the reduction of $\Delta\psi$ ($\Delta\psi$ hypersensitivity) is independent of its presequence but rather is linked to the mature portion of the polypeptide chain. Pam17 recruitment by the receptor Tim50 is specifically required for the import of these $\Delta\psi$-hypersensitive precursors but is largely dispensable for import of precursors with low $\Delta\psi$ sensitivity. Accordingly, the $\Delta\psi$ energizes a second step in matrix translocation in a presequence-independent manner.

Results

Matrix-destined precursor proteins display differential dependencies on Tim50

Tim50 is the major presequence receptor of the TIM23 complex in the inner mitochondrial membrane and regulates gating of the Tim23 pore. A surprising and still unresolved observation is that a loss of Tim50 leads to robust import defects for matrix proteins, but has a much lesser effect on precursors sorted into the inner membrane (Geissler et al., 2002). To assess the function of Tim50 in protein transport, we isolated mitochondria from *Saccharomyces cerevisiae* cells in which *TIM50* was under control of the *GAL1* promoter. Growing yeast in glucose-containing medium represses the *GAL1* promoter and concomitantly blocks transcription of *TIM50*. To avoid secondary effects, levels of Tim50 were maintained at 20% of the wild-type (WT) amount. Under these conditions, the protein levels of other TIM23 complex components were similar between Tim50-depleted and WT mitochondria (Fig. 1 A). Because Tim50 regulates Tim23 channel activity, we assessed $\Delta\psi$ in mitochondria with reduced amounts of Tim50 using a potential-sensitive dye. Tim50-depleted and WT mitochondria were equally able to quench the fluorescent dye, indicating that the mitochondrial $\Delta\psi$ was not affected under our conditions of controlled Tim50 depletion (Fig. 1 B). We assessed the import capacity of matrix proteins in Tim50-depleted mitochondria with in vitro transport assays. Import of $F_1\beta$ and the model matrix protein $b_2(167)_\Delta$–dihydrofolate reductase (DHFR), which consists of an N-terminal portion of cytochrome b_2 fused to DHFR, was strongly affected, whereas inner membrane–sorted precursors (e.g., cytochrome c_1) were much less Tim50 dependent, as previously reported (Fig. 1, C and D; and Fig. S1 A; Geissler et al., 2002). Considering that Tim50 serves as a presequence receptor in the intermembrane space and hence acts upstream of the import motor, the stronger reliance of motor-dependent substrates on Tim50, compared with motor-independent precursors, is surprising and still lacks an explanation (Geissler et al., 2002). To better understand the Tim50 dependence of mitochondrial proteins, we imported other matrix-targeted precursor proteins, like Tim44, a component of the import motor, and $F_1\alpha$, a soluble subunit of the F_1F_o-ATP synthase. Surprisingly, the import of both precursor proteins was only mildly affected in Tim50-depleted mitochondria (Fig. 1, E and F). In fact, the import efficiency was similar to the mild import defect observed for inner membrane–sorted precursor proteins (Geissler et al., 2002).

To ascertain that the observed import defects were directly linked to Tim50 function, we screened for temperature-conditional *tim50* mutants (Fig. S1 B). The mutant *tim50-19* was selected for analysis because purified mitochondria exhibited WT-like $\Delta\psi$ (Fig. S1 C). Upon heat shock of isolated mitochondria, import of $F_1\alpha$ was clearly more efficient than $F_1\beta$ in *tim50-19* mitochondria (Fig. S1, D and E). Importantly, steady-state levels of mitochondrial proteins in *tim50-19* mitochondria were similar to WT (Fig. S1 F). We conclude that impairment of Tim50 function, either by depletion of the protein or by mutagenesis of the *TIM50* gene, affects the import of different matrix proteins to different extents.

Tim50 is important for Pam17 recruitment

To assess whether depletion of Tim50 affects TIM23 complex organization, we immunoisolated the TIM23 complex with Tim23-specific antibodies. No significant differences of the tested motor or core complex constituents associated with Tim23 were apparent. However, although steady-state levels of Pam17 were WT-like in Tim50-depleted mitochondria (Fig. 1 A), the amount of Pam17 copurified with Tim23 was drastically reduced (Fig. 2 A). A lack of Pam17 leads to a matrix protein import defect (van der Laan et al., 2005; Schiller, 2009). However, only a small set of model matrix proteins had been tested as import substrates. We therefore assessed whether import defects of *pam17Δ* mitochondria resembled those of Tim50-depleted mitochondria. To exclude unspecific effects, we confirmed that the $\Delta\psi$ was not affected in *pam17Δ* mutant mitochondria (Fig. 2 C) and in intact yeast cells (Figs. 2 B and S1 G). As reported, import of $b_2(167)_\Delta$-DHFR and $F_1\beta$ was strongly affected in *pam17Δ* mitochondria (Fig. 2, D and E; van der Laan et al., 2005). In addition, import of Pam18 and Atp14 depended on Pam17 (Fig. S2, A and C). In contrast, import of $F_1\alpha$, Tim44, Atp5, and Mdj1 was only mildly affected in the absence of Pam17 (Fig. 2, F and G; and Fig. S2, B and D). Interestingly, this differential matrix import phenotype resembled the defects observed in mitochondria with reduced Tim50 levels (Fig. 2 H). To exclude the possibility that the observed differences in *pam17Δ* mitochondria were caused by different dependencies of the precursors on import motor activity, we imported $F_1\alpha$ and $F_1\beta$ into mitochondria isolated from temperature-conditional mtHsp70 (Ssc1 in yeast) mutant cells (*ssc1-3*). For this, *ssc1-3* cells were grown at a permissive temperature, and the phenotype was induced by shifting purified mitochondria to a nonpermissive temperature before the import reaction. After heat inactivation of mtHsp70, the import of both precursors, $F_1\alpha$ and $F_1\beta$, was compromised, demonstrating that both precursors depend to the same extent on motor function (Fig. S2, E and F). To assess whether Pam17-dependent precursors also accumulated in vivo, we generated cell lysates from WT and *pam17Δ* mutant cells. As expected, we found that the precursor of Atp14 was detectable in *pam17Δ* cells. Moreover, the amount of Pam18 was drastically reduced in the *pam17Δ* mutant (Fig. S2 G).

Pam17 affects matrix protein import independent of motor function

The selective role of Pam17 in matrix protein import suggested that Pam17 participates in import motor function (van der Laan et al., 2005). We therefore directly assessed the inward-driving force generated by the motor in WT and *pam17Δ* mitochondria. To this end, radiolabeled $b_2(167)_\Delta$-DHFR was imported into

Downloaded from on January 8, 2017

Published December 23, 2016

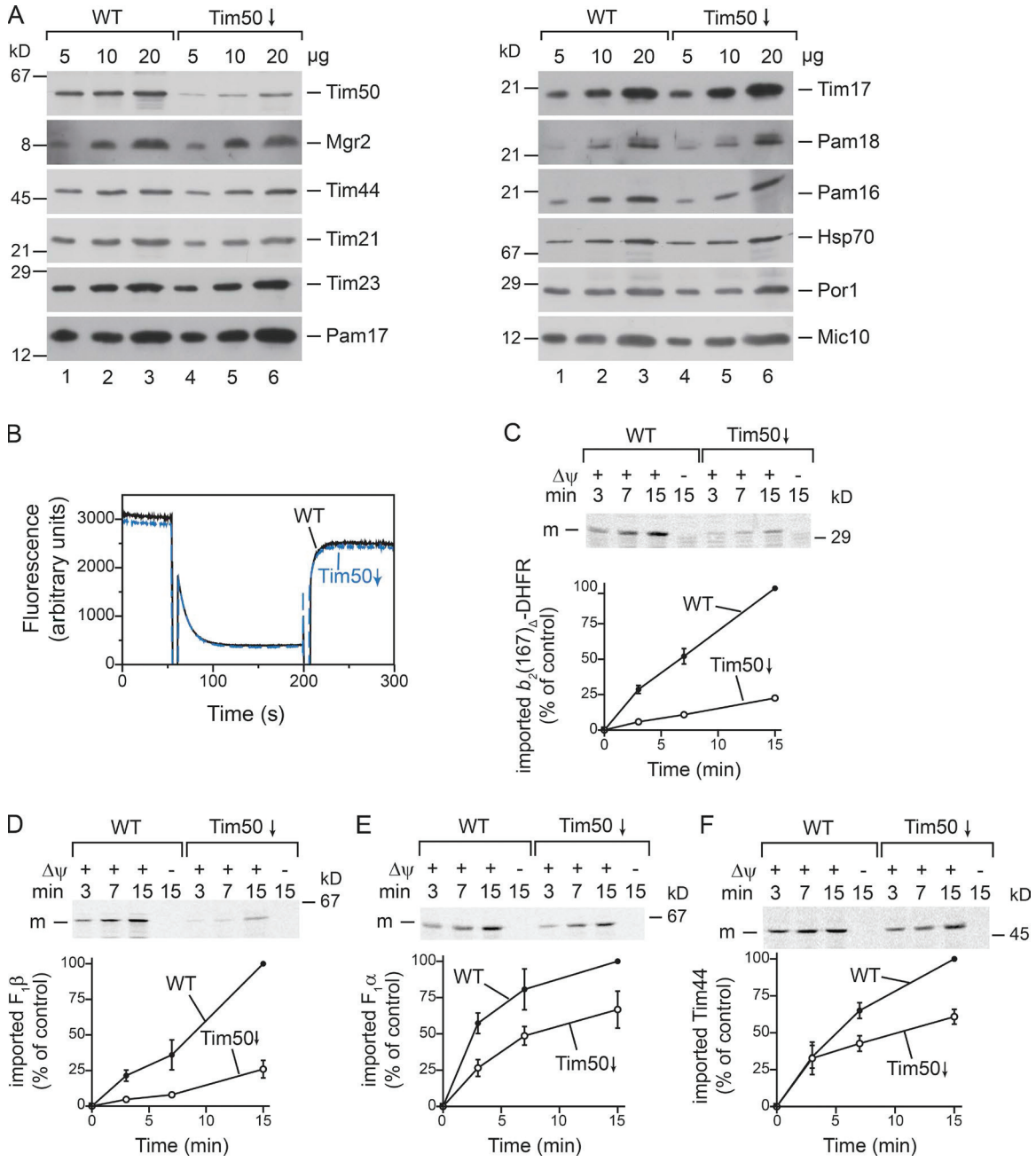

Figure 1. **Protein import is impaired in Tim50-depleted mitochondria.** (A) Steady-state Western blot analysis of WT and Tim50-depleted mitochondria. (B) Δψ of isolated mitochondria was assessed using the Δψ-sensitive dye $DiSC_3(5)$. Fluorescence was recorded before and after addition of valinomycin. (C–F) ^{35}S-labeled precursors were imported into isolated mitochondria, and import stopped at the indicated time points with antimycin A, valinomycin, and oligomycin (AVO). Samples were PK treated and analyzed by SDS-PAGE and autoradiography. Results are presented as mean ± SEM. $n = 3$. The longest import time of the WT sample was set to 100%. m, mature protein.

mitochondria in the presence of methotrexate (MTX). MTX leads to a tight folding of the C-terminal DHFR moiety. The unfolded N-terminal part of the precursor is imported through the TOM and TIM23 complexes, whereas the DHFR moiety is pulled tightly against the TOM complex by the import motor. After initial import, the Δψ was dissipated, and proteinase K (PK) was added after different time points. In the absence of a Δψ, the import motor prevents the precursor from backsliding. Because the tightly folded DHFR moiety only becomes protease accessible if the precursor slides back, this assay enables an estimation of the pulling force of the import motor (Voisine et al., 1999). Remarkably, *pam17Δ* mitochondria did not display a pulling defect when the model protein $b_2(167)_\Delta$-DHFR was used, whereas mutant mitochondria affected in Pam16 function showed a clear pulling defect for this precursor (Fig. 3 A). Our previous work showed that *pam17Δ* mitochondria displayed a defect in this assay when inner membrane–sorted $b_2(220)$-DHFR was used (van der Laan et al., 2005). Because of the presence of a heme-binding domain, import of this precursor into mitochondria is motor dependent. Interestingly, mitochondria lacking Mgr2 also display protease sensitivity of the accumulated $b_2(220)$-DHFR, caused by an accelerated release

Downloaded from on January 8, 2017

Published December 23, 2016

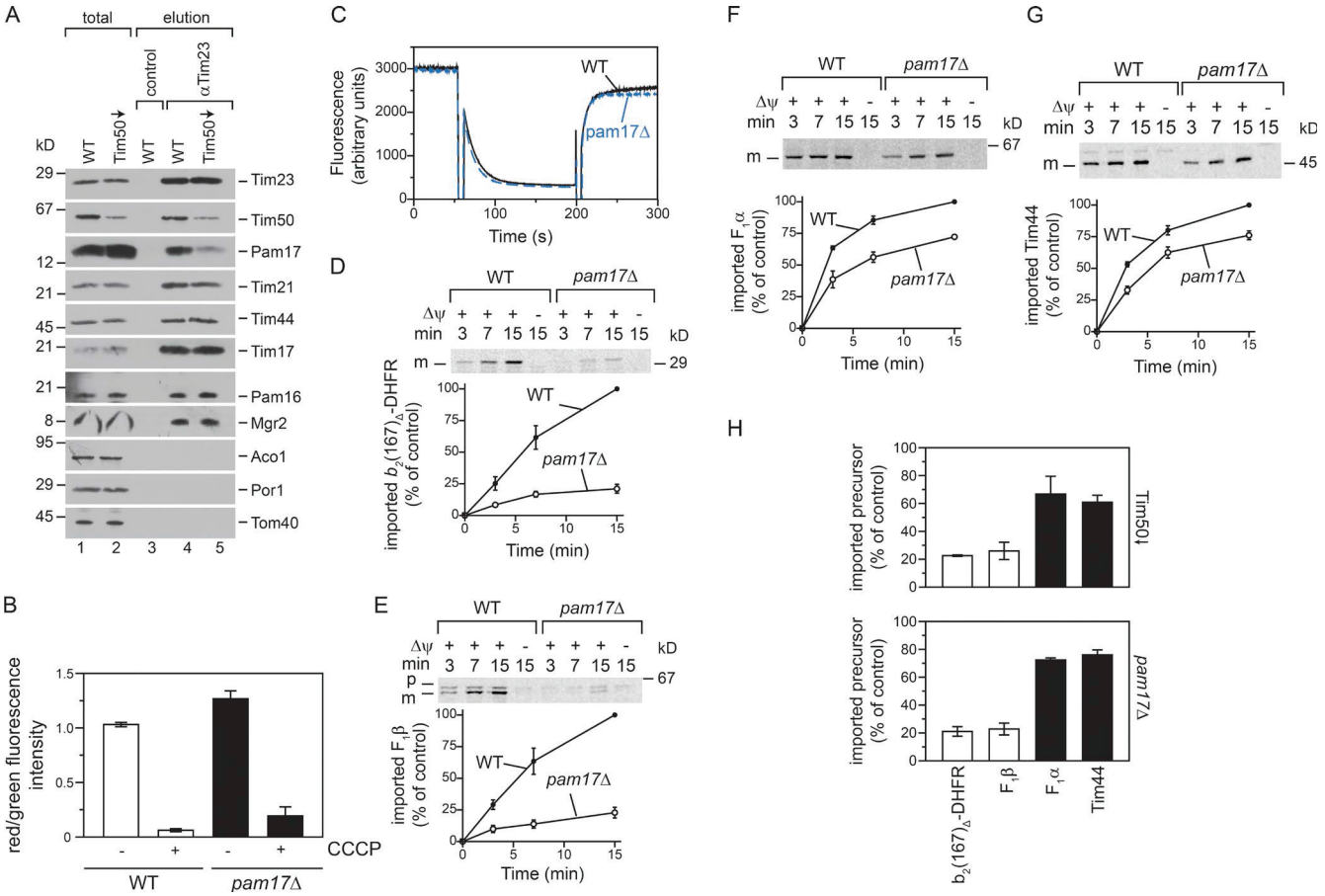

Figure 2. ***pam17Δ* mitochondria display similar import defects as mitochondria lacking Tim50.** (A) WT and Tim50-depleted mitochondria were solubilized with digitonin and subjected to α-Tim23 immunoisolation. Samples were analyzed by Western blotting. Total, 10%; elution, 100%. (B) Quantification of mean red/green fluorescence intensities from WT and *pam17Δ* cells. For each condition, three independent clones were analyzed and 150–1,500 cells were quantified. Results are presented as mean ± SEM. $n = 3$. (C) Δψ of WT and *pam17Δ* mitochondria was assessed as described in Fig. 1 B. (D–G) ^{35}S-labeled precursors were imported as described in Fig. 1 (C–F). p, precursor; m, mature protein. (H) Comparison of import efficiency of indicated ^{35}S-labeled precursors into Tim50-depleted or *pam17Δ* mitochondria after 15 min (results from Fig. 1 [C–F] and D–G).

from the TIM23 complex into the inner membrane (Ieva et al., 2014; Schulz and Rehling, 2014). Surprisingly, Mgr2 levels were strongly reduced in mitochondria lacking Pam17 (Fig. S3 A). Hence, we compared the ability of *mgr2Δ* mitochondria to prevent backsliding of the two precursors $b_2(167)_\Delta$-DHFR and b_2(220)-DHFR. A significant amount of the b_2(220)-DHFR intermediate became protease accessible in *mgr2Δ* mitochondria, whereas the protease sensitivity of $b_2(167)_\Delta$-DHFR was similar in WT and *mgr2Δ* mitochondria (Fig. 3 B; Ieva et al., 2014). We concluded that the apparent pulling defect in *pam17Δ* was likely an indirect defect caused by loss of Mgr2 in these mitochondria.

Pam17 dynamically associates with the TIM23 core complex, and its recruitment is triggered by presequence recognition (Popov-Celeketić et al., 2008; Lytovchenko et al., 2013). However, once a precursor spans the TOM and TIM23 complexes and engages the import motor, Pam17 is released from the translocation intermediate (Fig. S3 B). We asked whether differences between the import efficiencies of Tim44 and $F_1\alpha$, and of $F_1\beta$ and $b_2(167)_\Delta$-DHFR, were caused by distinct properties of their presequences. To test this hypothesis, the presequences of $F_1\alpha$ and $F_1\beta$ were swapped. If the presequence is the determining factor, the import defects should be reversed (Fig. 3 C). However, the presequence swap did not alter the import defects observed in mitochondria lacking either Tim50 or Pam17 (Fig. 3, D and E). Thus, the presequences do not determine the differential Tim50 and Pam17 dependence of the precursors.

Two matrix protein classes display distinct Δψ dependencies

Because a presequence swap between $F_1\alpha$ and $F_1\beta$ did not affect their import properties in *pam17Δ* mitochondria, we investigated other factors that might be responsible for the disparities in import efficiency. Previous analyses demonstrated that the unfolding of precursors did not rescue import into *pam17Δ* mitochondria (Schiller, 2009), indicating that the folding state of the preprotein does not influence its Pam17 dependency. Therefore, we analyzed whether the tested precursors displayed characteristic differences with regard to their Δψ dependence. We imported precursors into isolated mitochondria in the absence or presence of increasing amounts of the protonophore carbonyl cyanide m-chlorophenyl hydrazone (CCCP). For all tested proteins, the import efficiency decreased with lower Δψ, as expected. However, the import of $F_1\alpha$ and Tim44 was significantly more efficient at low Δψ than the import of $F_1\beta$ and $b_2(167)_\Delta$-DHFR (Fig. 4, A–F). Compared with $F_1\alpha$ and Tim44, $F_1\beta$ and $b_2(167)_\Delta$-DHFR displayed Δψ hypersensitivity. Intriguingly, the Δψ-hypersensitive precursors were also Pam17 and

Downloaded from on January 8, 2017

Published December 23, 2016

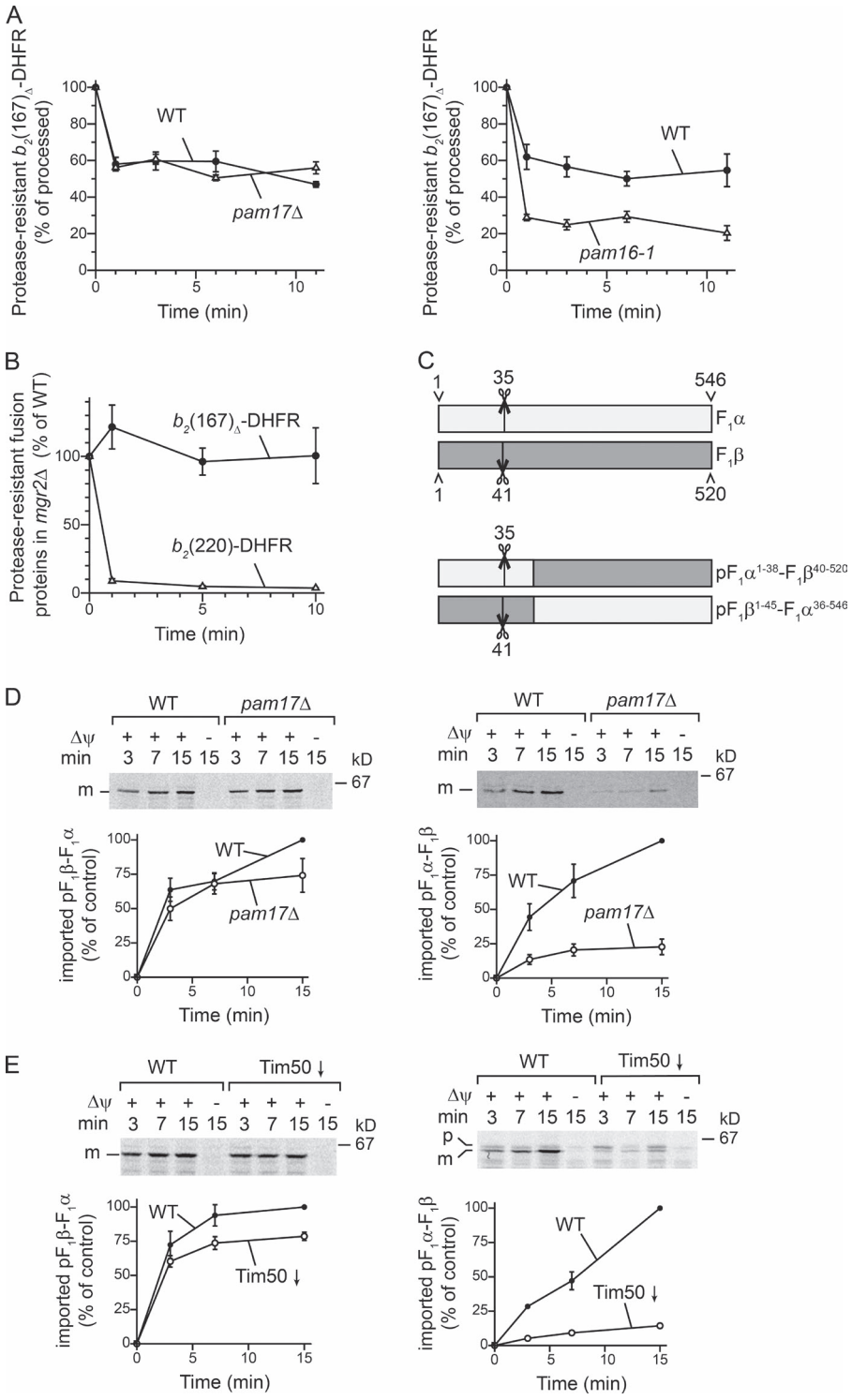

Figure 3. **Pam17 plays a motor-independent role in protein import.** (A and B) The inward driving force of the motor was assessed using ^{35}S-labeled $b_2(167)_\Delta$-DHFR (A and B) or $b_2(220)$-DHFR (B alone) in the presence of MTX. After an initial import reaction, membrane potential was dissipated with valinomycin. The precursor was chased in a second incubation step for indicated time points before PK was added. The amount of processed intermediate was quantified (100%: amount of processed intermediate without protease treatment). Results are presented as mean ± SEM. n = 3. (C) Schematic representation of $F_1\alpha$, $F_1\beta$, $pF_1\alpha$-$F_1\beta$, and $pF_1\beta$-$F_1\alpha$. For $pF_1\alpha$-$F_1\beta$, the first 38 aa of $F_1\alpha$ were fused to the mature part of $F_1\beta$ (40–end). For $pF_1\beta$-$F_1\alpha$, the first 45 aa of $F_1\beta$ were fused to the mature part of $F_1\alpha$ (36–end). (D and E) ^{35}S-labeled $pF_1\alpha$-$F_1\beta$ and $pF_1\beta$-$F_1\alpha$ were imported into isolated mitochondria from indicated strains as described in Fig. 1. p, precursor; m, mature protein.

Tim50 dependent. This effect could also be recapitulated in vivo. When yeast cells were treated with increasing amounts of CCCP to gradually decrease the Δψ, the Pam17-dependent precursor Atp14 accumulated at a lower CCCP concentration than the Pam17-independent precursor of Mdj1 (Fig. S3 C).

The current concepts of presequence-mediated protein import into mitochondria state that the Δψ acts on positively charged residues of the presequence, and thereby drives the initial import of preproteins in an electrophoretic manner until the import motor engages with the preprotein. Accordingly, the Δψ dependence of a precursor should be mainly determined by presequence properties. However, we show that a swap of presequences between $F_1\alpha$ and $F_1\beta$ does not affect the observed import phenotype in mitochondria affected in Pam17 or Tim50 function. We therefore tested whether a presequence swap can reverse Δψ hypersensitivity of the precursor proteins. To this end, we performed CCCP titration experiments for the mature portion of $F_1\beta$ carrying the $F_1\alpha$ presequence ($pF_1\alpha$-$F_1\beta$) and the mature portion of $F_1\alpha$ fused to the presequence of $F_1\beta$ ($pF_1\beta$-$F_1\alpha$). Astonishingly, the presequence did not alter the Δψ dependence

Downloaded from on January 8, 2017

Published December 23, 2016

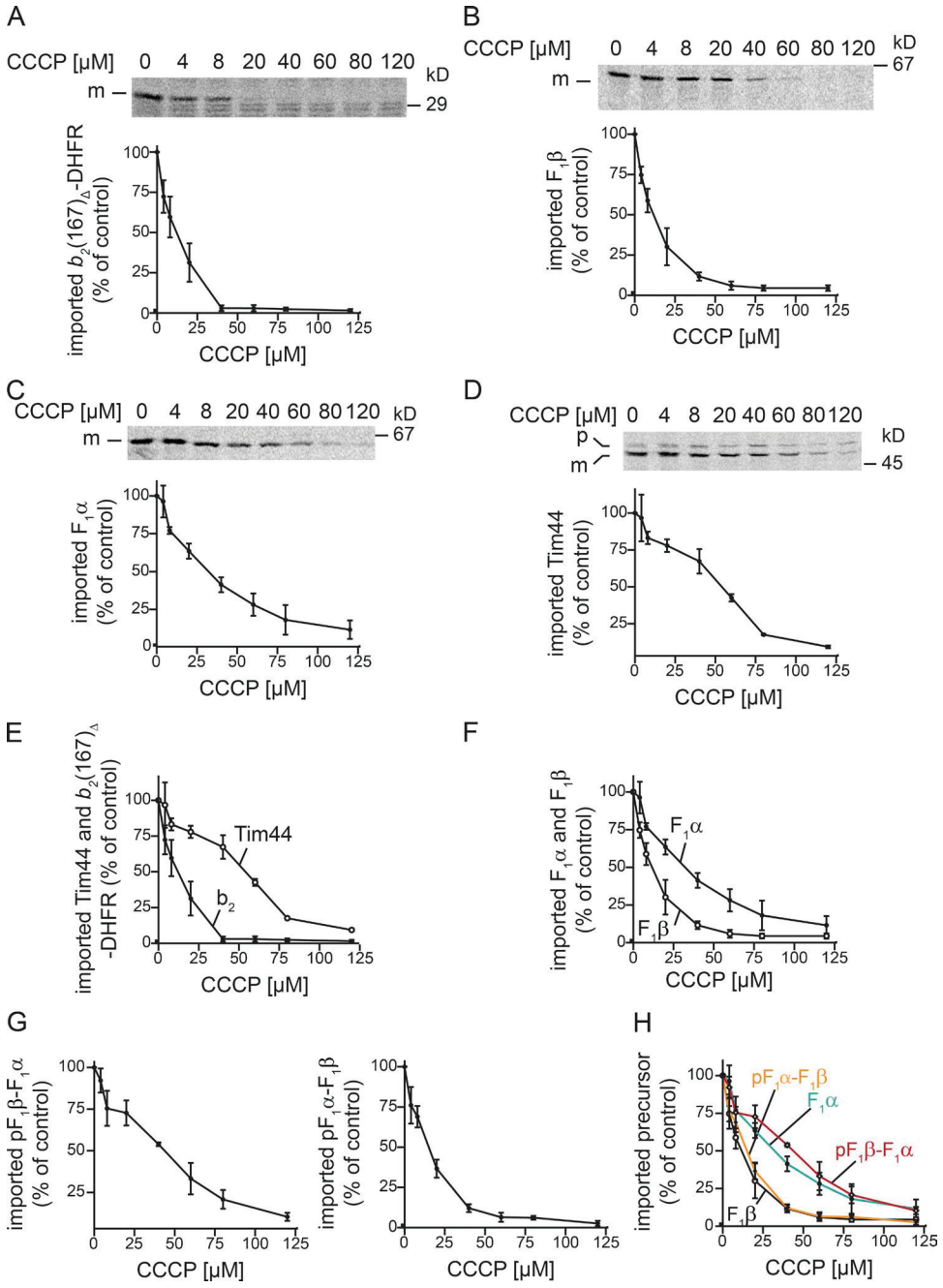

Figure 4. **Import of matrix proteins depends to different extents on membrane potential.** (A–H) Isolated WT mitochondria were treated with the indicated amounts of CCCP for 5 min before import. After 15 min of import, reactions were stopped with AVO, and import was analyzed by SDS-PAGE and digital autoradiography. Results are presented as mean ± SEM. $n = 3$. p, precursor; m, mature protein. (E and F) Overlay of results from CCCP titration experiments with $F_1\alpha$, $F_1\beta$, Tim44, and $b_2(167)_\Delta$-DHFR. (H) Overlay of results from CCCP titration experiments with $F_1\alpha$, $F_1\beta$, $pF_1\alpha$-$F_1\beta$, and $pF_1\beta$-$F_1\alpha$.

of the imported precursor, but rather the mature portion of the polypeptide determined Δψ hypersensitivity (Fig. 4, G and H). To address whether a depletion of the Δψ affects the association of Pam17 with the translocase, we immunoisolated the TIM23 complex in the presence of CCCP. At a concentration of 40 µM, when import of Δψ hypersensitivity precursors is significantly affected, Pam17 remained bound to TIM23 (Fig. S3 D). We also analyzed the association of Pam17 with Tim23 by chemical cross-linking in the presence or absence of Δψ (Hutu et al., 2008). The reported Pam17–Tim23 cross-link was not affected by CCCP addition (Fig. S3 E). Accordingly, the observed Δψ hypersensitivity of precursors is not linked to a dissociation of Pam17 from the import machinery. We conclude that in addition to the universal Δψ-driven translocation of the presequence, a second Δψ-dependent translocation step promotes the transport of the mature portion in a class of mitochondrial matrix proteins.

Discussion

The mitochondrial Δψ is a crucial driving force for inner membrane translocation that acts on precursor proteins in the vicinity

Downloaded from on January 8, 2017

Published December 23, 2016

of the inner membrane. We report that mitochondrial matrix proteins do not display a uniform dependency on Δψ. Although import of some matrix-targeted proteins is already severely impaired when the Δψ is slightly reduced, other precursors are hardly affected until Δψ is strongly compromised. Previous work defined the concept of two energy-dependent translocation stages (Chacinska et al., 2009; Neupert, 2015; Schulz et al., 2015). First, the Δψ acts on the positive charges of the presequence to drive precursor translocation in an electrophoretic manner. Second, mtHsp70 engages with precursors to energize the ATP-dependent unfolding of precursor proteins and their matrix translocation. We now show that the observed Δψ hypersensitivity of the precursors cannot be alleviated by replacement of the presequence with that of a less Δψ-dependent precursor protein. Our findings reveal an unexpected shortcoming in the current concepts of mitochondrial protein import. They confine a critical Δψ dependency also to the mature portion of matrix-targeted proteins. Accordingly, precursor translocation is facilitated by two independent Δψ-driven steps.

We show that Pam17 specifically promotes the transport of Δψ-hypersensitive precursors into the matrix and that the presequence receptor Tim50 is critical for efficient Pam17 recruitment to the TIM23 channel. Consequently, mitochondria affected in Tim50 function mimic the *pam17Δ* phenotype with regard to import defects for Δψ-hypersensitive precursors. Because the Pam17 dependency of precursor proteins is determined by their mature domain and because Tim50 likely contains more than one precursor protein binding site (Qian et al., 2011; Schulz et al., 2011; Lytovchenko et al., 2013; Rahman et al., 2014), it is tempting to speculate that Tim50 may not only interact with presequences, but also with segments of the mature region of precursors. Because there are no specific mutations defined that affect Tim50's interaction with a presequence, the question of whether this domain also acts on the mature part can currently not be assessed experimentally. Our findings suggest that Tim50 may translate information about the nature of the precursor protein into an energy supply requirement. Pam17 has been considered to affect the functionality of the import motor (van der Laan et al., 2005; Hutu et al., 2008; Schiller, 2009). This model is based on matrix protein import defects observed in *pam17Δ* mutant mitochondria and the protease sensitivity of arrested b_2(220)-DHFR (van der Laan et al., 2005). However, in this study, we show that the matrix protein import defect in *pam17Δ* is specific for Δψ-hypersensitive precursors and that the observed protease sensitivity of b_2(220)-DHFR is likely caused by a loss of Mgr2, leading to enhanced lateral release of this precursor into the inner membrane. We therefore conclude that motor function is not rate limiting to the import of matrix proteins in *pam17Δ* mitochondria, but that the matrix protein import defect is linked to a Δψ-sensitive translocation step particularly affecting those precursors that are Δψ hypersensitive.

How does the Δψ affect the transport of Δψ-hypersensitive precursor proteins? Work by Huang et al. (2002) demonstrated that the Δψ participates in the unfolding of the mature portion of precursor proteins. However, this Δψ-mediated unfolding activity has been shown to depend on the precursor's presequence. In line with this, chemical unfolding of the precursor does not alleviate the *pam17Δ* import defect (Schiller, 2009). Accordingly, the Pam17 dependence and Δψ hypersensitivity of precursors does not reflect an increased unfolding requirement during import. Regarding the order of transport events at the presequence translocase, the second Δψ-dependent transport step succeeds a presequence-dependent translocation event, but precedes the motor-requiring transport stages. Pam17 was shown to directly interact with the central core component, Tim23 (Hutu et al., 2008; Popov-Celeketić et al., 2008). Of note, Δψ affects the conformation of the Tim23 protein independently of presequence binding (Malhotra et al., 2013). In this light, we propose that the Tim23 channel gating activity contributes significantly to the passage of Δψ-hypersensitive precursors. This interpretation could link the transport reaction to an unresolved behavior of the Tim23 channel. Although the Tim23 channel is activated by presequences at low Δψ, in the absence of presequences the channel displays a biphasic activity pattern. At low Δψ, the gating activity of the Tim23 channel is low; however, it becomes activated at high Δψ (Truscott et al., 2001; van der Laan et al., 2007). Our analyses are in agreement with the idea that Δψ-hypersensitive precursors especially depend on this second, presequence-independent channel activation step, which may be facilitated by Pam17 recruitment to the import channel.

Materials and methods

Yeast growth and handling

Yeast strains were grown in YP medium (1% yeast extract and 2% peptone) containing 2% glucose (YPD) or 3% glycerol (YPG) at 30°C. *pam17Δ* (van der Laan et al., 2005), *pam16-1* (Frazier et al., 2004), and corresponding WT strains were grown at 25°C, except for the experiment described in Fig. S2 G, for which *pam17Δ* and WT cells were grown at 30°C. *mgr2Δ* and the corresponding WT strain were shifted to 39°C for 24 h before harvesting (Gebert et al., 2012). A strain in which the *TIM50* gene was under the control of a *GAL1* promoter was described previously (Geissler et al., 2002). For down-regulation of Tim50 expression, yeast cells were precultured in YP medium containing 2% galactose, 1% raffinose, and 3% lactate, pH 5.0, and subsequently grown for 38 h at 30°C in YP medium containing 3% lactate, pH 5.0, and 0.2% glucose. In the absence of galactose and presence of glucose, the *GAL1* promoter is repressed. Consequently, Tim50 levels are reduced as a result of protein turnover and cell division.

For the generation of the temperature-sensitive allele *tim50-19*, a plasmid-encoded WT *TIM50* allele was replaced in the corresponding gene deletion strain derived from *S. cerevisiae* YPH499 by gap repair and shuffling of a *TIM50* version obtained by error-prone PCR. Temperature-conditional alleles were selected by comparing the growth of strains at permissive and nonpermissive temperatures. Sequence analysis of the *tim50-19* allele revealed four mutations, K93N in the matrix domain, F345L and W376R in the core domain, and I422V in the C-terminal presequence-binding domain.

For detection of import defects in cells, WT and *pam17Δ* strains were grown in YPD medium at 30°C overnight. The next morning, cells were diluted to OD_{600} = 0.2 and grown for 10 h in YPG at 30°C. Afterward, cells were harvested and cell lysates were analyzed by SDS-PAGE and Western blotting.

Microscopy

To assess mitochondrial membrane potential in cells, yeast strains were grown in YPG medium supplemented with 20 mg/L adenine at 25°C overnight. The next morning, cells were harvested at OD_{600} = 2–3, pelleted, and washed with 10 mM Tris/HCl, pH 6.8. Next, cells were incubated with 20 µM CCCP or the same volume of ethanol for 5 min at 25°C before addition of 2 µM JC-1. After 10 min of incubation at

Downloaded from on January 8, 2017

Published December 23, 2016

25°C, cells were washed three times with 10 mM Tris/HCl, pH 6.8, and analyzed by microscopy.

For this, a 1:25 dilution of cells in a 384-well microtitre plate was automatically imaged at 30°C on an Imaging Machine 03-dual widefield high content screening microscope (Acquifer) equipped with a white light-emitting diode array for brightfield imaging, a light-emitting diode fluorescence excitation light source, an sCMOS (2,048 × 2,048 pixel) camera, a temperature-controlled incubation chamber, and a stationary plate holder in combination with movable optics. Images were acquired in brightfield and with 470-nm and 590-nm filter cubes (exitation 469/35 nm, emission 525/39 nm, and dichroic 497 nm; and exitation 590/20 nm, emission 628/32 nm, and dichroic 607 nm; respectively) with a 40× CFI Super Plan Fluor ELWD NA 0.60 (Nikon). Integration times were fixed at 200 ms for both fluorescence channels. The focal plane was detected in the brightfield channel using a yeast autofocus algorithm.

Fluorescence was quantified using a Knime (Berthold et al., 2009) pipeline to automate segmentation of the individual cells in the brightfield channel, followed by quantification of the mean cell fluorescence in both channels.

Import of precursor proteins

Precursor proteins were radiolabeled by translation in the presence of [^{35}S]methionine using rabbit reticulocyte lysate (Promega). Mitochondria were resuspended in import buffer (250 mM sucrose, 10 mM MOPS/KOH, pH 7.2, 80 mM KCl, 2 mM KH_2PO_4, 5 mM $MgCl_2$, 5 mM methionine, and 3% fatty acid–free BSA) supplemented with 2 mM ATP and 2 mM NADH. Membrane potential was dissipated using a final concentration of 8 µM antimycin A, 1 µM valinomycin, and 20 µM oligomycin. 20-µg/ml PK treatment was performed for 10 min on ice. 2 mM PMSF was added for 10 min on ice to inactivate PK. Mitochondria were sedimented, washed with SEM (250 mM sucrose, 1 mM EDTA, and 20 mM MOPS, pH 7.2) and further analyzed by SDS-PAGE and autoradiography. Quantifications were performed using ImageQuant TL (GE Healthcare) using a rolling ball background subtraction.

Protein complex isolation

Coimmunoprecipitation experiments using Tim23-specific serum were performed essentially as described previously (Herrmann et al., 2001). In brief, mitochondria were resuspended to 1 mg/ml in solubilization buffer (20 mM Tris/HCl, pH 7.4, 150 mM NaCl, 10% glycerol [wt/vol], 1 mM PMSF, and 1% digitonin) and incubated for 30 min on ice. After a clarifying spin, supernatant was loaded on protein A–Sepharose beads cross-linked to Tim23 antibodies, incubated for 1.5 h at 4°C on a rotating wheel, washed 10× (solubilization buffer with 0.3% digitonin), and eluted with a 50-µl double-bed volume of 0.1 M glycine, pH 2.8 (neutralized with 1-M Tris base). To address Pam17 association with the TIM23 complex at low membrane potential, mitochondria were incubated with CCCP in solubilization buffer lacking digitonin for 5 min on ice before solubilization with 1% (wt/vol) digitonin and coimmunoprecipitation.

Membrane potential measurements

Mitochondrial membrane potential was assessed using 3,3′-dipropylthiadicarbocyanine iodide ($DiSC_3(5)$). Mitochondria were suspended in buffer containing 600 mM sorbitol, 1% (wt/vol) BSA, 10 mM $MgCl_2$, and 20 mM KPi, pH 7.4, to a concentration of 166 µg/ml. Changes in fluorescence were recorded using a F-7000 fluorescence spectrophotometer (Hitachi) at 25°C with excitation at 622 nm, emission at 670 nm, and slits of 5 nm. Components were added to the cuvette containing 500 µl of buffer in the following order: $DiSC_3(5)$, 83 µg of mitochondria, and valinomycin (5 µl from 100-µM stock in EtOH, 1 µM final) to dissipate the membrane potential. The difference in fluorescence before and after the addition of valinomycin was used to compare relative membrane potential between strains.

Cloning

Presequence swap of *Neurospora crassa* $F_1\beta$ and *S. cerevisiae* $F_1\alpha$ was performed by overlap PCR. For $pF_1\alpha$-$F_1\beta$, the first 38 aa of yeast $F_1\alpha$ were fused to the mature part of *N. crassa* $F_1\beta$ (40–end). For $pF_1\beta$-$F_1\alpha$, the first 45 aa of $F_1\beta$ were fused to the mature part of $F_1\alpha$ (36–end).

Assessing import-driving activity

Import-driving activity was assessed as previously described (Voisine et al., 1999). For import experiments, temperature-sensitive strains were incubated in import buffer for 15 min at 37°C, and subsequently 2 mM ATP, 2 mM NADH, 5 mM creatine phosphate, and 0.01 mg/ml creatine kinase were added. Radiolabeled $b_2(167)_\Delta$-DHFR was imported at 25°C for 15 min in the presence of 5 µM MTX, and membrane potential was dissipated using 1 µM valinomycin. A sample was taken ($\Delta t = 0$ min), the precursor was chased at 25°C, and samples were treated with PK after 1, 3, 6, and 11 min for 15 min on ice. Samples were analyzed by SDS-PAGE and autoradiography. The amount of PK-resistant intermediate was quantified and standardized to the total amount of generated intermediate ($\Delta t = 0$) for each strain.

Membrane potential reduction by CCCP titration

For reduction of membrane potential, the protonophore CCCP was used as previously reported (van der Laan et al., 2006). Mitochondria were resuspended in import buffer with 1% BSA and 20 µM oligomycin to prevent regeneration of membrane potential by the reverse function of the F_1F_o-ATPase. CCCP was added from a 4 mM stock in EtOH, and mitochondria were incubated for 5 min at 25°C before import.

For in vivo CCCP titration, cells were grown at 30°C overnight in YPD medium. The next day, cells were diluted to $OD_{600} = 0.5$ in 2× YPAD, and grown for another 5 h. Then, cells were diluted back to $OD_{600} = 1$ in 2× YPAD, and CCCP was added from a 50 mM stock solution. After 30 min of incubation, cells were harvested and cell lysates were analyzed by SDS-PAGE and Western blotting. For quantification, the amount of accumulated precursor at 80 µM CCCP was set to 100%.

Chemical cross-linking

For cross-linking, mitochondria were resuspended in import buffer without BSA to a final concentration of 1 mg/ml. CCCP was added from a 5 mM stock solution, and mitochondria were incubated for 5 min on ice. Next, disuccinimidyl glutarate in DMSO was added to a final concentration of 500 µM, and mitochondria were incubated for 30 min on ice. Afterward, excess cross-linker was quenched using 100 mM glycine, pH 8.0, for 10 min on ice. After reisolation of mitochondria, cross-links were analyzed by SDS-PAGE and Western blotting.

Generation and isolation of the TIM23–TOM supercomplex

A TIM23–TOM supercomplex was isolated essentially as described previously (Chacinska et al., 2003). In brief, recombinant $b_2(167)_\Delta$-DHFR was imported into mitochondria in import buffer with BSA in the presence of 5 µM MTX for 15 min at 25°C. Next, mitochondria were reisolated, washed with SEM, resuspended to 1 mg/ml in solubilization buffer (20 mM Tris/HCl, pH 7.4, 150 mM NaCl, 10% glycerol [wt/vol], 1 mM PMSF, and 1% digitonin), and incubated for 30 min on ice. After a clarifying spin, complexes were isolated by incubating lysates with Tim23- or Tom22-specific antibodies coupled to protein A–Sepharose beads. Beads were washed 10× with solubilization buffer containing 0.3% (wt/vol) digitonin and eluted with 100 mM glycine, pH 2.8.

Downloaded from on January 8, 2017

Published December 23, 2016

Isolation of mitochondria

Mitochondria were isolated essentially as previously described (Meisinger et al., 2006). If not stated otherwise, yeast cells were grown in YPG medium and harvested at OD_{600} = 2–3. After treatment with buffer A (10 mM DTT and 100 mM Tris/H_2SO_4, pH 9.4) for 30 min at 30°C, cells were washed and treated with zymolyase buffer (20 mM KPO_4, pH 7.4, 1.2 M sorbitol, and 0.57 mg/L zymolyase) for 1–2 h at 30°C. After additional washing in zymolyase buffer without enzyme, cells were resuspended in ice-cold homogenization buffer (600 mM sorbitol, 10 mM Tris/HCl, pH 7.4, 1 g/L BSA, 1 mM PMSF, and 1 mM EDTA) and opened using a cell homogenizer. The mitochondrial fraction was obtained by differential centrifugation, resuspended in SEM buffer, and frozen in liquid nitrogen.

Online supplemental material

Fig. S1 shows corresponding import experiments to Fig. 1 in *tim50-19* mitochondria. Moreover, in vivo membrane potential assessment in *pam17Δ* cells and WT cells are shown. Fig. S2 shows precursor imports in *pam17Δ* mitochondria and in vivo precursor accumulation, extending Fig. 2 (D–G). Also, $F_1\alpha$ and $F_1\beta$ imports in *ssc1-3* mitochondria show that both precursors are to the same extent motor dependent for import. Fig. S3 relates to Fig. 3 and shows steady-state protein analysis of *pam17Δ* mitochondria and the Pam17 association with the TIM23 complex when a precursor spans both TOM and TIM23 complexes. Fig. S3 also shows in vivo CCCP titration and Pam17 association with the TIM23 complex under low-membrane potential conditions supporting data in Fig. 4.

Acknowledgments

We thank M. Meinecke for discussion, S. Callegari for critical reading, and Á. Farkas for support in data analyses.

This work was supported by the Deutsche Forschungsgemeinschaft (DFG) grants SFB860 to P. Rehling, SFB746 to M. van der Laan, and SFB1190/Z03 to A. Clancy. This work was also supported by the Molecular Biology PhD program at the International Max Planck Research School and Göttingen Graduate School for Neurosciences and Molecular Biosciences DFG grant GSC 226/1 to A.B. Schendzielorz and C. Schulz, the Excellence Initiative of the German federal and state governments EXC 294 BIOSS grant to M. van der Laan, the Centre National de la Recherche Scientifique–Institut National de la Santé et de la Recherche Médicale ATIP-Avenir program grant to R. Ieva, Boehringer Ingelheim Fonds grant to C. Schulz, and the Max Planck Society (to P. Rehling).

The authors declare no competing financial interests.

Submitted: 18 July 2016
Revised: 30 September 2016
Accepted: 28 November 2016

References

Berthold, M.R., N. Cebron, F. Dill, T.R. Gabriel, T. Kötter, T. Meinl, P. Ohl, K. Thiel, and B. Wiswedel. 2009. KNIME - the konstanz information miner: version 2.0 and beyond. *SIGKDD Explor.* 11:26–31. http://dx.doi.org/10.1145/1656274.1656280

Chacinska, A., P. Rehling, B. Guiard, A.E. Frazier, A. Schulze-Specking, N. Pfanner, W. Voos, and C. Meisinger. 2003. Mitochondrial translocation contact sites: separation of dynamic and stabilizing elements in formation of a TOM-TIM-preprotein supercomplex. *EMBO J.* 22:5370–5381. http://dx.doi.org/10.1093/emboj/cdg532

Chacinska, A., C.M. Koehler, D. Milenkovic, T. Lithgow, and N. Pfanner. 2009. Importing mitochondrial proteins: machineries and mechanisms. *Cell.* 138:628–644. http://dx.doi.org/10.1016/j.cell.2009.08.005

D'Silva, P.D., B. Schilke, W. Walter, A. Andrew, and E.A. Craig. 2003. J protein cochaperone of the mitochondrial inner membrane required for protein import into the mitochondrial matrix. *Proc. Natl. Acad. Sci. USA.* 100:13839–13844. http://dx.doi.org/10.1073/pnas.1936150100

Endo, T., and K. Yamano. 2010. Transport of proteins across or into the mitochondrial outer membrane. *Biochim. Biophys. Acta.* 1803:706–714. http://dx.doi.org/10.1016/j.bbamcr.2009.11.007

Frazier, A.E., J. Dudek, B. Guiard, W. Voos, Y. Li, M. Lind, C. Meisinger, A. Geissler, A. Sickmann, H.E. Meyer, et al. 2004. Pam16 has an essential role in the mitochondrial protein import motor. *Nat. Struct. Mol. Biol.* 11:226–233. http://dx.doi.org/10.1038/nsmb735

Gebert, M., S.G. Schrempp, C.S. Mehnert, A.K. Heißwolf, S. Oeljeklaus, R. Ieva, M. Bohnert, K. von der Malsburg, S. Wiese, T. Kleinschroth, et al. 2012. Mgr2 promotes coupling of the mitochondrial presequence translocase to partner complexes. *J. Cell Biol.* 197:595–604. http://dx.doi.org/10.1083/jcb.201110047

Geissler, A., A. Chacinska, K.N. Truscott, N. Wiedemann, K. Brandner, A. Sickmann, H.E. Meyer, C. Meisinger, N. Pfanner, and P. Rehling. 2002. The mitochondrial presequence translocase: an essential role of Tim50 in directing preproteins to the import channel. *Cell.* 111:507–518. http://dx.doi.org/10.1016/S0092-8674(02)01073-5

Herrmann, J.M., B. Westermann, and W. Neupert. 2001. Analysis of protein–protein interactions in mitochondria by coimmunoprecipitation and chemical cross-linking. *Methods Cell Biol.* 65:217–230. http://dx.doi.org/10.1016/S0091-679X(01)65013-1

Huang, S., K.S. Ratliff, and A. Matouschek. 2002. Protein unfolding by the mitochondrial membrane potential. *Nat. Struct. Biol.* 9:301–307. http://dx.doi.org/10.1038/nsb772

Hutu, D.P., B. Guiard, A. Chacinska, D. Becker, N. Pfanner, P. Rehling, and M. van der Laan. 2008. Mitochondrial protein import motor: differential role of Tim44 in the recruitment of Pam17 and J-complex to the presequence translocase. *Mol. Biol. Cell.* 19:2642–2649. http://dx.doi.org/10.1091/mbc.E07-12-1226

Ieva, R., S.G. Schrempp, L. Opaliński, F. Wollweber, P. Höß, A.K. Heißwolf, M. Gebert, Y. Zhang, B. Guiard, S. Rospert, et al. 2014. Mgr2 functions as lateral gatekeeper for preprotein sorting in the mitochondrial inner membrane. *Mol. Cell.* 56:641–652. http://dx.doi.org/10.1016/j.molcel.2014.10.010

Kozany, C., D. Mokranjac, M. Sichting, W. Neupert, and K. Hell. 2004. The J domain–related cochaperone Tim16 is a constituent of the mitochondrial TIM23 preprotein translocase. *Nat. Struct. Mol. Biol.* 11:234–241. http://dx.doi.org/10.1038/nsmb734

Liu, Q., P. D'Silva, W. Walter, J. Marszalek, and E.A. Craig. 2003. Regulated cycling of mitochondrial Hsp70 at the protein import channel. *Science.* 300:139–141. http://dx.doi.org/10.1126/science.1083379

Lytovchenko, O., J. Melin, C. Schulz, M. Kilisch, D.P. Hutu, and P. Rehling. 2013. Signal recognition initiates reorganization of the presequence translocase during protein import. *EMBO J.* 32:886–898. http://dx.doi.org/10.1038/emboj.2013.23

Malhotra, K., M. Sathappa, J.S. Landin, A.E. Johnson, and N.N. Alder. 2013. Structural changes in the mitochondrial Tim23 channel are coupled to the proton-motive force. *Nat. Struct. Mol. Biol.* 20:965–972. http://dx.doi.org/10.1038/nsmb.2613

Mapa, K., M. Sikor, V. Kudryavtsev, K. Waegemann, S. Kalinin, C.A.M. Seidel, W. Neupert, D.C. Lamb, and D. Mokranjac. 2010. The conformational dynamics of the mitochondrial Hsp70 chaperone. *Mol. Cell.* 38:89–100. http://dx.doi.org/10.1016/j.molcel.2010.03.010

Martin, J., K. Mahlke, and N. Pfanner. 1991. Role of an energized inner membrane in mitochondrial protein import. Delta psi drives the movement of presequences. *J. Biol. Chem.* 266:18051–18057.

Meinecke, M., R. Wagner, P. Kovermann, B. Guiard, D.U. Mick, D.P. Hutu, W. Voos, K.N. Truscott, A. Chacinska, N. Pfanner, and P. Rehling. 2006. Tim50 maintains the permeability barrier of the mitochondrial inner membrane. *Science.* 312:1523–1526. http://dx.doi.org/10.1126/science.1127628

Meisinger, C., N. Pfanner, and K.N. Truscott. 2006. Isolation of yeast mitochondria. *Methods Mol. Biol.* 313:33–39.

Neupert, W. 2015. A perspective on transport of proteins into mitochondria: a myriad of open questions. *J. Mol. Biol.* 427:1135–1158. http://dx.doi.org/10.1016/j.jmb.2015.02.001

Neupert, W., and M. Brunner. 2002. The protein import motor of mitochondria. *Nat. Rev. Mol. Cell Biol.* 3:555–565. http://dx.doi.org/10.1038/nrm878

Downloaded from on January 8, 2017

Published December 23, 2016

Neupert, W., and J.M. Herrmann. 2007. Translocation of proteins into mitochondria. *Annu. Rev. Biochem.* 76:723–749. http://dx.doi.org/10.1146/annurev.biochem.76.052705.163409

Popov-Celeketić, D., K. Mapa, W. Neupert, and D. Mokranjac. 2008. Active remodelling of the TIM23 complex during translocation of preproteins into mitochondria. *EMBO J.* 27:1469–1480.

Qian, X., M. Gebert, J. Höpker, M. Yan, J. Li, N. Wiedemann, M. van der Laan, N. Pfanner, and B. Sha. 2011. Structural basis for the function of Tim50 in the mitochondrial presequence translocase. *J. Mol. Biol.* 411:513–519. http://dx.doi.org/10.1016/j.jmb.2011.06.020

Rahman, B., S. Kawano, K. Yunoki-Esaki, T. Anzai, and T. Endo. 2014. NMR analyses on the interactions of the yeast Tim50 C-terminal region with the presequence and Tim50 core domain. *FEBS Lett.* 588:678–684. http://dx.doi.org/10.1016/j.febslet.2013.12.037

Roise, D., and G. Schatz. 1988. Mitochondrial presequences. *J. Biol. Chem.* 263:4509–4511.

Schiller, D. 2009. Pam17 and Tim44 act sequentially in protein import into the mitochondrial matrix. *Int. J. Biochem. Cell Biol.* 41:2343–2349. http://dx.doi.org/10.1016/j.biocel.2009.06.011

Schleyer, M., B. Schmidt, and W. Neupert. 1982. Requirement of a membrane potential for the posttranslational transfer of proteins into mitochondria. *Eur. J. Biochem.* 125:109–116. http://dx.doi.org/10.1111/j.1432-1033.1982.tb06657.x

Schulz, C., and P. Rehling. 2014. Remodelling of the active presequence translocase drives motor-dependent mitochondrial protein translocation. *Nat. Commun.* 5. http://dx.doi.org/10.1038/ncomms5349

Schulz, C., O. Lytovchenko, J. Melin, A. Chacinska, B. Guiard, P. Neumann, R. Ficner, O. Jahn, B. Schmidt, and P. Rehling. 2011. Tim50's presequence receptor domain is essential for signal driven transport across the TIM23 complex. *J. Cell Biol.* 195:643–656. http://dx.doi.org/10.1083/jcb.201105098

Schulz, C., A. Schendzielorz, and P. Rehling. 2015. Unlocking the presequence import pathway. *Trends Cell Biol.* 25:265–275. http://dx.doi.org/10.1016/j.tcb.2014.12.001

Truscott, K.N., P. Kovermann, A. Geissler, A. Merlin, M. Meijer, A.J. Driessen, J. Rassow, N. Pfanner, and R. Wagner. 2001. A presequence- and voltage-sensitive channel of the mitochondrial preprotein translocase formed by Tim23. *Nat. Struct. Biol.* 8:1074–1082. http://dx.doi.org/10.1038/nsb726

Truscott, K.N., W. Voos, A.E. Frazier, M. Lind, Y. Li, A. Geissler, J. Dudek, H. Müller, A. Sickmann, H.E. Meyer, et al. 2003. A J-protein is an essential subunit of the presequence translocase-associated protein import motor of mitochondria. *J. Cell Biol.* 163:707–713. http://dx.doi.org/10.1083/jcb.200308004

Turakhiya, U., K. von der Malsburg, V.A.M. Gold, B. Guiard, A. Chacinska, M. van der Laan, and R. Ieva. 2016. Protein import by the mitochondrial presequence translocase in the absence of a membrane potential. *J. Mol. Biol.* 428:1041–1052. http://dx.doi.org/10.1016/j.jmb.2016.01.020

Ungermann, C., W. Neupert, and D.M. Cyr. 1994. The role of Hsp70 in conferring unidirectionality on protein translocation into mitochondria. *Science.* 266:1250–1253. http://dx.doi.org/10.1126/science.7973708

van der Laan, M., A. Chacinska, M. Lind, I. Perschil, A. Sickmann, H.E. Meyer, B. Guiard, C. Meisinger, N. Pfanner, and P. Rehling. 2005. Pam17 is required for architecture and translocation activity of the mitochondrial protein import motor. *Mol. Cell. Biol.* 25:7449–7458. http://dx.doi.org/10.1128/MCB.25.17.7449-7458.2005

van der Laan, M., N. Wiedemann, D.U. Mick, B. Guiard, P. Rehling, and N. Pfanner. 2006. A role for Tim21 in membrane-potential-dependent preprotein sorting in mitochondria. *Curr. Biol.* 16:2271–2276. http://dx.doi.org/10.1016/j.cub.2006.10.025

van der Laan, M., M. Meinecke, J. Dudek, D.P. Hutu, M. Lind, I. Perschil, B. Guiard, R. Wagner, N. Pfanner, and P. Rehling. 2007. Motor-free mitochondrial presequence translocase drives membrane integration of preproteins. *Nat. Cell Biol.* 9:1152–1159. http://dx.doi.org/10.1038/ncb1635

Vögtle, F.-N., S. Wortelkamp, R.P. Zahedi, D. Becker, C. Leidhold, K. Gevaert, J. Kellermann, W. Voos, A. Sickmann, N. Pfanner, and C. Meisinger. 2009. Global analysis of the mitochondrial N-proteome identifies a processing peptidase critical for protein stability. *Cell.* 139:428–439. http://dx.doi.org/10.1016/j.cell.2009.07.045

Voisine, C., E.A. Craig, N. Zufall, O. von Ahsen, N. Pfanner, and W. Voos. 1999. The protein import motor of mitochondria: unfolding and trapping of preproteins are distinct and separable functions of matrix Hsp70. *Cell.* 97:565–574. http://dx.doi.org/10.1016/S0092-8674(00)80768-0

Downloaded from on January 8, 2017

Schendzielorz et al., https://doi.org/10.1083/jcb.201607066

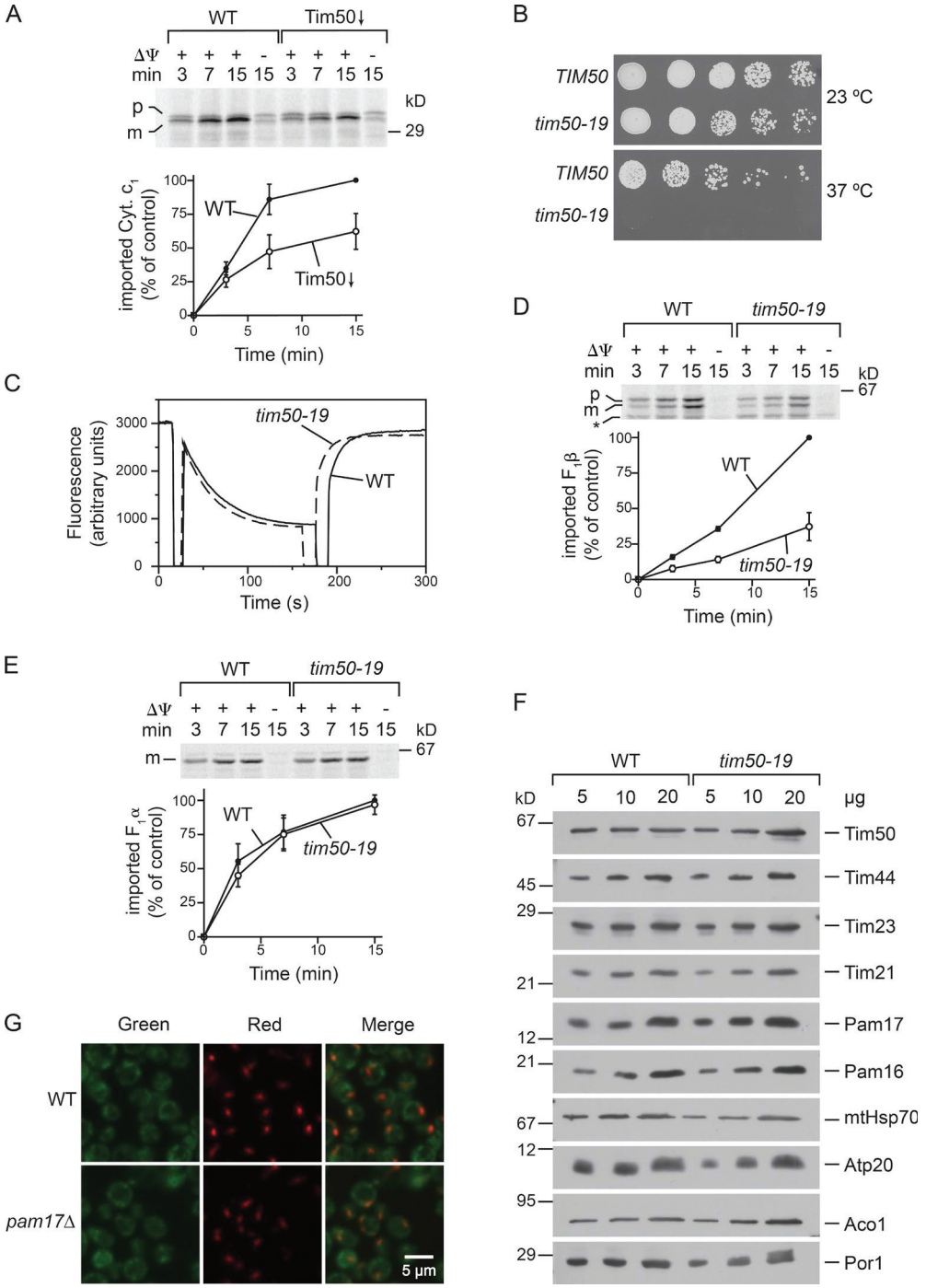

Figure S1. **Corresponding import experiments to Fig. 1 in *tim50-19* mitochondria.** (A) ^{35}S-labeled precursor was imported as described in Fig. 1 for the indicated times. After stopping the import reaction with AVO, all samples were PK treated and analyzed by SDS-PAGE and digital autoradiography. (B) Serial dilutions of WT and *tim50-19* cells were spotted onto YPD medium and incubated at 23°C or 37°C. (C) Membrane potential of WT and *tim50-19* mitochondria was assessed as described in Figs. 1 and 2. (D and E) Isolated mitochondria were incubated for 15 min at a nonpermissive temperature before import of ^{35}S-labeled precursors for the indicated times. After stopping import, all samples were PK treated and analyzed by SDS-PAGE and digital autoradiography. The asterisk indicates an unspecific degradation product. (A, D, and E) Results are presented as mean ± SEM. $n = 3$. p, precursor; m, mature protein. (F) Steady-state Western blot analysis of mitochondria isolated from WT and *tim50-19*. (G) WT and *pam17Δ* cells were grown in YPG medium at 25°C overnight. To analyze mitochondrial membrane potential, cells were harvested and incubated with 20 µM CCCP or the same volume of ethanol for 5 min at 25°C before the addition of 2 µM JC-1 for 10 min at 25°C. JC-1 accumulates in a membrane potential–dependent manner in mitochondria and changes its emission spectrum from green to red light.

THE JOURNAL OF CELL BIOLOGY

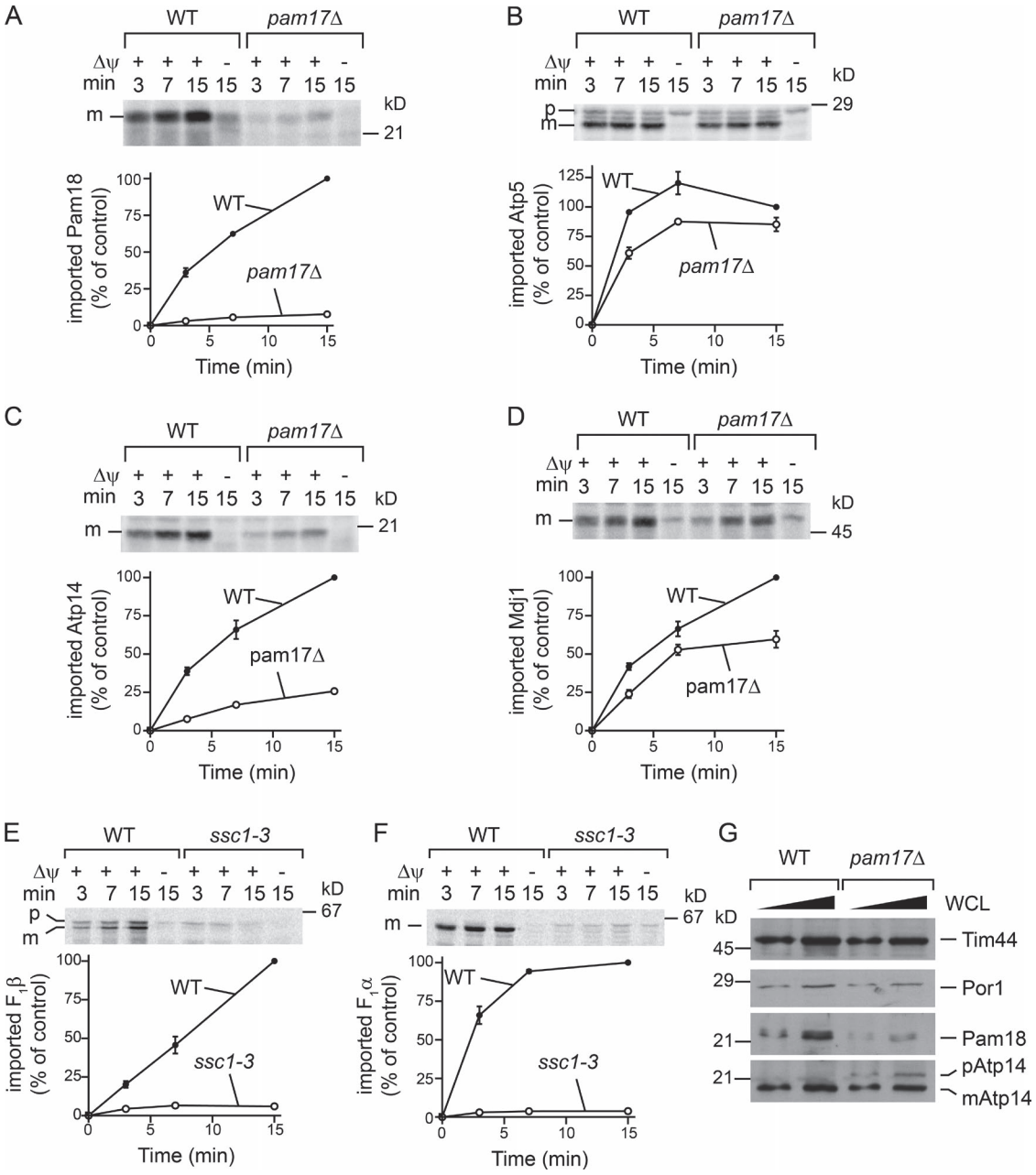

Figure S2. **Protein import is impaired in *pam17Δ* mitochondria and cells.** (A–D) ^{35}S-labeled precursors were imported into isolated mitochondria as described in Fig. 1. After 15 min of import, reactions were stopped and import was analyzed by SDS-PAGE and autoradiography. Results are presented as mean ± SEM. *n* = 3. (E and F) Mitochondria were incubated at 37°C for 15 min, and import was performed as described in A–D. p, precursor; m, mature protein. (G) To assess mitochondrial precursor accumulation in cells, WT and *pam17Δ* cells were grown overnight in YPD medium at 30°C. Cells were diluted in YPG medium and grown for 10 h. Subsequently, cells were harvested and cell lysates were analyzed by SDS-PAGE and Western blotting. WCL, whole cell lysate amount.

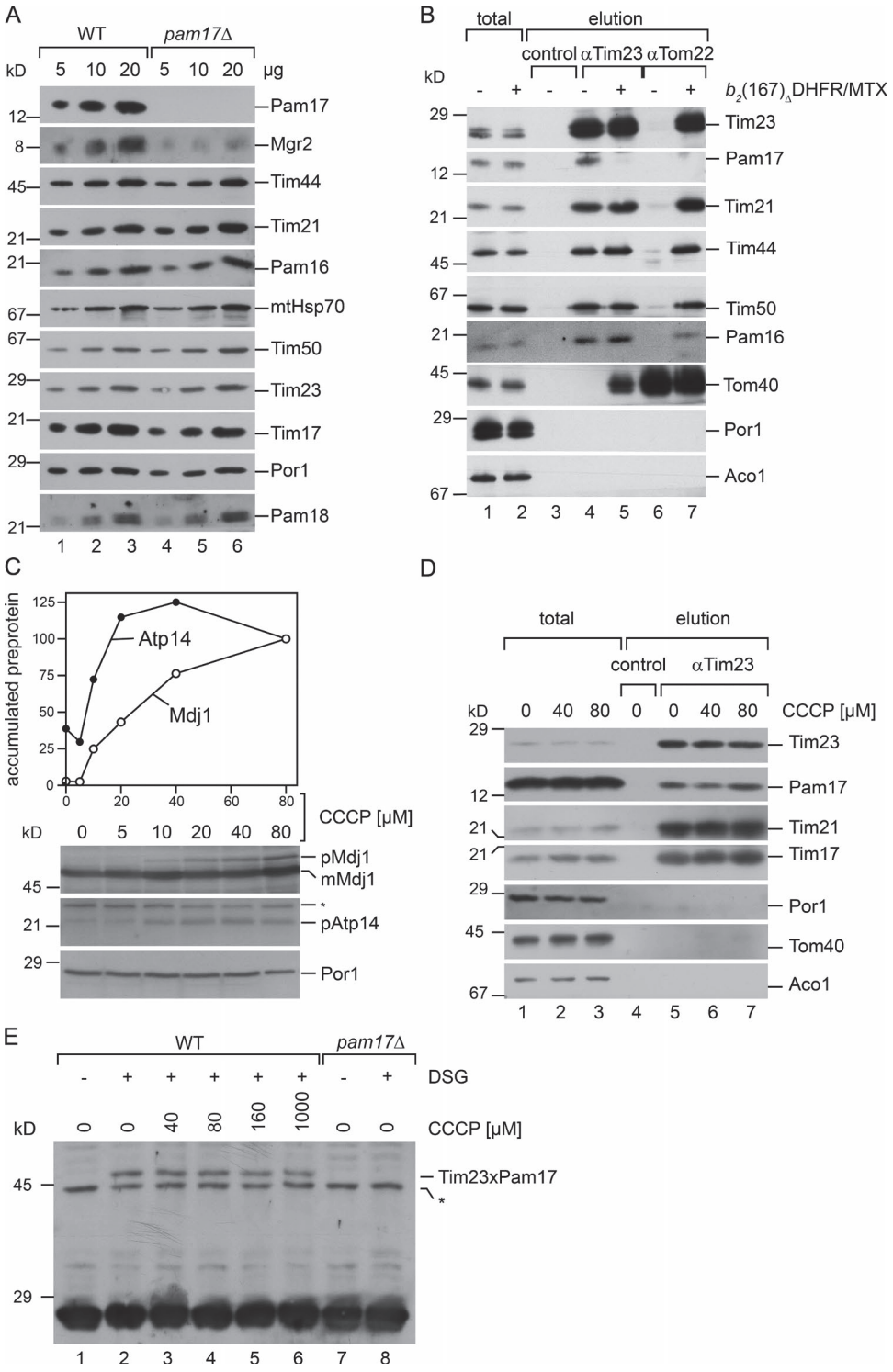

Figure S3. **Pam17 is not part of the active motor complex, and its association with TIM23 complex is not Δψ dependent.** (A) Steady-state Western blot analysis of mitochondria isolated from WT and *pam17Δ*. (B) Mitochondria were incubated in import buffer with or without b_2(167)Δ-DHFR and MTX for 15 min at 25°C. Afterward, mitochondria were solubilized in digitonin, and TIM23 and TOM complexes were immunoisolated using Tim23- and Tom22-specific antibodies, respectively. Total (5%) and elution fractions were analyzed by SDS-PAGE and Western blotting. (C) Cells were grown overnight at 30°C. After dilution, cells were grown for an additional 5 h in 2× YPAD medium at 30°C. Cell amounts were adjusted to OD_{600} = 1, and indicated amounts of CCCP were added for 30 min at 30°C. Cells were harvested and lysed before analysis by Western blotting. The amounts of Mdj1- and Atp14-accumulated precursors were quantified and plotted as percentages of accumulated precursors at 80 µM CCCP. The asterisk indicates a nonspecific cross-reaction band. *n* = 1. (D) Mitochondria were resuspended in solubilization buffer without digitonin and treated with the indicated amounts of CCCP for 5 min on ice. Afterward, digitonin was added and the TIM23 complex was isolated using Tim23-specific antibodies. Total (10%) and elution fractions were analyzed by SDS-PAGE and Western blotting. (E) Isolated mitochondria were incubated with indicated amounts of CCCP for 5 min before cross-linking with the amino group–specific cross-linker disuccinimidyl glutarate (DSG). After quenching of the cross-linker with glycine, mitochondria were reisolated and analyzed by SDS-PAGE and Western blotting. The asterisk indicates the nonspecific signal of the antibody.

2.2 Manuscript 2: Cation selectivity of the presequence translocase Tim23 is crucial for efficient protein import

eLIFE elifesciences.org

RESEARCH ARTICLE

Cation selectivity of the presequence translocase channel Tim23 is crucial for efficient protein import

Niels Denkert[1†], Alexander Benjamin Schendzielorz[1†], Mariam Barbot[1], Lennart Versemann[1], Frank Richter[1], Peter Rehling[1,2,3*], Michael Meinecke[1,3,4*]

[1]Department of Cellular Biochemistry, University Medical Center Göttingen, Göttingen, Germany; [2]Max Planck Institute for Biophysical Chemistry, Göttingen, Germany; [3]Göttinger Zentrum für Molekulare Biowissenschaften, Göttingen, Germany; [4]European Neuroscience Institute Göttingen, Göttingen, Germany

Abstract Virtually all mitochondrial matrix proteins and a considerable number of inner membrane proteins carry a positively charged, N-terminal presequence and are imported by the TIM23 complex (presequence translocase) located in the inner mitochondrial membrane. The voltage-regulated Tim23 channel constitutes the actual protein-import pore wide enough to allow the passage of polypeptides with a secondary structure. In this study, we identify amino acids important for the cation selectivity of Tim23. Structure based mutants show that selectivity is provided by highly conserved, pore-lining amino acids. Mutations of these amino acid residues lead to reduced selectivity properties, reduced protein import capacity and they render the Tim23 channel insensitive to substrates. We thus show that the cation selectivity of the Tim23 channel is a key feature for substrate recognition and efficient protein import.
DOI: https://doi.org/10.7554/eLife.28324.001

***For correspondence:** peter.rehling@medizin.uni-goettingen.de (PR); michael.meinecke@med.uni-goettingen.de (MM)

[†]These authors contributed equally to this work

Competing interests: The authors declare that no competing interests exist.

Funding: See page 13

Received: 03 May 2017
Accepted: 31 July 2017

Reviewing editor: Nikolaus Pfanner, University of Freiburg, Germany

© Copyright Denkert et al. This article is distributed under the terms of the Creative Commons Attribution License, which permits unrestricted use and redistribution provided that the original author and source are credited.

Introduction

Double membrane bounded mitochondria import over 1000 different proteins synthesized on cytosolic ribosomes (***Endo and Yamano, 2009***; ***Neupert and Herrmann, 2007***; ***Schmidt et al., 2010***). Different targeting signals direct the proteins into one of the four mitochondrial sub-compartments: outer membrane (OM), intermembrane space (IMS), inner membrane (IM) and matrix. Approximately, 70% of these mitochondrial proteins are synthesized with an N-terminal presequence (***Vögtle et al., 2009***), which directs them across the OM. Once threaded through the OM, the presequence directs preproteins to the presequence translocase (TIM23 complex), located in the inner boundary membrane (***Barbot and Meinecke, 2016***; ***Chacinska et al., 2005***). The TIM23 complex transports precursor proteins across the inner membrane, or, if they contain additional sorting signals, inserts them into the IM (***Neupert and Herrmann, 2007***; ***van der Laan et al., 2007***). The membrane potential ($\Delta\Psi$) across the energy coupling inner membrane exerts an electrophoretic force on the positively charged presequences, thereby providing energy for the translocation of preproteins. $\Delta\Psi$ is necessary and sufficient for membrane insertion of IM proteins (***van der Laan et al., 2007***), whereas full translocation of proteins into the mitochondrial matrix depends on additional energy provided by the ATP consuming presequence translocase-associated import motor PAM (***Neupert and Brunner, 2002***; ***Schendzielorz et al., 2017***). The TIM23 complex consists of the channel forming Tim23 subunit and its homolog Tim17 (***Lohret et al., 1997***; ***Maarse et al., 1994***; ***Meinecke et al., 2006***; ***Ryan et al., 1998***; ***Truscott et al., 2001***). Additionally, the receptor protein Tim50 as well as Mgr2 are constitutive subunits of the presequence translocase, whereas Tim21 is specific to the TIM23 complex in the absence of the PAM motor (***Chacinska et al., 2005***; ***Ieva et al.,***

eLife digest The cells of animals, plants and other eukaryotic organisms contain compartments known as organelles that play many different roles. For example, compartments called mitochondria are responsible for supplying the chemical energy cells need to survive and grow. Two membranes surround each mitochondrion and energy is converted on the surface of the inner one.

Mitochondria contain over 1,000 different proteins, most of which are produced in the main part of the cell and have to be transported into the mitochondria. A transport protein called Tim23 is part of a larger group or 'complex' of proteins that helps to import many other proteins into the mitochondria. This complex sits in the inner membrane, with the Tim23 protein forming a large, water-filled pore through its core that provides a route for proteins to pass through the membrane.

Proteins are made of building blocks called amino acids. The proteins transported by the complex containing Tim23 all have a short chain of amino acids at one end known as an N-terminal presequence. However, it is not clear how the inside of the Tim23 channel identifies and transports this presequence to allow the right proteins to pass through the inner membrane.

Denkert, Schendzielorz et al. studied the normal and mutant versions of a Tim23 channel from yeast to find out which parts of the protein are involved in detecting the N-terminal presequence after it enters the pore. The experiments show that there are several amino acids in Tim23 that play important roles in this process. Furthermore, mitochondria containing mutant Tim23 channels, that are less able to identify the N-terminal presequence, are impaired in their ability to import proteins.

Tim23 proteins in humans and other organisms also contain most or all of the specific amino acids identified in this study, suggesting that the findings of Denkert, Schendzielorz et al. will also apply to other species. Furthermore, the experimental strategy used in this study could be adapted to investigate transport proteins in other cell compartments.

DOI: https://doi.org/10.7554/eLife.28324.002

2014). Tim23 was identified as the central pore-forming component of the TIM23 complex by electrophysiological characterization of purified Tim23 as well as patch-clamp analyses of inner membrane derived vesicles, depleted of Tim17 (***Martinez-Caballero et al., 2007***; ***Truscott et al., 2001***). Tim23 forms a voltage-activated, water-filled pore with a diameter of 1.3–2.4 nm. To maintain the permeability barrier of the inner membrane it is voltage-regulated by the Tim50 receptor and shows sensitivity towards presequence peptides and full-length preproteins (***Meinecke et al., 2006***; ***Truscott et al., 2001***). Many electrophysiological features of purified Tim23, such as voltage-gating, substrate sensitivity and selectivity, were also found in measurements of the TIM23 complex. The role of Tim17 is less clear, though recent studies suggest it might be involved in channel regulation within the complex (***Martinez-Caballero et al., 2007***; ***Ramesh et al., 2016***).

Despite its channel dimension, which would allow the simultaneous passage of multiple ions, Tim23 shows a clear preference to conduct cations over anions. Since its discovery this selectivity was speculated to be important to recognize and transport positively charged presequences through the channel. The lack of high-resolution 3D structures on the one hand, and the missing amphipathic character of the predicted transmembrane helices hindered the possibility to construct structure based mutants to investigate the molecular nature and physiological importance of the basic electrophysiological characteristics of the Tim23 channel. In recent years efforts have been made to overcome this issue. Fluorescent mapping has allowed for the first time to show which amino acid residues of the transmembrane helices of Tim23 are likely facing the aqueous channel lumen (***Alder et al., 2008***; ***Malhotra et al., 2013***).

In this study, we identify pore-lining amino acids of the Tim23 channel that contribute to ion selectivity. Mutations of these highly conserved amino acids specifically affect the channels selective properties while leaving other electrophysiological characteristics intact. Yeast cells expressing mutant Tim23 channels with decreased selectivity show growth defects and are impaired in the import of mitochondrial proteins. On the protein level, selectivity reduction leads to a highly decreased sensitivity towards substrates. Our data provide evidence for the idea that the biophysical properties of protein-conducting Tim23 channel are essential for its physiological functions.

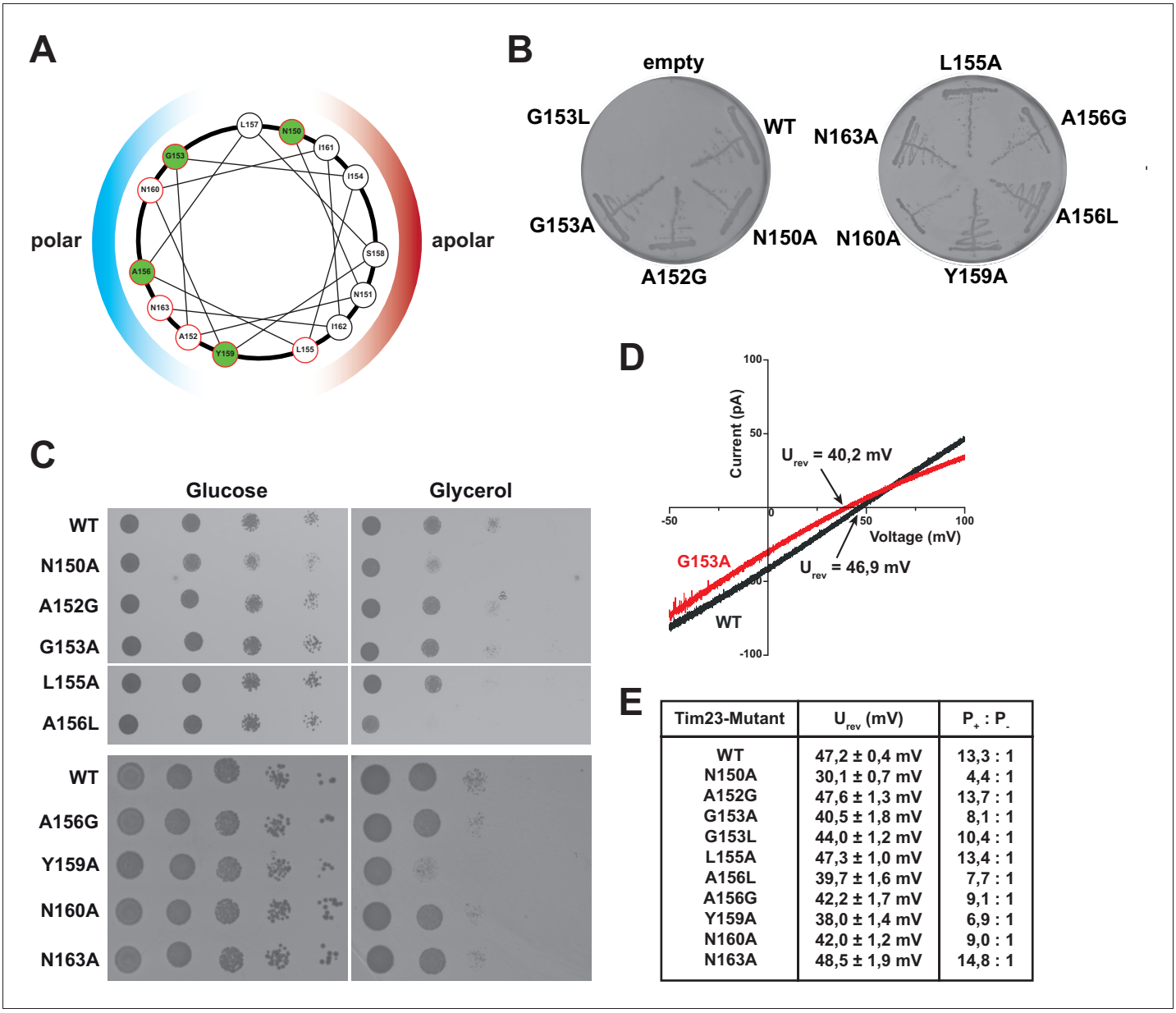

Tim23-Mutant	U_{rev} (mV)	$P_+ : P_-$
WT	47,2 ± 0,4 mV	13,3 : 1
N150A	30,1 ± 0,7 mV	4,4 : 1
A152G	47,6 ± 1,3 mV	13,7 : 1
G153A	40,5 ± 1,8 mV	8,1 : 1
G153L	44,0 ± 1,2 mV	10,4 : 1
L155A	47,3 ± 1,0 mV	13,4 : 1
A156L	39,7 ± 1,6 mV	7,7 : 1
A156G	42,2 ± 1,7 mV	9,1 : 1
Y159A	38,0 ± 1,4 mV	6,9 : 1
N160A	42,0 ± 1,2 mV	9,0 : 1
N163A	48,5 ± 1,9 mV	14,8 : 1

Figure 1. Substitutions of pore-lining residues of Tim23 reduce the channel's ion selectivity and lead to a growth defect in *S. cerevisiae*. (**A**) Helical wheel projection of amino acid residues 150–163 of the second transmembrane helix of Tim23. Highlighted residues in green indicate near 100% conservation. Colored hemispheres indicates polar/apolar facing regions of helix. Residues mutated in this study are circled in red. (**B**) *S. cerevisiae* strains with chromosomal deletion of the *TIM23* gene, complemented by a plasmid carrying both *URA3* and *TIM23* gene, were transformed with plasmids containing wild type *TIM23* or mutants and tested for viability after plasmid loss on 5-FOA containing medium. (**C**) *tim23*Δ yeast cells with plasmids containing wild type *TIM23* or pore-lining mutants were grown on fermentable (left) or non-fermentable (right) media at 37°C. Strains WT to A156L were grown on a single plate each for glucose and glycerol respectively. (**D**) Electrophysiological current-voltage (I–V) curves were recorded at asymmetrical buffer conditions with 12.5-fold KCl gradient for Tim23 (grey) or $Tim23^{G153A}$ (red) to determine reversal potentials. (**E**) Reversal potentials U_{rev} were experimentally determined for wild type Tim23 and all mutants by independent triplicates at asymmetrical buffer conditions, the ion selectivity was calculated from the mean reversal potential following the Goldman-Hodgkin-Katz equation. Errors represent standard deviation.

DOI: https://doi.org/10.7554/eLife.28324.003

The following figure supplements are available for figure 1:

Figure supplement 1. Electrophysiological screening of Tim23 mutants.

DOI: https://doi.org/10.7554/eLife.28324.004

Figure supplement 2. Sequence conservation of Tim23.

DOI: https://doi.org/10.7554/eLife.28324.005

Results

To investigate the physiological function of highly conserved, pore-lining amino acid residues of Tim23 (**Alder et al., 2008**; **Malhotra et al., 2013**) from *Saccharomyces cerevisiae in vivo*, we employed mutants based on substitution of amino acids in the second transmembrane helix (**Figure 1A**). *S. cerevisiae* cells with chromosomal deletion of *TIM23*, rescued by a *URA3*-containing plasmid carrying wild type *TIM23*, were transformed with plasmids carrying the *HIS3* gene as a selection marker and either a wild type copy of *TIM23* or *TIM23* mutant alleles. Transformants were selected on medium lacking Histidine (**Figure 1—figure supplement 1A**). The ability of *TIM23* mutants to complement Tim23 function was monitored by plasmid shuffle on 5-fluoroorotic acid (5-FOA)-containing medium (**Figure 1B**). Transformation was successful for all constructs, while 5-FOA selection showed that Tim23^{G153L} exhibited a lethal phenotype as published previously (**Demishtein-Zohary et al., 2015**). *TIM23* mutants that grew on 5-FOA were subsequently analyzed for growth on fermentable (glucose) and non-fermentable (glycerol) carbon sources (**Figure 1C**). Four mutants, encoding Tim23^{N150A}, Tim23^{L155A}, Tim23^{A156L} and Tim23^{Y159A}, exhibited a significant growth defect on non-fermentable media at 37°C, with Tim23^{A156L} showing the strongest phenotype (**Figure 1C**).

To analyze whether the growth defects could be explained by changed channel characteristics of Tim23, we expressed wild type and mutant forms of Tim23 in *E. coli*. The proteins were purified from inclusion bodies to homogeneity, incorporated into preformed large unilamellar vesicles (LUVs) and subjected to single-channel planar lipid bilayer experiments (**Krüger et al., 2012**; **Montilla-Martinez et al., 2015**). Interestingly, in a wide screen for basic electrophysiological parameters we found that a number of mutants (*Tim23^{N150A}*, *Tim23^{A156L}*, *Tim23^{Y159A}*) that showed growth defects exhibited a significantly reduced reversal potential (**Figures 1D** and **3D** and **Figure 1—figure supplement 1B**), which translates to a severe reduction of the channels cation preference (**Figure 1E**), while other parameters remained unaffected (**Figure 1—figure supplement 1B–D**). The strongest reduction was observed for Tim23^{N150A}, where the selectivity dropped down to 33% of wild type level. A slightly weaker reduction in cation preference (between 50–70% of wild type level) was observed for Tim23^{G153A}, Tim23^{A156G}, Tim23^{A156L}, Tim23^{Y159A} and Tim23^{N160A}. All residues with decreased selectivity are highly conserved between Tim23 in different species (**Figure 1—figure supplement 2**).

To analyze if the observed growth defects could be directly linked to altered channel characteristics or if they were secondary effects, we examined the integrity of the TIM23 complex in the inner membrane. Mitochondrial lysates of all mutants and wild type were analyzed for steady state protein levels of Tim23 (**Figure 2A**). Reduced levels of Tim23 were found for the mutants Tim23^{L155A}, Tim23^{A156L}, Tim23^{Y159A} and Tim23^{N160A} (**Figure 2A**, lanes 5, 7, 8 and 9). Tim23^{L155A}, Tim23^{A156L}, Tim23^{Y159A} all showed impaired growth phenotypes, which might result from decreased Tim23 levels. To gain more insight into TIM23 complex integrity of the mutants we performed co-immunoprecipitation of wild type and all mutants using antibodies against Tim23 (**Figure 2B**). Interestingly, TIM23 and PAM subunits could be efficiently co-purified. The altered levels of some subunits (for example Tim17 and Tim50) can probably be attributed to decreased Tim23 levels in mitochondria. As an alternative approach, we analyzed TIM23 complex integrity of selected mutants by size exclusion chromatography. To this end, mitochondrial extracts carrying Tim23, Tim23^{N150A}, or Tim23^{Y159A} were generated and subjected to chromatographic separation of protein complexes. In agreement with the results of the immunoisolation analyses, the TIM23 complex apparently remained intact and associated with the import motor (**Figure 2—figure supplement 1**).

Hence, after carefully testing the suitability of Tim23 mutants for subsequent analysis, Tim23^{N150A} was the only mutation that led to impaired growth, decreased ion-selectivity and exhibited normal protein levels and complex assembly and was therefore further analyzed in *in organello* assays. Mitochondrial steady state levels of selected proteins were analyzed, that is, TIM23 complex components, PAM complex subunits and mitochondrial marker proteins (**Figure 2C**). Here, all protein levels in mitochondria from Tim23^{N150A} expressing cells were unchanged compared to wild type.

To assess that the inner membrane potential was not affected in mitochondria containing Tim23^{N150A}, we tested the $\Delta\Psi$ *in organello*, using the membrane-permeable fluorophore $DiSC_3(5)$ (**Figure 2D**). The measurements showed that $\Delta\Psi$ was not significantly altered in Tim23^{N150A}-expressing cells compared to the wild type control (**Figure 2D and E**). In agreement with this unchanged membrane potential, in single-channel measurements the IMS domain of Tim50 exhibited the same

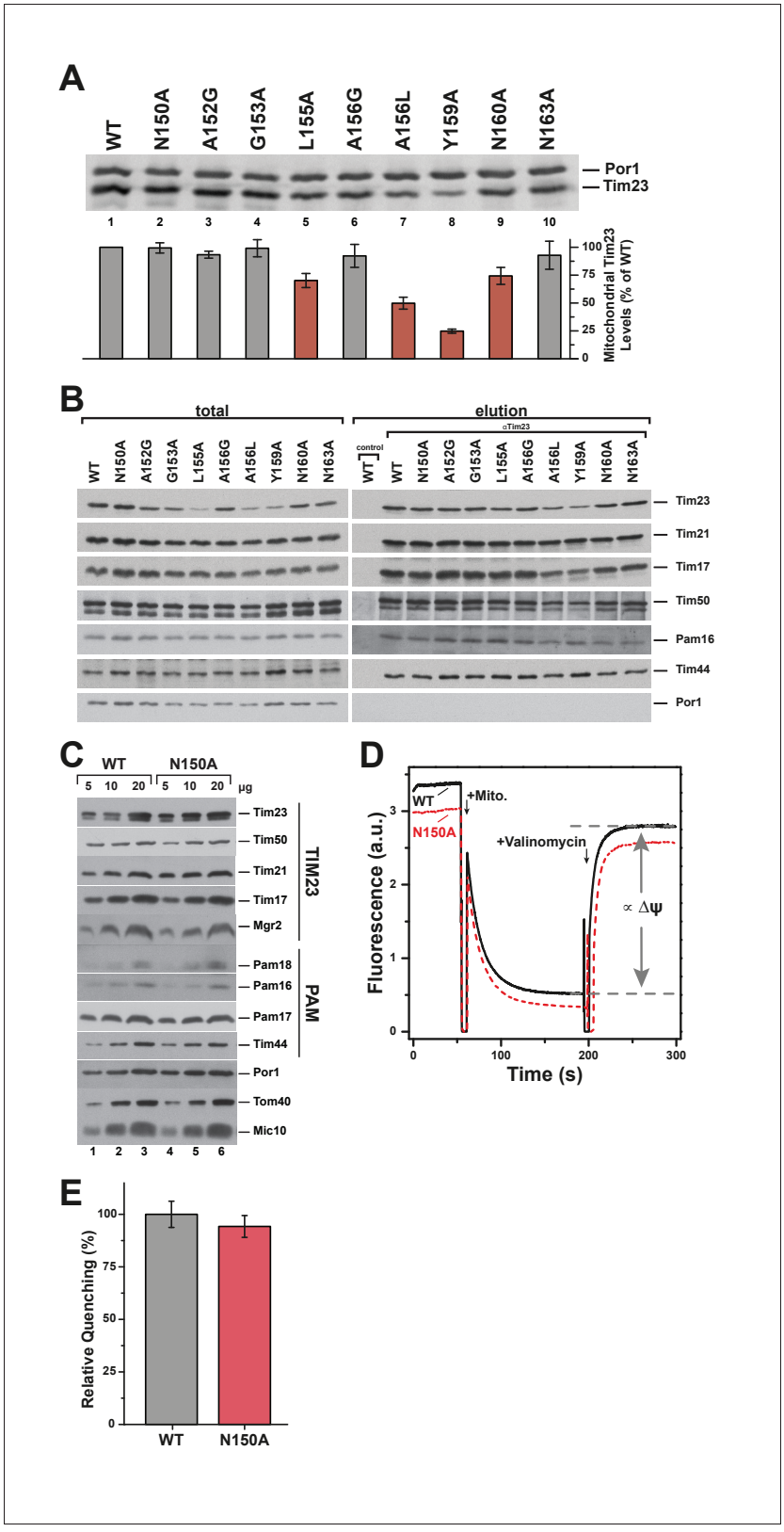

Figure 2. Pore-lining mutant Tim23^{N150A} is properly expressed and integrated into TIM23 complexes. (**A**) Mitochondrial steady state levels of yeast expressing wild type Tim23 or mutants were assessed by Western blot analysis (upper) with decoration against Tim23 and Por1 (mitochondrial outer membrane). Protein levels were quantified using fluorescently labelled secondary antibodies in four independent experiments and normalized by

Figure 2 continued on next page

Figure 2 continued

mitochondrial Por1 levels. Significantly reduced levels are indicated in red. Error bars represent standard error of the mean. (**B**) TIM23 complex integrity and recruitment of PAM complex of wild type and Tim23 mutants was examined by co-immunoprecipitation of mitochondrial lysates using Tim23 antibodies. (**C**) Isolated mitochondria containing Tim23 or $Tim23^{N150A}$ were Western blotted and decorated against proteins of the TIM23 complex, the PAM complex, Por1 and Tom40 (both mitochondrial outer membrane) and Mic10 (mitochondrial inner membrane). (**D**) Membrane potential $\Delta\Psi$ was assessed by adding isolated mitochondria containing Tim23 (black solid) or $Tim23^{N150A}$ (red dashed) to the fluorophore $DiSC_3(5)$, then dissipating $\Delta\Psi$ with valinomycin and determining the amount of quenching. Grey dashed lines and arrows indicate the parameter quantified in (**D**). (**E**) Relative fluorophore quenching as a measure of membrane potential $\Delta\Psi$ for Tim23 (grey) and $Tim23^{N150A}$ (red) was quantified (as depicted in C) in three independent experiments. Error bars represent standard error of the mean before normalization.

DOI: https://doi.org/10.7554/eLife.28324.006

The following figure supplement is available for figure 2:

Figure supplement 1. TIM23 complex characterization by size exclusion chromatography profiles.

DOI: https://doi.org/10.7554/eLife.28324.007

voltage-regulation on wild type and $Tim23^{N150A}$ that we reported before (***Figure 3E and F***) (***Meinecke et al., 2006***).

In our initial screen for altered electrophysiological characteristics, we found that specifically the ion-selectivity of $Tim23^{N150A}$ was decreased (***Figure 1E and 3D***). We next performed an in-depth analysis of this mutant form of the channel to confirm that no other channel parameters were affected. Wild type as well as $Tim23^{N150A}$ channels exhibited complex voltage-dependent gating patterns (***Figure 3A and B***). Both pores gated with the same main-conductance state of ~460 pS (at 250 mM KCl) and showed similar sub-conductance states of ~170 pS and ~60 pS (***Figure 3C***). Again $Tim23^{N150A}$ displayed a reduced reversal potential, while the wild type and mutant Tim23 showed the same voltage-dependent open probability (***Figure 3E and F***) and were efficiently voltage-regulated by $Tim50^{IMS}$ as published before (***Figure 3E and F***) (***Meinecke et al., 2006***). In summary, $Tim23^{N150A}$ is found in wild type levels in mitochondria, integrates properly into the TIM23 complex, and has no effect on the integrity of the inner membrane. In addition, it displays wild type-like channel characteristics except for a significantly reduced cation preference.

We next asked whether the reduced selectivity for cations impacted the import capabilities of the presequence translocase. To this end, isolated mitochondria were incubated with radiolabeled matrix proteins bearing typical, positively charged presequences: $F_1\beta$ (***Figure 4A***), a subunit of the F_1F_O-ATP synthase, Cox4 (***Figure 4B***), a subunit of the cytochrome *c* oxidase, and the model fusion proteins $b_2(167)_\Delta$-DHFR (***Figure 4C***) and $b_2(220)$-DHFR (***Figure 4D***) which is sorted into the inner membrane. The import reaction was stopped after 10, 20 or 30 min by dissipation of $\Delta\Psi$ and mitochondria were subsequently treated with Proteinase K to remove non-imported precursor proteins. Even at permissive temperature, quantified import efficiency in the linear phase revealed significant reductions for both types of imported substrates (***Figure 4E***), showing that $Tim23^{N150A}$ is clearly affected in protein import. Import experiments conducted at 37˚C show the same trend with an even more pronounced reduction (***Figure 4—figure supplement 1***), while import experiments using the ADP/ATP carrier (AAC) and Cox12 revealed that other import pathways into mitochondria (TIM22 and MIA) were not impaired by the mutation (***Figure 4F and G***). In fact, a slightly increased import efficiency for AAC is frequently observed when transport along the TIM23 pathway is affected (***Geissler et al., 2002***; ***Schulz et al., 2011***).

These observations led us to hypothesize that the reduced import capabilities of $Tim23^{N150A}$ were linked to the altered cation selectivity, which could be explained if selectivity defects lead to changed sensitivity of the mutant channel towards substrates. To test this, we analyzed the channel response of wild type Tim23 and $Tim23^{N150A}$ to presequences in single-channel experiments. As a substrate we used a peptide corresponding to the presequence of Cox4 (***Allison and Schatz, 1986***), a subunit of the cytochrome *c* oxidase, which is well characterized to study import processes and signal recognition biochemically (***Chacinska et al., 2005***; ***Lytovchenko et al., 2013***; ***Schulz et al., 2011***) and channel excitation electrophysiologically (***Lohret et al., 1997***; ***Martinez-Caballero et al., 2007***; ***Meinecke et al., 2006***; ***Ramesh et al., 2016***; ***Truscott et al., 2001***; ***van der Laan et al., 2007***). The presequence peptide was titrated in increasing concentrations to the intermembrane

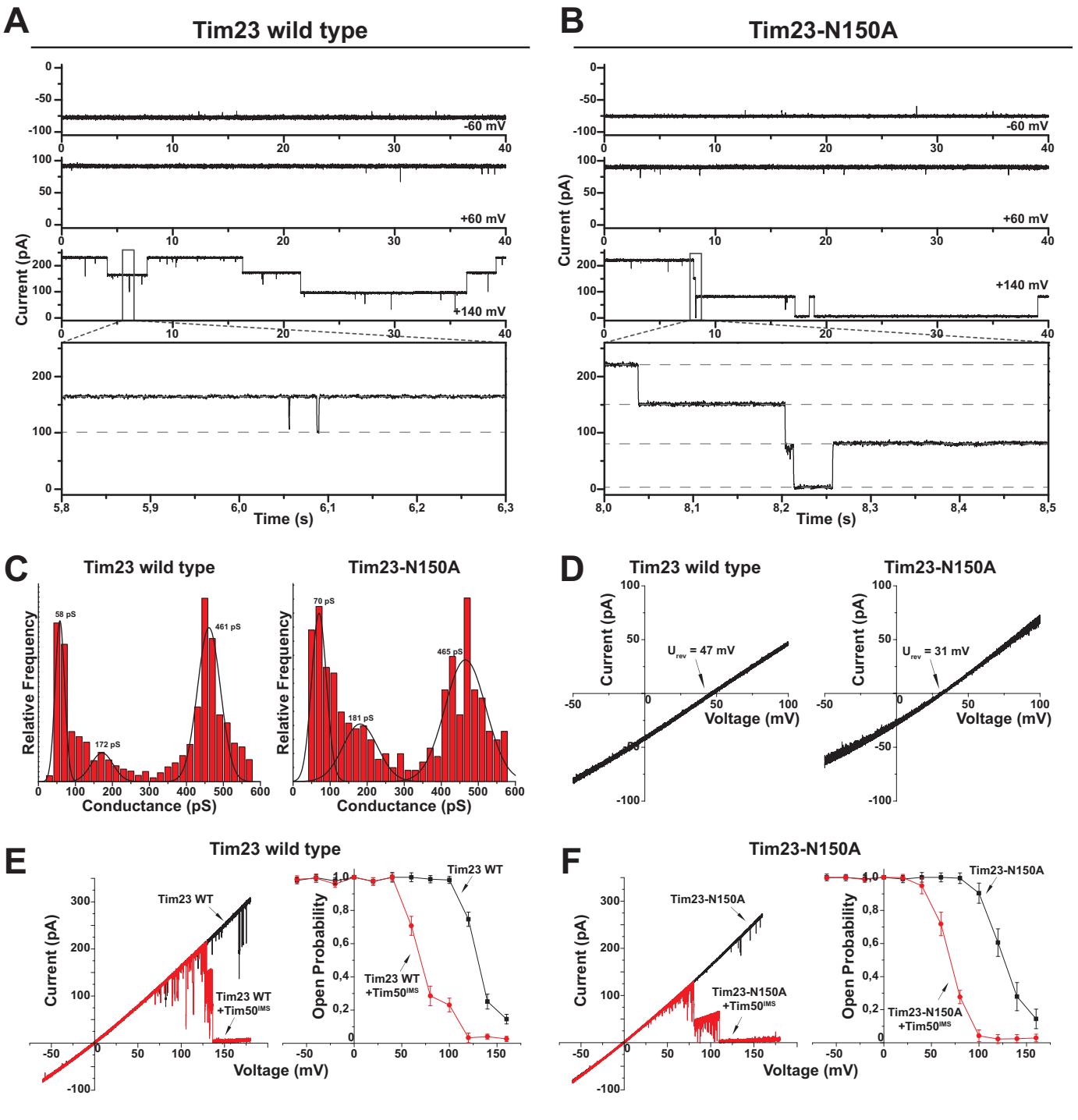

Figure 3. Tim23^{N150A} displays reduced cation preference. (**A**)/(**B**) Tim23- (**A**) or Tim23^{N150A}-containing (**B**) proteoliposomes were fused with planar lipid bilayers and single-channel activity was characterized by electrophysiological current recordings. (**C**) Gating event histograms for Tim23 (left) and Tim23^{N150A} (right) were calculated from constant-voltage recordings (as depicted in A) with at least 2000 gating events each. The three most prominent classes of conductance changes were modeled with a Gaussian fit. (**D**) I-V curves at asymmetrical buffer conditions were recorded for Tim23 (left) and Tim23^{N150A} (right) with indicated reversal potential U_{rev} for 12.5-fold KCl-gradient. (**E**)/(**F**) I-V curves (left) and open probabilities (right) were determined for bilayer incorporated Tim23 (**E**) or Tim23^{N150A} (**F**) before (black) and after (red) addition of 700 nM Tim50^{IMS} to IMS-side of the channel. Error bars represent standard deviation (SD, n = 3).

DOI: https://doi.org/10.7554/eLife.28324.008

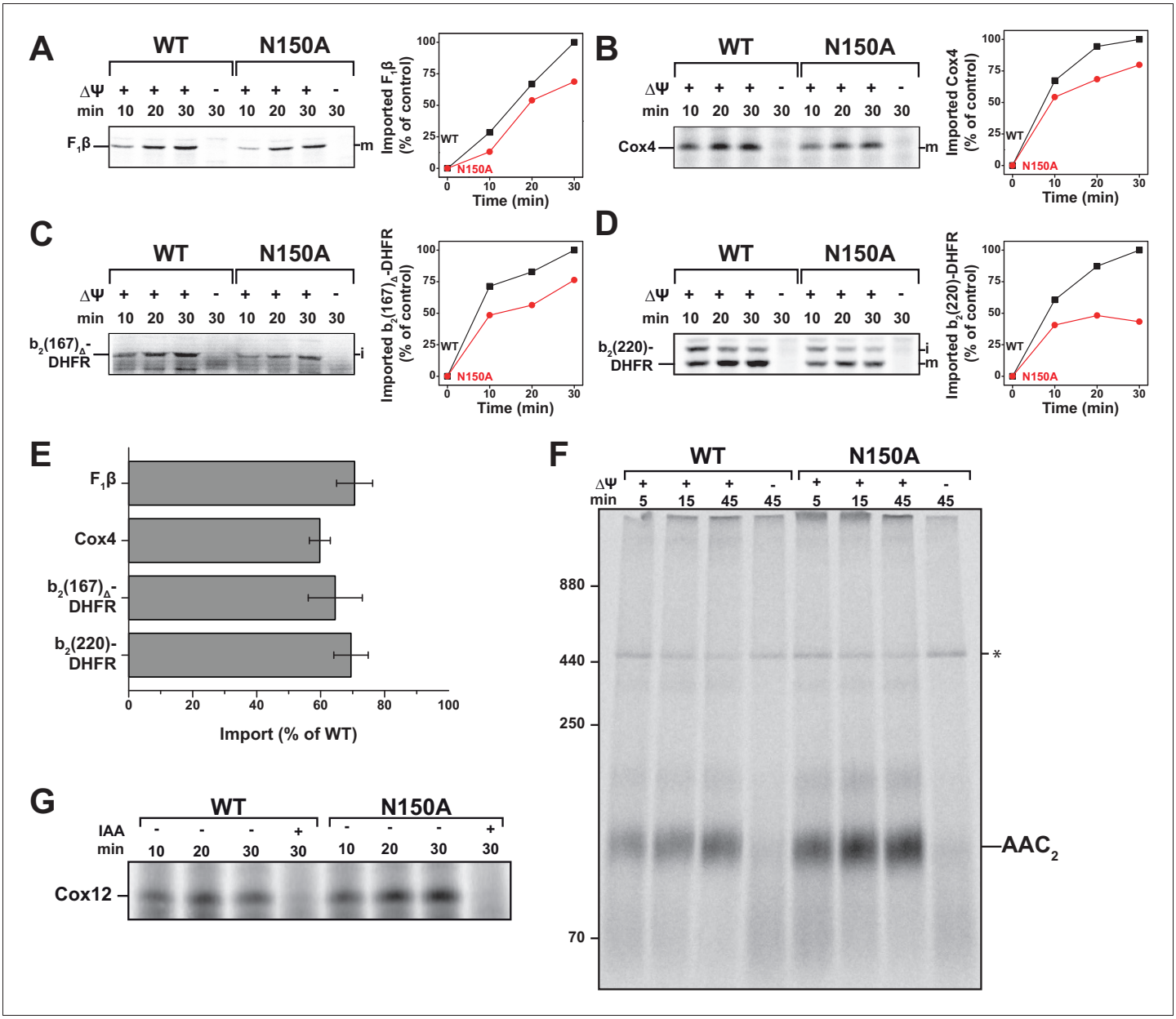

Figure 4. Tim23^{N150A} exhibits significant import defects for various TIM23 substrates. (**A–D**) Import capability of wild type and tim23^{N150A} mutant mitochondria was determined by incubating [^{35}S]-radiolabeled matrix destined precursors $F_1\beta$ (**A**), Cox4 (**B**), $b_2(167)_\Delta$-DHFR (**C**) or the inner membrane sorted b_2(220)-DHFR (**D**) with isolated mitochondria for 10, 20 or 30 min. The import reactions were stopped by dissipating ΔΨ and subsequent Proteinase K (PK)-digest. Digital autoradiographs (left) were analyzed and quantified (right). Maximum import into wild type mitochondria was set to 100%. (**E**) Relative import efficiency after 15 min of import into mitochondria containing Tim23^{N150A} was quantified for different substrates. Error bars represent standard error of the mean (SEM, n = 3). (**F**) Carrier import into Tim23^{N150A}-containing mitochondria was assessed via ADP/ATP carrier (AAC) complex assembly by incubating [^{35}S]-radiolabeled AAC with isolated mitochondria for 15, 30 or 45 min. The import reaction was stopped by dissipating ΔΨ and subsequent PK-digest. Assembly of AAC dimer was monitored by BN-PAGE. (**G**) The MIA substrate Cox12 was [^{35}S]-radiolabeled and imported into Tim23^{N150A}-containing mitochondria for 10, 20 or 30 min. The import reaction was stopped by addition of iodoacetamide (IAA) and subsequent PK-digest.

DOI: https://doi.org/10.7554/eLife.28324.009

The following figure supplement is available for figure 4:

Figure supplement 1. Import of TIM23-substrates at non-permissive temperatures.

DOI: https://doi.org/10.7554/eLife.28324.010

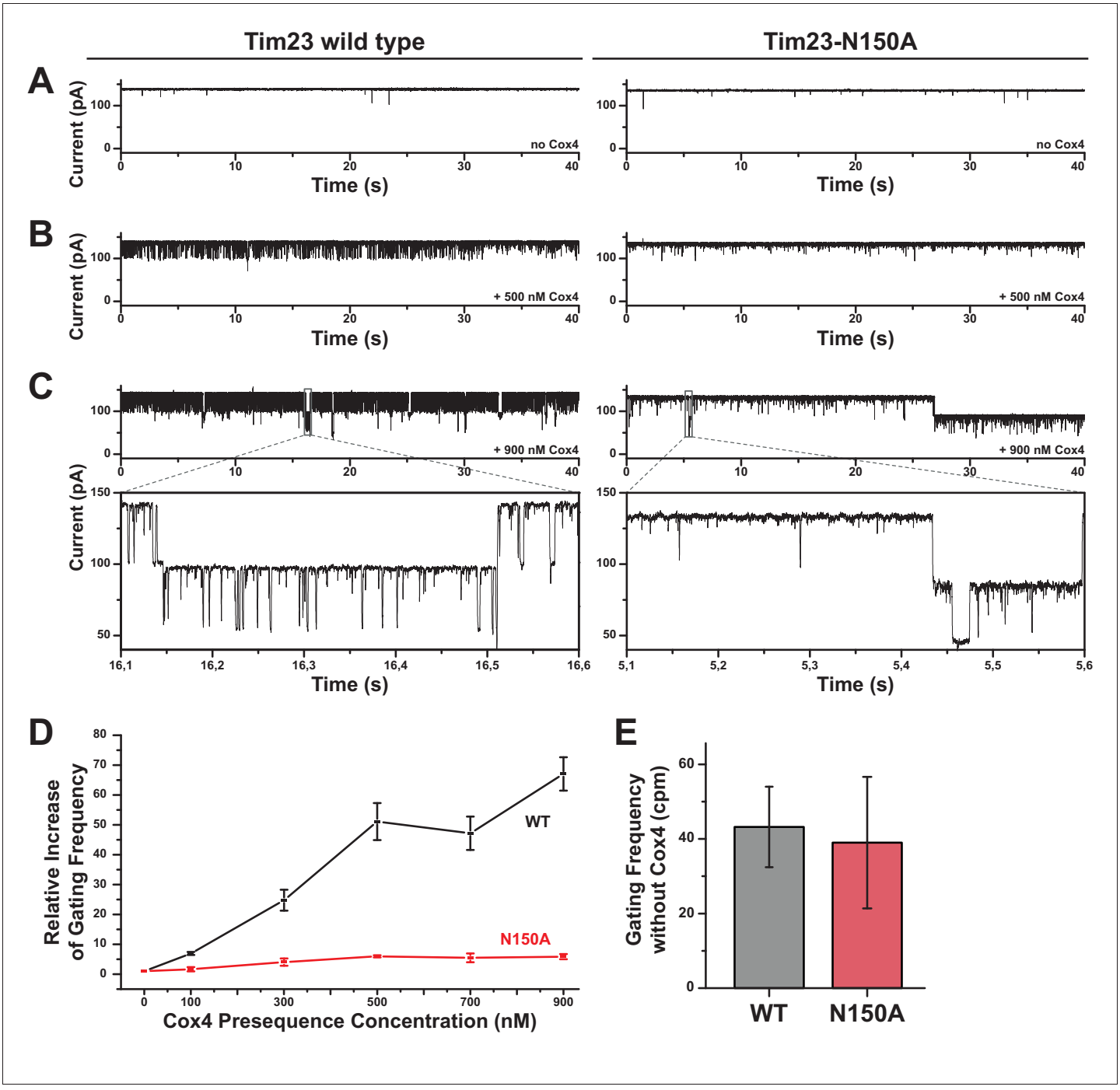

Figure 5. Increased gating frequency as a measure of channel response to presequence titration is heavily reduced for Tim23^{N150A}. (**A**) Bilayer-incorporated Tim23 (left) or Tim23^{N150A} (right) single-channel currents were recorded at +80 mV before addition of Cox4 presequence peptide. (**B**)/(**C**) Current recordings of wild type (left) and mutant (right) channels were performed after each titration step. (**D**) Channel response of Tim23 (black) and Tim23^{N150A} (red) after addition of Cox4 presequence was quantified by counting gating events and calculating the relative increase in activity compared to unstimulated channels. Error bars represent standard deviation. (**E**) Absolute gating frequency of unstimulated Tim23 and Tim23^{N150A} was determined from current recordings before presequence titration. Error bars represent standard deviation (SD, n = 3).

DOI: https://doi.org/10.7554/eLife.28324.011

space corresponding side of bilayer-incorporated wild type or Tim23^{N150A} channels and current was recorded at constant holding potentials after each titration step. Tim23 reacted to higher holding potentials by partial or complete closing (***Figure 3A,B,E and F***), which could mask presequence-

induced activity increase or change channel behavior. Hence, we aimed to minimize such secondary effects by recording at lower holding potentials. We applied voltages of +80 mV, where the channel stayed primarily in an open state even during prolonged exposure but reacts to presequence activation. Wild type Tim23 showed a distinct activity increase, characterized by fast gating (flickering), after addition of Cox4 (***Figure 5A,B and C***). While $Tim23^{N150A}$ also responded with an increased gating frequency to Cox4 addition, the effect was drastically reduced in comparison to wild type Tim23. Where wild type Tim23 channels could be activated to a relative increase in gating frequency of factor 50 (***Figure 5D***, black curve), the gating frequency of $Tim23^{N150A}$ only changed by a factor 6 (***Figure 5D***, red curve), resulting in an 88% reduction of voltage-activated gating from wild type to mutant Tim23. To further prove that the relative reduction in gating frequency did not originate from e.g. a higher baseline of gating frequency of $Tim23^{N150A}$ compared to wild type Tim23, we analyzed absolute gating frequencies in the absence of substrate peptides (***Figure 5E***). Both proteins have near identical average gating frequencies in unstimulated conditions, excluding pre-activation effects.

In summary, our data show that a decreased selectivity of Tim23 leads to reduced substrate sensitivity, which explains the impaired protein import capacity of mitochondria expressing a Tim23 selectivity mutant.

Discussion

Tim23, the eponymous core subunit of the TIM23 complex, was identified as the import channel for presequence carrying substrates more than 15 years ago (***Lohret et al., 1997***; ***Truscott et al., 2001***). Although the basic channel characteristics have been described to some extend (***Martinez-Caballero et al., 2007***; ***Meinecke et al., 2006***; ***Truscott et al., 2001***), the physiological relevance of these parameters as well as the molecular mode of function of the import pore are still enigmatic. Due to lack of structural information the current understanding is little more than that at the heart of the TIM23 complex a water-filled pore facilitates the passage of preproteins across the inner membrane.

In this study, we investigated the molecular basis of Tim23's ion-selectivity to link biophysical properties of the import channel to its physiological function. We report the identification of pore-lining amino acids that contribute to the channels cation selectivity. Interestingly, we found that a number of different residues are involved in discriminating between ions. All amino acids detected to be important for channel selectivity are strictly conserved in evolution, suggesting an essential role for the selectivity in protein transport across the inner membrane. In recent studies these residues were successfully cross-linked to preproteins *in transit*, showing their accessibility and exposure to the channel lumen (***Alder et al., 2008***; ***Malhotra et al., 2013***). Our results imply that selectivity is not necessarily provided by a confined restriction zone within the channel but rather by specific channel surface characteristics throughout the length of the pore, which facilitate the passage of certain ions over others. Such a mechanism was proposed for other large pores to explain their selective properties (***Im and Roux, 2002***; ***Kutzner et al., 2011***). Even though these reports were mainly made for β-barrel proteins, the similarity of the electrophysiological properties between some β-barrel pores, like Tom40 or Sam50, and α-helical import pores, like Tim23 or Tim22, makes it appealing to speculate that the selectivity of these pores has a similar molecular nature. Most of the detected selectivity mutants in our study showed impaired growth. As an outlier $Tim23^{G153A}$ shows a mediocre reduction in selectivity while growth is relatively unaffected and we therefore hypothesize that a certain impairment of the selective properties can be compensated. We rigorously excluded mutant forms of Tim23 that showed decreased mitochondrial steady state levels or with a compromised TIM23 complex assembly and hence could not be used to link *in vitro* single-channel results with *in vivo* and *in organello* experiments. This led to the identification of $Tim23^{N150A}$, which is expressed and assembled as wild type Tim23. The potential across the inner membrane is unaffected in cells expressing $Tim23^{N150A}$. In line with the uncompromised mitochondrial fitness, all channel parameters, especially $Tim50^{IMS}$ voltage-regulation, but selectivity and substrate sensitivity, are comparable with wild type Tim23. Importantly, mitochondria containing $Tim23^{N150A}$ channels showed significantly reduced import capacity for matrix proteins. We therefore conclude that the drastically reduced selectivity renders Tim23 channels insensitive towards positively charged substrate peptides, which in turn explains the reduced import rates of preproteins. The position of the amino acid

substitution N150A is found close to the beginning of transmembrane helix 2 and is therefore located at the matrix side of the channel. This suggests that the decreased substrate sensitivity characterized by an inactive, slowly gating channel in the presence of prepeptides cannot be explained by binding and activation of the substrate to the IMS side of the channel. Instead the substrate has to reach deep into the channel to be affected by a mutation at the matrix side. Similar to what was described for Tom40 (**Mahendran et al., 2012**), the active, fast-gating Tim23 is therefore likely a transport competent state of the channel, triggered by peptides in transit within the channel that are discriminated by the channels selective properties. A decreased selectivity of Tim23 leads to an inability to be activated and therefore directly to decreased import rates.

The strategy used in this study allowed us to link the biophysical properties of a protein translocase to its physiological function. While water-filled pores were identified at the heart of most organellar translocation complexes (**du Plessis et al., 2011**; **Harsman et al., 2010**; **Meinecke et al., 2016**; **Neupert and Herrmann, 2007**; **Schmidt et al., 2010**; **Sjuts et al., 2017**), only basic channel characteristics were described in most cases. A correlation between the fascinating electrophysiological properties of these large pores and their physiological function remained circumstantial evidence. It was for example speculated for almost 20 years, that the cation selectivity of the Tim23 channel is important for recognition or transport of positively charged presequences, though no direct evidence was reported. Interestingly, many translocation pores show partially similar electrophysiological properties. Although structurally diverse, Tim23, Tim22, Tom40 and Sam50 all display comparable channel diameters and a preference for cations. The molecular nature of these characteristics as well as their physiological importance will be highly important problems to tackle in the future.

Materials and methods

Protein expression and purification

*Sc*Tim23 wild type and mutants were expressed from the plasmid pET10N containing an N-Terminal His_{10}-Tag in *E. coli* strain BL21 (DE3). All mutants were generated from the wild type plasmid by site-directed mutagenesis. Inoculated cultures in LB-medium were grown to $OD_{600} \approx 0.7$, after expression (induced by 1 mM isopropyl-β-D-thiogalactopyranoside (IPTG), 37°C, 3 hr) cells were lysed and inclusion bodies were purified (**Meinecke et al., 2006**; **Tarasenko et al., 2017**). Inclusion bodies were then denatured by 8 M Urea, 150 mM NaCl, 10 mM Tris-HCl, 50 mM Imidazole, pH 8.0, applied to NiNTA-Agarose and eluted by the same buffer with 500 mM Imidazole. Isolated Tim23 was further subjected to size exclusion chromatography using a HiLoad 16/600 Superdex 75 column (GE Healthcare, NJ, USA) and single band purity was confirmed by SDS-PAGE.

The presequence-peptide Cox4 (MLSLRQSIRFFKPATRTLCSSRYLL) was purchased from JPT Peptide Technologies (DE) as N-terminal amine and C-terminal amide.

The IMS domain of Tim50 (aa 132–476) was recombinantly expressed and purified to single band purity as described elsewhere (**Geissler et al., 2002**; **Schulz et al., 2011**).

Liposome preparation and protein incorporation

Lipids were purchased as L-α-Phosphatidylcholine (PC), L-α-Phosphatidylethanolamine (PE), L-α-Phosphatidylinositol (PI), L-α-Phosphatidylserine (PS) and Cardiolipin (CL) from Avanti Polar Lipids (AL, USA). The lipid mixture of 45:20:15:5:15 mol% PC:PE:PI:PS:CL in $CHCl_3$, closely resembling inner mitochondrial lipid composition (**van Meer et al., 2008**), was dried with a nitrogen stream and resuspended in 100 mM KCl, 10 mM MOPS-Tris, pH 7.0. Lipid suspension was thoroughly vortexed, subjected to seven freeze-thaw cycles and extruded through 200 nm membranes (Whatman plc, UK) to ensure unilamellarity and defined size distribution. Both liposomes and protein in urea were incubated with the mild detergent MEGA-9 (Glycon, DE) above CMC at 80 mM first separately then combined, at room temperature. Subsequently the liposome-protein-detergent mixture was subjected to dialysis against 5 L of liposome buffer to remove both urea and MEGA-9. Incorporation success was monitored by Histodenz flotation assay and sodium carbonate extractions as described elsewhere (**Barbot et al., 2015**).

Electrophysiological experiments

Electrophysiological experiments with Tim23 were carried out using the planar lipid bilayer technique, described in detail before (**Harsman et al., 2011**; **Reinhold et al., 2012**). Briefly, Tim23-containing proteoliposomes were added next to the bilayer in the *cis* chamber to enable fusion of liposomes with the bilayer. Asymmetrical buffer conditions for osmotically-driven fusion were 250 mM KCl, 10 mM MOPS-Tris, pH 7.0 in the *cis* chamber and 20 mM KCl, 10 mM MOPS-Tris, pH 7.0, for a 12.5-fold KCl-gradient over the bilayer. The electric recordings were performed using two Ag/AgCl electrodes in glass tubes, embedded in a 2 M KCl agar-bridge to minimize junction potentials, with one electrode per chamber. The electrode in the *trans* chamber was the reference electrode as it was connected to the headstage (CV-5-1GU) of a Geneclamp 500B current amplifier (both Molecular Devices, CA, USA), with the cis-electrode acting as ground. Currents were digitized by a Digidata 1440A A/D converter and recorded using the software AxoScope 10.3 and Clampex 10.3 (all Molecular Devices). Analysis of the data was carried out using R-packages *stepR* (**Hotz et al., 2013**) and dbacf (**Tecuapetla-Gómez and Munk, 2015**) and OriginPro 8.5 (OriginLab, MA, USA). After incorporation of Tim23 into the lipid bilayer, symmetrical conditions were set by perfusion with 20x chamber volume of 250 mM KCl, 10 mM MOPS-Tris, pH 7.0. These symmetrical buffer conditions were used for constant-voltage recordings and current-voltage relations. Asymmetrical buffers identical to the fusion conditions were used for reversal potential measurements. Tim23 typically inserts unidirectionally into the bilayer, with the IMS-domain of Tim23 exposed to *trans*. For concentration-dependent quantification of gating events, the synthetic peptide representing the presequence of the TIM23-substrate cytochrome c oxidase subunit 4 was titrated to the *trans* chamber in increasing concentrations. After addition, the buffer in the chamber was stirred for 2 min and then rests for 2 min before current recordings start. Constant-voltage currents were recorded for one minute, all gating events were counted and used to determine the gating frequency, i.e. events per minute. The open probability was calculated by dividing the mean by the maximum current.

Yeast growth and handling

All yeast strains were grown in YP medium (1% yeast extract, 2% peptone) with 2% glucose (YPD) or 3% glycerol (YPG) medium at 30°C. For plate growth test, synthetic medium containing 3% glycerol or 2% glucose was used. For generation of a Tim23 shuffling strain MB29 (**Geissler et al., 2002**), endogenous *TIM23* was replaced by homologous recombination with a *LYS2* cassette in a strain expressing *TIM23* from a *URA3* containing plasmid. Wild type and mutant Tim23 were expressed by cloning *TIM23* gene +1 kb upstream and downstream of the gene into pRS413. Point mutations were introduced by side-directed mutagenesis. After transformation of these plasmids into the shuffling strain, 5-Fluoroorotic acid (5-FOA) was used to select against *URA3* containing plasmids harboring wild type *TIM23*. For subsequent isolation of mitochondria, yeast cells were first grown in YPD medium at 30°C overnight, then diluted to OD_{600} = 0.2 in YPG medium and continued to grow for 24 hr at 30°C. Cells were then transferred to a bigger culture at OD_{600} = 0.2 in YPG and grown at 30°C for 16 hr, reaching a final OD_{600} of 2–3. Isolation of mitochondria was handled as described before (**Schendzielorz et al., 2017**).

Import of precursor proteins

For import of [^{35}S]-methionine labeled precursors into isolated mitochondria, proteins were translated using rabbit reticulocyte lysate (Promega, WI, USA). Reaction was performed in import buffer (250 mM sucrose, 10 mM MOPS/KOH pH 7.2, 80 mM KCl, 2 mM KH_2PO_4, 5 mM $MgCl_2$, 5 mM methionine and 3% fatty acid-free BSA) supplemented with 2 mM ATP and 2 mM NADH. To stop the import reaction, membrane potential was disrupted using final concentration of 1 µM valinomyin, 8 µM antimycin A and 20 µM oligomycin and samples were Proteinase K (PK, 20 µg/ml) treated for 10 min on ice. PK was inhibited with 2 mM phenylmethylsulphonyl fluoride (PMSF) for 10 min on ice; mitochondria were pelleted, washed with SEM (250 mM sucrose, 20 mM MOPS pH 7.2, 1 mM EDTA) and further analyzed by SDS-PAGE and autoradiography. Import and assembly of the ADP/ATP carrier protein (AAC) via TIM22 was performed using the standard protocol and further analyzed by Blue Native PAGE and autoradiography as described before (**Schulz et al., 2011**). Import of Cox12 via MIA was performed as described (**Gornicka et al., 2014**). Briefly, in addition to the standard protocol the reticulocyte lysate was diluted 1:2 in saturated ammonium sulfate ($(NH_4)_2SO_4$)

and precipitated on ice. The pellet was resuspended in 8 M urea, 10 mM DTT, 30 mM MOPS, pH 7.2 and then added to mitochondria in import buffer without BSA. The Cox12 import reaction was stopped with 25 mM iodoacetamide (IAA) and PK.

Quantifications were performed using ImageQuant TL (GE Healthcare, NJ, USA) using a rolling ball background subtraction.

Protein complex isolation

TIM23 complex isolation was carried out essentially as described (***Herrmann et al., 2001***). Briefly, mitochondria were resuspended to 1 mg/ml in solubilization buffer (20 mM Tris/HCl pH 7.4, 150 mM NaCl, 10% glycerol (w/v), 1 mM PMSF, 1% digitonin) and kept on ice for 20 min. Insoluble parts were removed by centrifugation at 14000 x g for 10 min and supernatant was incubated with Tim23-specific antibodies cross-linked to Protein A sepharose beads. After 30 min of binding on a rotating wheel at 4°C and 5x washing with 500 µl washing buffer (solubilization buffer with 0.3% digitonin), samples where eluted with 50 µl 0.1 mM glycine pH 2.8 (neutralized with 5 µl 1 M Tris base).

Membrane potential measurements

Membrane potential was measured using 3,3'-dipropylthiadicarbocyanine iodide ($DiSC_3(5)$). Mitochondria were resuspended in buffer containing 600 mM sorbitol, 1% (wt/vol) BSA, 10 mM $MgCl_2$ and 20 mM KPi, pH 7.4 to a concentration of 166 µg/ml. Changes in fluorescence were assessed with a F-7000 fluorescence spectrophotometer (Hitachi, JP) at room temperature with excitation at 622 nm, emission at 670 nm and slits of 5 nm. Components were added to the cuvette in the fowling order: 500 µl of buffer, $DiSC_3(5)$, 83 µg of mitochondria, 1 µM valinomycin. To compare relative differences in membrane potential, the difference in fluorescence before and after addition of valinomycin was used.

Complex characterization by size exclusion chromatographie

Mitochondria were solubilized as described for protein complex isolation, with 2 mg/ml instead of 1 mg/ml, and 50 µl were loaded to a Superose 6 increase 3.2/300 and eluted in solubilization buffer containing 0.3% digitonin. The first 1250 µl were discarded, the following 750 µl were collected in 50 µl fractions and subjected to SDS-PAGE and Western blot. Quantifications were performed using ImageQuant TL (GE Healthcare, NJ, USA) using a rolling ball background subtraction.

Acknowledgements

We thank Robert Rucktäschel for technical assistance with size exclusion chromatography. The work was supported by the Deutsche Forschungsgemeinschaft SFB1190, P12 (MM), SFB860, B1 (PR), FOR 1905, TP1 (ND), the Boehringer Ingelheim Foundation (FR), the Max Planck Society (PR) and the Ph. D program 'Molecular Biology' – International Max Planck Research School and the Göttingen Graduate School for Neurosciences and Molecular Biosciences (GGNB; DFG grant GSC 226/1 (ABS)).

Additional information

Funding

Funder	Grant reference number	Author
Deutsche Forschungsgemeinschaft	SFB1190	Michael Meinecke
Deutsche Forschungsgemeinschaft	SFB860	Peter Rehling
Deutsche Forschungsgemeinschaft	FOR1905	Niels Denkert

The funders had no role in study design, data collection and interpretation, or the decision to submit the work for publication.

Author contributions

Niels Denkert, Data curation, Formal analysis, Investigation, Methodology, Writing—original draft; Alexander Benjamin Schendzielorz, Formal analysis, Investigation, Methodology; Mariam Barbot, Conceptualization, Investigation; Lennart Versemann, Frank Richter, Investigation; Peter Rehling, Conceptualization, Supervision, Writing—review and editing; Michael Meinecke, Conceptualization, Data curation, Supervision, Funding acquisition, Writing—original draft

Author ORCIDs

Niels Denkert, http://orcid.org/0000-0002-2551-0360
Alexander Benjamin Schendzielorz, http://orcid.org/0000-0003-3360-9130
Peter Rehling, http://orcid.org/0000-0001-5661-5272
Michael Meinecke, http://orcid.org/0000-0003-1414-6951

Decision letter and Author response

Decision letter https://doi.org/10.7554/eLife.28324.013
Author response https://doi.org/10.7554/eLife.28324.014

Additional files

Supplementary files

- Transparent reporting form

DOI: https://doi.org/10.7554/eLife.28324.012

References

Alder NN, Jensen RE, Johnson AE. 2008. Fluorescence mapping of mitochondrial TIM23 complex reveals a water-facing, substrate-interacting helix surface. *Cell* **134**:439–450. DOI: https://doi.org/10.1016/j.cell.2008.06.007, PMID: 18692467

Allison DS, Schatz G. 1986. Artificial mitochondrial presequences. *PNAS* **83**:9011–9015. DOI: https://doi.org/10.1073/pnas.83.23.9011, PMID: 3024162

Barbot M, Jans DC, Schulz C, Denkert N, Kroppen B, Hoppert M, Jakobs S, Meinecke M. 2015. Mic10 oligomerizes to bend mitochondrial inner membranes at cristae junctions. *Cell Metabolism* **21**:756–763. DOI: https://doi.org/10.1016/j.cmet.2015.04.006, PMID: 25955211

Barbot M, Meinecke M. 2016. Reconstitutions of mitochondrial inner membrane remodeling. *Journal of Structural Biology* **196**:20–28. DOI: https://doi.org/10.1016/j.jsb.2016.07.014, PMID: 27456366

Chacinska A, Lind M, Frazier AE, Dudek J, Meisinger C, Geissler A, Sickmann A, Meyer HE, Truscott KN, Guiard B, Pfanner N, Rehling P. 2005. Mitochondrial presequence translocase: switching between TOM tethering and motor recruitment involves Tim21 and Tim17. *Cell* **120**:817–829. DOI: https://doi.org/10.1016/j.cell.2005.01.011, PMID: 15797382

Demishtein-Zohary K, Marom M, Neupert W, Mokranjac D, Azem A. 2015. GxxxG motifs hold the TIM23 complex together. *FEBS Journal* **282**:2178–2186. DOI: https://doi.org/10.1111/febs.13266, PMID: 25765297

du Plessis DJ, Nouwen N, Driessen AJ. 2011. The Sec translocase. *Biochimica et Biophysica Acta (BBA) - Biomembranes* **1808**:851–865. DOI: https://doi.org/10.1016/j.bbamem.2010.08.016, PMID: 20801097

Endo T, Yamano K. 2009. Multiple pathways for mitochondrial protein traffic. *Biological Chemistry* **390**:723–730. DOI: https://doi.org/10.1515/BC.2009.087, PMID: 19453276

Geissler A, Chacinska A, Truscott KN, Wiedemann N, Brandner K, Sickmann A, Meyer HE, Meisinger C, Pfanner N, Rehling P. 2002. The mitochondrial presequence translocase: an essential role of Tim50 in directing preproteins to the import channel. *Cell* **111**:507–518. DOI: https://doi.org/10.1016/S0092-8674(02)01073-5, PMID: 12437924

Gornicka A, Bragoszewski P, Chroscicki P, Wenz LS, Schulz C, Rehling P, Chacinska A. 2014. A discrete pathway for the transfer of intermembrane space proteins across the outer membrane of mitochondria. *Molecular Biology of the Cell* **25**:3999–4009. DOI: https://doi.org/10.1091/mbc.E14-06-1155, PMID: 25318675

Harsman A, Bartsch P, Hemmis B, Krüger V, Wagner R. 2011. Exploring protein import pores of cellular organelles at the single molecule level using the planar lipid bilayer technique. *European Journal of Cell Biology* **90**:721–730. DOI: https://doi.org/10.1016/j.ejcb.2011.04.012, PMID: 21684628

Harsman A, Krüger V, Bartsch P, Honigmann A, Schmidt O, Rao S, Meisinger C, Wagner R. 2010. Protein conducting nanopores. *Journal of Physics: Condensed Matter* **22**:454102. DOI: https://doi.org/10.1088/0953-8984/22/45/454102, PMID: 21339590

Herrmann JM, Westermann B, Neupert W. 2001. Analysis of protein-protein interactions in mitochondria by coimmunoprecipitation and chemical cross-linking. *Methods in cell biology* **65**:217–230. DOI: https://doi.org/10.1016/S0091-679X(01)65013-1, PMID: 11381595

Hotz T, Schütte OM, Sieling H, Polupanow T, Diederichsen U, Steinem C, Munk A. 2013. Idealizing ion channel recordings by a jump segmentation multiresolution filter. *IEEE Transactions on NanoBioscience* **12**:376–386. DOI: https://doi.org/10.1109/TNB.2013.2284063, PMID: 24235310

Ieva R, Schrempp SG, Opaliński L, Wollweber F, Höß P, Heißwolf AK, Gebert M, Zhang Y, Guiard B, Rospert S, Becker T, Chacinska A, Pfanner N, van der Laan M. 2014. Mgr2 functions as lateral gatekeeper for preprotein sorting in the mitochondrial inner membrane. *Molecular Cell* **56**:641–652. DOI: https://doi.org/10.1016/j.molcel.2014.10.010, PMID: 25454944

Im W, Roux B. 2002. Ion permeation and selectivity of OmpF porin: a theoretical study based on molecular dynamics, Brownian dynamics, and continuum electrodiffusion theory. *Journal of Molecular Biology* **322**:851–869. DOI: https://doi.org/10.1016/S0022-2836(02)00778-7, PMID: 12270719

Krüger V, Deckers M, Hildenbeutel M, van der Laan M, Hellmers M, Dreker C, Preuss M, Herrmann JM, Rehling P, Wagner R, Meinecke M. 2012. The mitochondrial oxidase assembly protein1 (Oxa1) insertase forms a membrane pore in lipid bilayers. *Journal of Biological Chemistry* **287**:33314–33326. DOI: https://doi.org/10.1074/jbc.M112.387563, PMID: 22829595

Kutzner C, Grubmüller H, de Groot BL, Zachariae U. 2011. Computational electrophysiology: the molecular dynamics of ion channel permeation and selectivity in atomistic detail. *Biophysical Journal* **101**:809–817. DOI: https://doi.org/10.1016/j.bpj.2011.06.010, PMID: 21843471

Lohret TA, Jensen RE, Kinnally KW. 1997. Tim23, a protein import component of the mitochondrial inner membrane, is required for normal activity of the multiple conductance channel, MCC. *The Journal of Cell Biology* **137**:377–386. DOI: https://doi.org/10.1083/jcb.137.2.377, PMID: 9128249

Lytovchenko O, Melin J, Schulz C, Kilisch M, Hutu DP, Rehling P. 2013. Signal recognition initiates reorganization of the presequence translocase during protein import. *The EMBO Journal* **32**:886–898. DOI: https://doi.org/10.1038/emboj.2013.23, PMID: 23403928

Maarse AC, Blom J, Keil P, Pfanner N, Meijer M. 1994. Identification of the essential yeast protein MIM17, an integral mitochondrial inner membrane protein involved in protein import. *FEBS Letters* **349**:215–221. DOI: https://doi.org/10.1016/0014-5793(94)00669-5, PMID: 8050569

Mahendran KR, Romero-Ruiz M, Schlösinger A, Winterhalter M, Nussberger S. 2012. Protein translocation through Tom40: kinetics of peptide release. *Biophysical Journal* **102**:39–47. DOI: https://doi.org/10.1016/j.bpj.2011.11.4003, PMID: 22225796

Malhotra K, Sathappa M, Landin JS, Johnson AE, Alder NN. 2013. Structural changes in the mitochondrial Tim23 channel are coupled to the proton-motive force. *Nature Structural & Molecular Biology* **20**:965–972. DOI: https://doi.org/10.1038/nsmb.2613, PMID: 23832274

Martinez-Caballero S, Grigoriev SM, Herrmann JM, Campo ML, Kinnally KW. 2007. Tim17p regulates the twin pore structure and voltage gating of the mitochondrial protein import complex TIM23. *Journal of Biological Chemistry* **282**:3584–3593. DOI: https://doi.org/10.1074/jbc.M607551200, PMID: 17148445

Meinecke M, Bartsch P, Wagner R. 2016. Peroxisomal protein import pores. *Biochimica Et Biophysica Acta (BBA) - Molecular Cell Research* **1863**:821–827. DOI: https://doi.org/10.1016/j.bbamcr.2015.10.013, PMID: 26497277

Meinecke M, Wagner R, Kovermann P, Guiard B, Mick DU, Hutu DP, Voos W, Truscott KN, Chacinska A, Pfanner N, Rehling P. 2006. Tim50 maintains the permeability barrier of the mitochondrial inner membrane. *Science* **312**:1523–1526. DOI: https://doi.org/10.1126/science.1127628, PMID: 16763150

Montilla-Martinez M, Beck S, Klümper J, Meinecke M, Schliebs W, Wagner R, Erdmann R. 2015. Distinct Pores for Peroxisomal Import of PTS1 and PTS2 Proteins. *Cell Reports* **13**:2126–2134. DOI: https://doi.org/10.1016/j.celrep.2015.11.016, PMID: 26673321

Neupert W, Brunner M. 2002. The protein import motor of mitochondria. *Nature Reviews Molecular Cell Biology* **3**:555–565. DOI: https://doi.org/10.1038/nrm878, PMID: 12154367

Neupert W, Herrmann JM. 2007. Translocation of proteins into mitochondria. *Annual Review of Biochemistry* **76**:723–749. DOI: https://doi.org/10.1146/annurev.biochem.76.052705.163409, PMID: 17263664

Ramesh A, Peleh V, Martinez-Caballero S, Wollweber F, Sommer F, van der Laan M, Schroda M, Alexander RT, Campo ML, Herrmann JM. 2016. A disulfide bond in the TIM23 complex is crucial for voltage gating and mitochondrial protein import. *The Journal of Cell Biology* **214**:417–431. DOI: https://doi.org/10.1083/jcb.201602074, PMID: 27502485

Reinhold R, Krüger V, Meinecke M, Schulz C, Schmidt B, Grunau SD, Guiard B, Wiedemann N, van der Laan M, Wagner R, Rehling P, Dudek J. 2012. The channel-forming Sym1 protein is transported by the TIM23 complex in a presequence-independent manner. *Molecular and Cellular Biology* **32**:5009–5021. DOI: https://doi.org/10.1128/MCB.00843-12, PMID: 23045398

Ryan KR, Leung RS, Jensen RE. 1998. Characterization of the mitochondrial inner membrane translocase complex: the Tim23p hydrophobic domain interacts with Tim17p but not with other Tim23p molecules. *Molecular and Cellular Biology* **18**:178–187. DOI: https://doi.org/10.1128/MCB.18.1.178, PMID: 9418865

Schendzielorz AB, Schulz C, Lytovchenko O, Clancy A, Guiard B, Ieva R, van der Laan M, Rehling P. 2017. Two distinct membrane potential-dependent steps drive mitochondrial matrix protein translocation. *The Journal of Cell Biology* **216**:83–92. DOI: https://doi.org/10.1083/jcb.201607066, PMID: 28011846

Schmidt O, Pfanner N, Meisinger C. 2010. Mitochondrial protein import: from proteomics to functional mechanisms. *Nature Reviews Molecular Cell Biology* **11**:655–667. DOI: https://doi.org/10.1038/nrm2959, PMID: 20729931

Schulz C, Lytovchenko O, Melin J, Chacinska A, Guiard B, Neumann P, Ficner R, Jahn O, Schmidt B, Rehling P. 2011. Tim50's presequence receptor domain is essential for signal driven transport across the TIM23 complex. *The Journal of Cell Biology* **195**:643–656. DOI: https://doi.org/10.1083/jcb.201105098, PMID: 22065641

Sjuts I, Soll J, Bölter B. 2017. Import of Soluble Proteins into Chloroplasts and Potential Regulatory Mechanisms. *Frontiers in Plant Science* **8**:168. DOI: https://doi.org/10.3389/fpls.2017.00168, PMID: 28228773

Tarasenko D, Barbot M, Jans DC, Kroppen B, Sadowski B, Heim G, Möbius W, Jakobs S, Meinecke M. 2017. The MICOS component Mic60 displays a conserved membrane-bending activity that is necessary for normal cristae morphology. *The Journal of Cell Biology* **216**:889–899. DOI: https://doi.org/10.1083/jcb.201609046, PMID: 28254827

Tecuapetla-Gómez I, Munk A. 2015. Autocovariance estimation in regression with a discontinuous signal and $m $-dependent errors: A difference-based approach. *arXiv*. 1507.02485.

Truscott KN, Kovermann P, Geissler A, Merlin A, Meijer M, Driessen AJ, Rassow J, Pfanner N, Wagner R. 2001. A presequence- and voltage-sensitive channel of the mitochondrial preprotein translocase formed by Tim23. *Nature Structural Biology* **8**:1074–1082. DOI: https://doi.org/10.1038/nsb726, PMID: 11713477

van der Laan M, Meinecke M, Dudek J, Hutu DP, Lind M, Perschil I, Guiard B, Wagner R, Pfanner N, Rehling P. 2007. Motor-free mitochondrial presequence translocase drives membrane integration of preproteins. *Nature Cell Biology* **9**:1152–1159. DOI: https://doi.org/10.1038/ncb1635, PMID: 17828250

van Meer G, Voelker DR, Feigenson GW. 2008. Membrane lipids: where they are and how they behave. *Nature Reviews Molecular Cell Biology* **9**:112–124. DOI: https://doi.org/10.1038/nrm2330, PMID: 18216768

Vögtle FN, Wortelkamp S, Zahedi RP, Becker D, Leidhold C, Gevaert K, Kellermann J, Voos W, Sickmann A, Pfanner N, Meisinger C. 2009. Global analysis of the mitochondrial N-proteome identifies a processing peptidase critical for protein stability. *Cell* **139**:428–439. DOI: https://doi.org/10.1016/j.cell.2009.07.045, PMID: 19837041

eLIFE elifesciences.org

RESEARCH ARTICLE

Figures and figure supplements

Cation selectivity of the presequence translocase channel Tim23 is crucial for efficient protein import

Niels Denkert *et al*

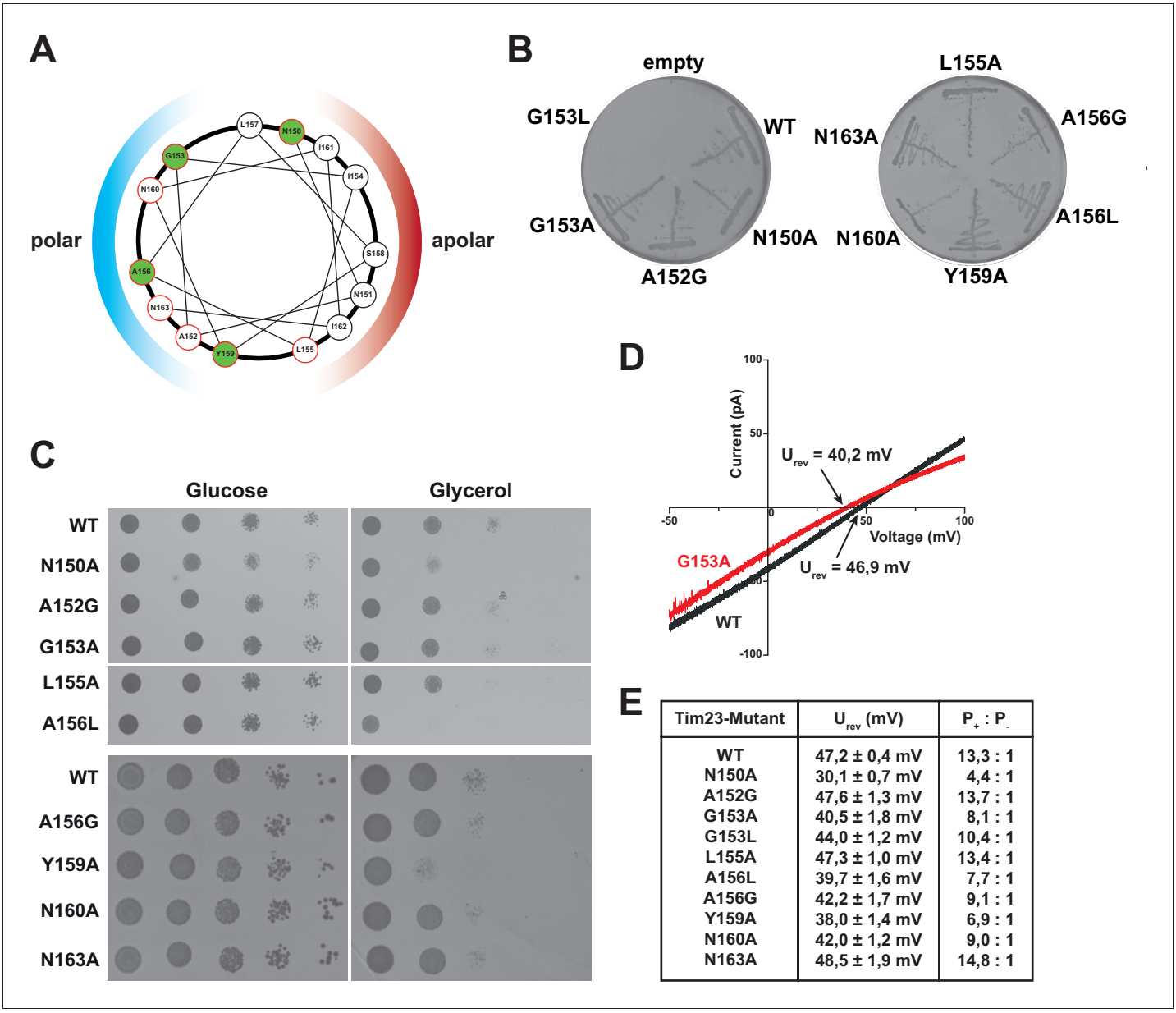

Tim23-Mutant	U_{rev} (mV)	$P_+ : P_-$
WT	47,2 ± 0,4 mV	13,3 : 1
N150A	30,1 ± 0,7 mV	4,4 : 1
A152G	47,6 ± 1,3 mV	13,7 : 1
G153A	40,5 ± 1,8 mV	8,1 : 1
G153L	44,0 ± 1,2 mV	10,4 : 1
L155A	47,3 ± 1,0 mV	13,4 : 1
A156L	39,7 ± 1,6 mV	7,7 : 1
A156G	42,2 ± 1,7 mV	9,1 : 1
Y159A	38,0 ± 1,4 mV	6,9 : 1
N160A	42,0 ± 1,2 mV	9,0 : 1
N163A	48,5 ± 1,9 mV	14,8 : 1

Figure 1. Substitutions of pore-lining residues of Tim23 reduce the channel's ion selectivity and lead to a growth defect in *S. cerevisiae*. (**A**) Helical wheel projection of amino acid residues 150–163 of the second transmembrane helix of Tim23. Highlighted residues in green indicate near 100% conservation. Colored hemispheres indicates polar/apolar facing regions of helix. Residues mutated in this study are circled in red. (**B**) *S. cerevisiae* strains with chromosomal deletion of the *TIM23* gene, complemented by a plasmid carrying both *URA3* and *TIM23* gene, were transformed with plasmids containing wild type *TIM23* or mutants and tested for viability after plasmid loss on 5-FOA containing medium. (**C**) *tim23Δ* yeast cells with plasmids containing wild type *TIM23* or pore-lining mutants were grown on fermentable (left) or non-fermentable (right) media at 37°C. Strains WT to A156L were grown on a single plate each for glucose and glycerol respectively. (**D**) Electrophysiological current-voltage (I–V) curves were recorded at asymmetrical buffer conditions with 12.5-fold KCl gradient for Tim23 (grey) or $Tim23^{G153A}$ (red) to determine reversal potentials. (**E**) Reversal potentials U_{rev} were experimentally determined for wild type Tim23 and all mutants by independent triplicates at asymmetrical buffer conditions, the ion selectivity was calculated from the mean reversal potential following the Goldman-Hodgkin-Katz equation. Errors represent standard deviation.
DOI: https://doi.org/10.7554/eLife.28324.003

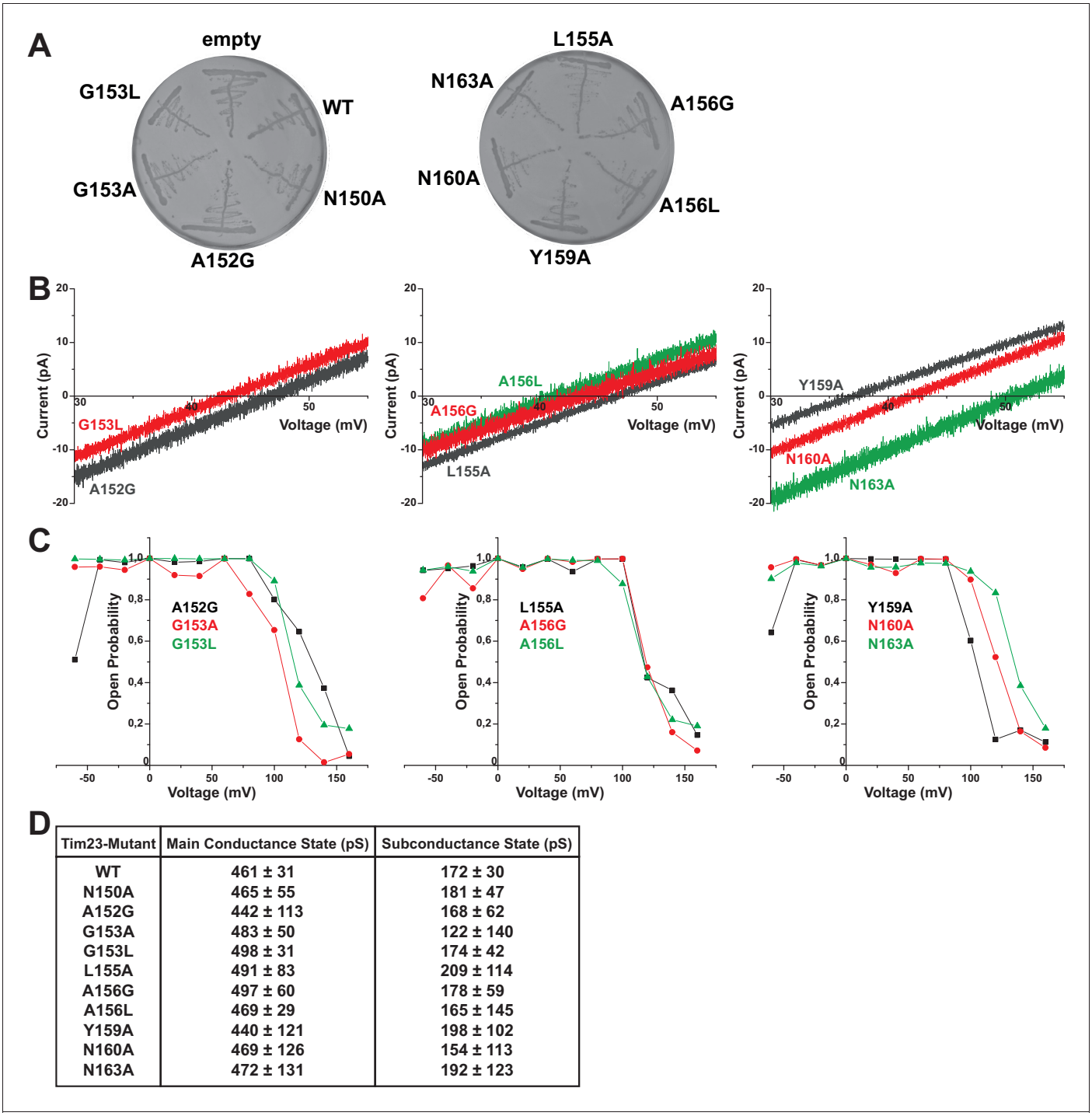

D

Tim23-Mutant	Main Conductance State (pS)	Subconductance State (pS)
WT	461 ± 31	172 ± 30
N150A	465 ± 55	181 ± 47
A152G	442 ± 113	168 ± 62
G153A	483 ± 50	122 ± 140
G153L	498 ± 31	174 ± 42
L155A	491 ± 83	209 ± 114
A156G	497 ± 60	178 ± 59
A156L	469 ± 29	165 ± 145
Y159A	440 ± 121	198 ± 102
N160A	469 ± 126	154 ± 113
N163A	472 ± 131	192 ± 123

Figure 1—figure supplement 1. Electrophysiological screening of Tim23 mutants. (**A**) *S. cerevisiae* cells with chromosomal deletion of the *TIM23* gene, complemented by a plasmid carrying both *URA3* and *TIM23* gene, were transformed with plasmids containing *HIS3* gene and wild type *TIM23* or mutants. Cells were tested for proper plasmid transformation on -His selective medium. (**B**) I-V curves of all mutants not shown in ***Figure 1*** or ***Figure 3***. Recorded under asymmetric buffer conditions with 12.5-fold KCl-gradient. (**C**) Open probabilities of all mutants not shown in ***Figure 3*** were calculated from one full set of constant-voltage recordings (from −60 mV to +160 mV) each. (**D**) Table of main and primary subconductance states of wild type Tim23 and all mutants were determined by Gaussian fits from gating event histograms (as shown in ***Figure 3B***). Mean and errors represent center and FWHM of Gaussian fits. For Tim23 and Tim23^{N150A}, more than 2000 gating events from three independent full sets of recordings and for every other mutant more than 700 gating events from one full set of recordings were analyzed each.

DOI: https://doi.org/10.7554/eLife.28324.004

Figure 1—figure supplement 2. Sequence conservation of Tim23. Sequence alignment of Tim23 proteins from different species (*Homo sapiens, Rattus norvegicus, Saccharomyces cerevisiae, Danio rerio, Neurospora crassa*). Sequence consensus as computed by ClustalW: * identity; : high similarity; . low similarity. Mutations used in this study are boxed in red.

DOI: https://doi.org/10.7554/eLife.28324.005

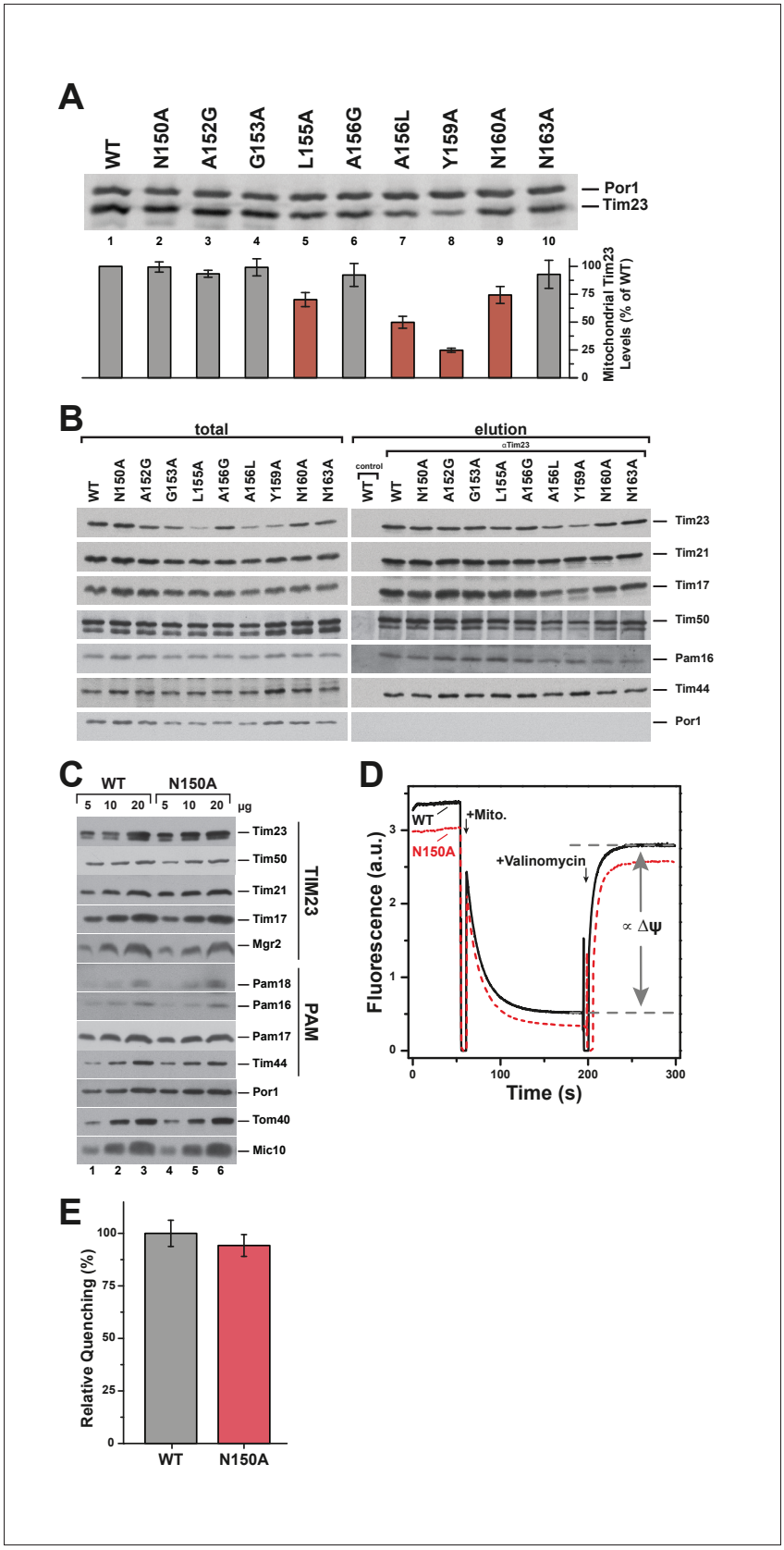

Figure 2. Pore-lining mutant Tim23^{N150A} is properly expressed and integrated into TIM23 complexes. (**A**) Mitochondrial steady state levels of yeast expressing wild type Tim23 or mutants were assessed by Western blot

Figure 2 continued on next page

Figure 2 continued

analysis (upper) with decoration against Tim23 and Por1 (mitochondrial outer membrane). Protein levels were quantified using fluorescently labelled secondary antibodies in four independent experiments and normalized by mitochondrial Por1 levels. Significantly reduced levels are indicated in red. Error bars represent standard error of the mean. (**B**) TIM23 complex integrity and recruitment of PAM complex of wild type and Tim23 mutants was examined by co-immunoprecipitation of mitochondrial lysates using Tim23 antibodies. (**C**) Isolated mitochondria containing Tim23 or $Tim23^{N150A}$ were Western blotted and decorated against proteins of the TIM23 complex, the PAM complex, Por1 and Tom40 (both mitochondrial outer membrane) and Mic10 (mitochondrial inner membrane). (**D**) Membrane potential $\Delta\Psi$ was assessed by adding isolated mitochondria containing Tim23 (black solid) or $Tim23^{N150A}$ (red dashed) to the fluorophore $DiSC_3(5)$, then dissipating $\Delta\Psi$ with valinomycin and determining the amount of quenching. Grey dashed lines and arrows indicate the parameter quantified in (**D**). (**E**) Relative fluorophore quenching as a measure of membrane potential $\Delta\Psi$ for Tim23 (grey) and $Tim23^{N150A}$ (red) was quantified (as depicted in C) in three independent experiments. Error bars represent standard error of the mean before normalization.

DOI: https://doi.org/10.7554/eLife.28324.006

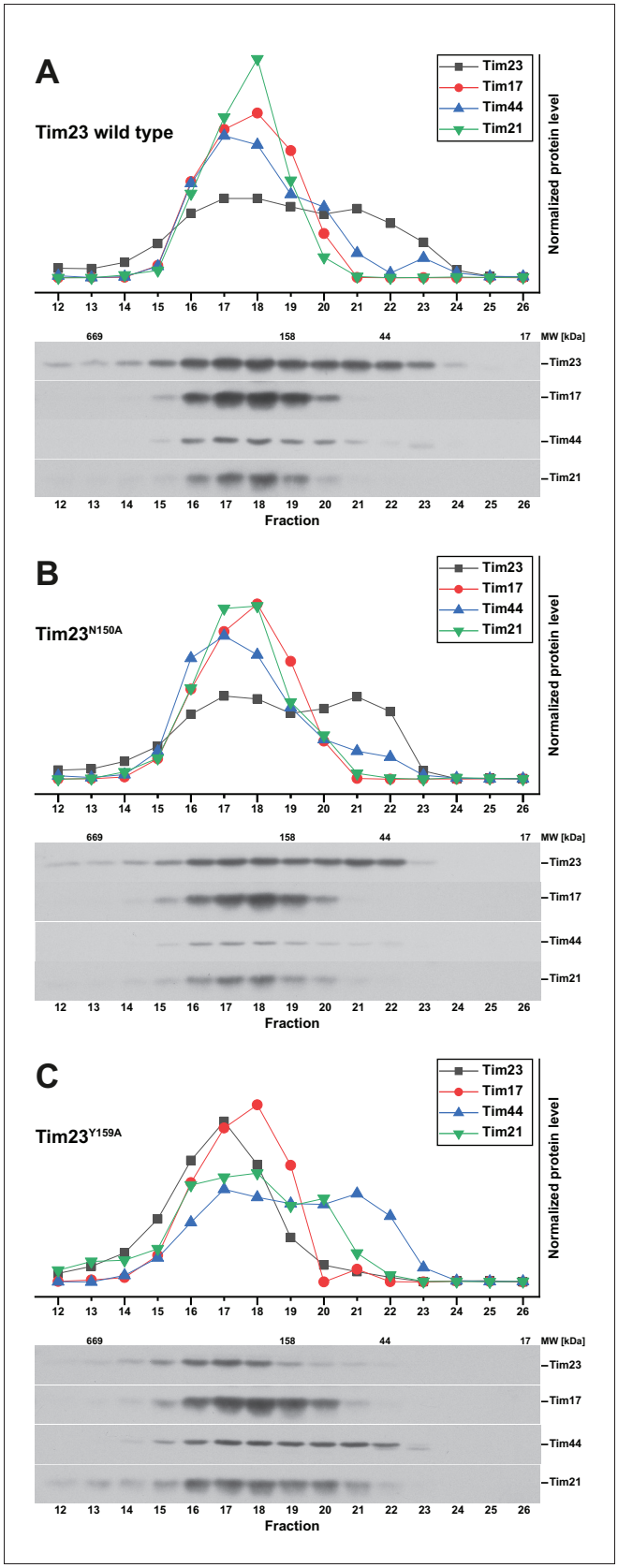

Figure 2—figure supplement 1. TIM23 complex characterization by size exclusion chromatography profiles. (**A**) – (**C**) Relative elution profile of the TIM23 complex (top) was assessed by quantification of Western blots (bottom)

Figure 2—figure supplement 1 continued on next page

Figure 2—figure supplement 1 continued

after size exclusion chromatography of solubilized mitochondria containing Tim23 wild type (**A**), Tim23^{N150A} (**B**) and Tim23^{Y159} (**C**).

DOI: https://doi.org/10.7554/eLife.28324.007

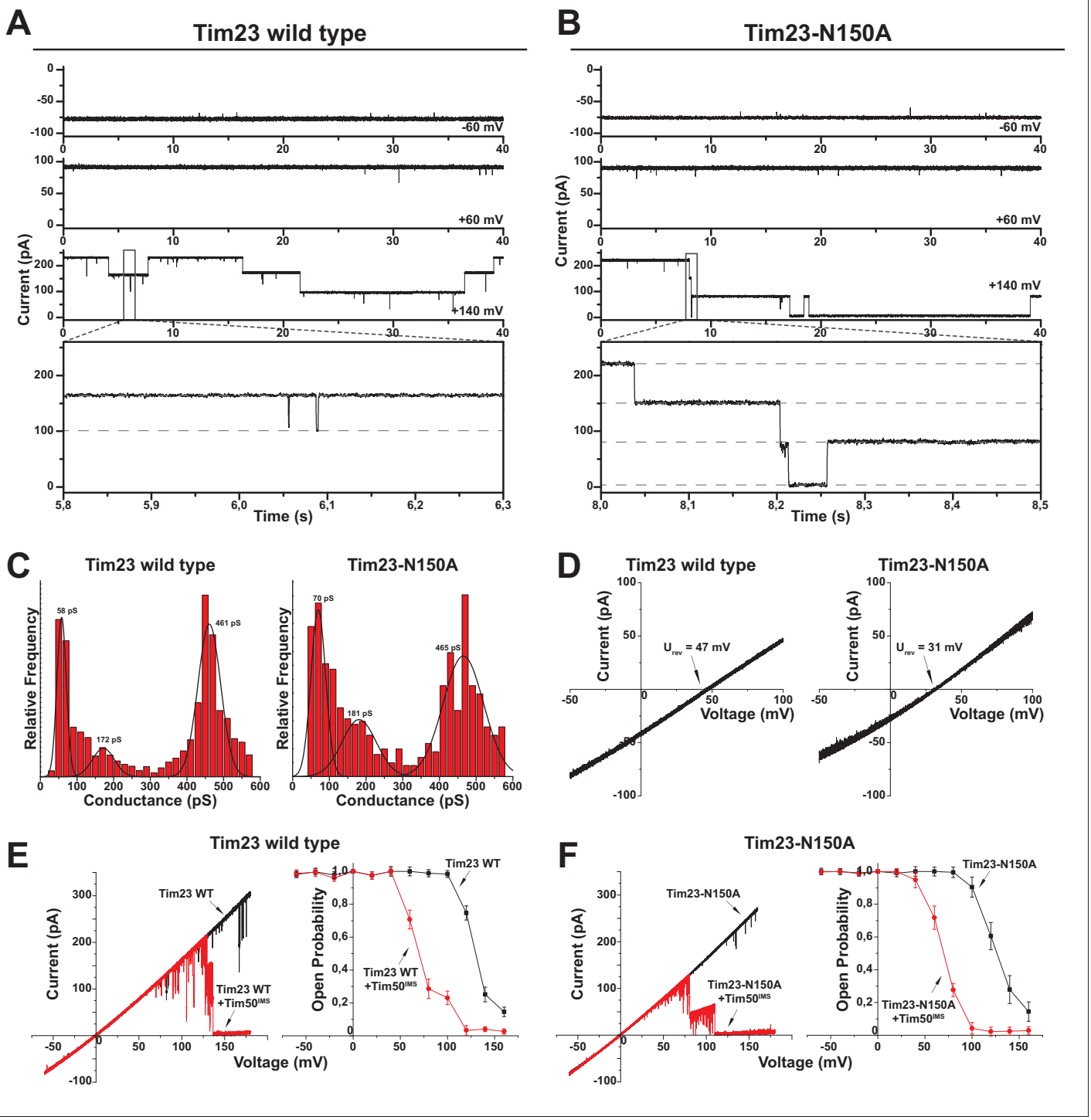

Figure 3. Tim23^{N150A} displays reduced cation preference. (**A**)/(**B**) Tim23- (**A**) or Tim23^{N150A}-containing (**B**) proteoliposomes were fused with planar lipid bilayers and single-channel activity was characterized by electrophysiological current recordings. (**C**) Gating event histograms for Tim23 (left) and Tim23^{N150A} (right) were calculated from constant-voltage recordings (as depicted in A) with at least 2000 gating events each. The three most prominent classes of conductance changes were modeled with a Gaussian fit. (**D**) I-V curves at asymmetrical buffer conditions were recorded for Tim23 (left) and Tim23^{N150A} (right) with indicated reversal potential U_{rev} for 12.5-fold KCl-gradient. (**E**)/(**F**) I-V curves (left) and open probabilities (right) were determined for bilayer incorporated Tim23 (**E**) or Tim23^{N150A} (**F**) before (black) and after (red) addition of 700 nM Tim50^{IMS} to IMS-side of the channel. Error bars represent standard deviation (SD, n = 3).

DOI: https://doi.org/10.7554/eLife.28324.008

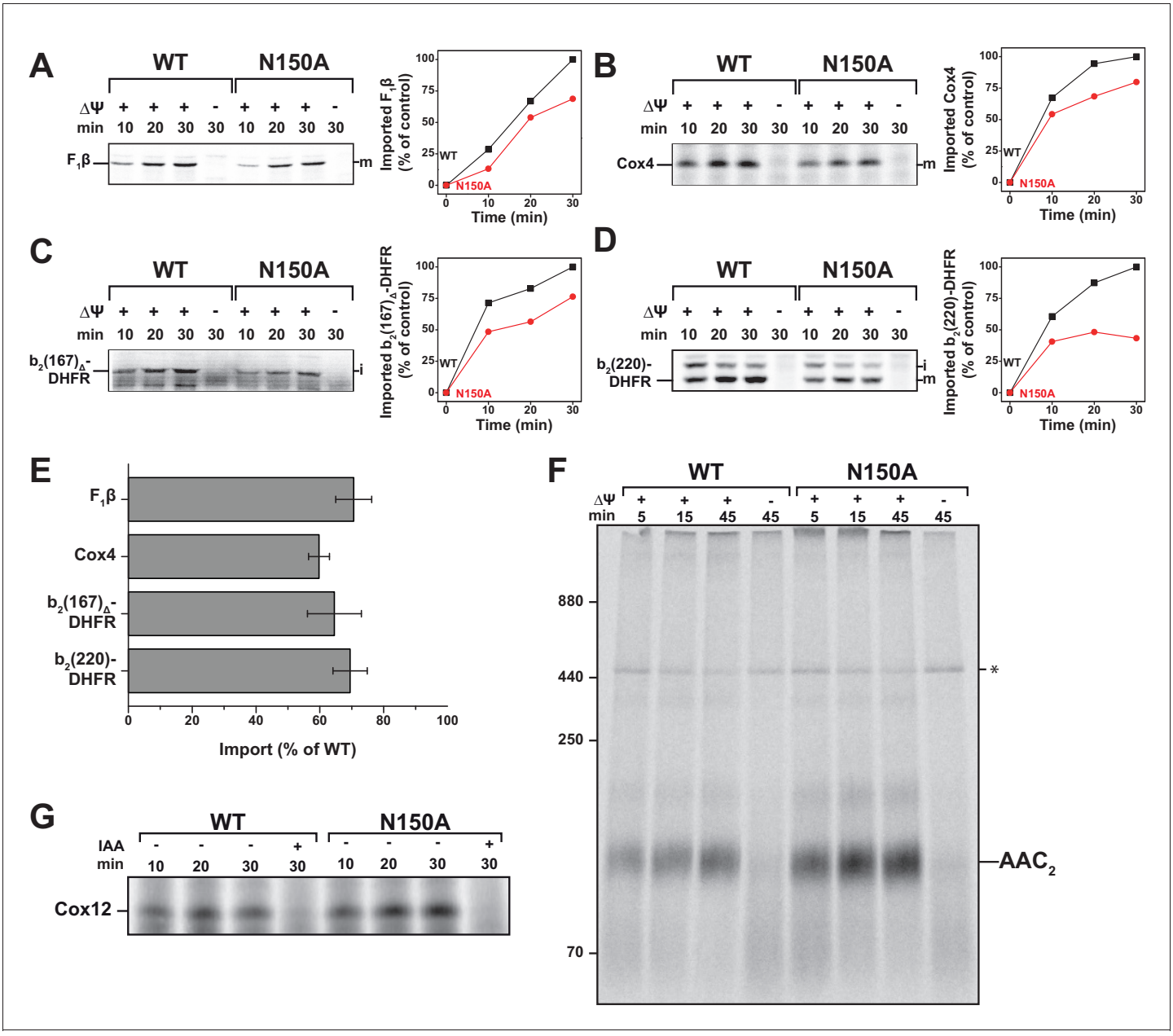

Figure 4. Tim23^{N150A} exhibits significant import defects for various TIM23 substrates. (**A–D**) Import capability of wild type and tim23^{N150A} mutant mitochondria was determined by incubating [^{35}S]-radiolabeled matrix destined precursors $F_1\beta$ (**A**), Cox4 (**B**), $b_2(167)_\Delta$-DHFR (**C**) or the inner membrane sorted b_2(220)-DHFR (**D**) with isolated mitochondria for 10, 20 or 30 min. The import reactions were stopped by dissipating $\Delta\Psi$ and subsequent Proteinase K (PK)-digest. Digital autoradiographs (left) were analyzed and quantified (right). Maximum import into wild type mitochondria was set to 100%. (**E**) Relative import efficiency after 15 min of import into mitochondria containing Tim23^{N150A} was quantified for different substrates. Error bars represent standard error of the mean (SEM, n = 3). (**F**) Carrier import into Tim23^{N150A}-containing mitochondria was assessed via ADP/ATP carrier (AAC) complex assembly by incubating [^{35}S]-radiolabeled AAC with isolated mitochondria for 15, 30 or 45 min. The import reaction was stopped by dissipating $\Delta\Psi$ and subsequent PK-digest. Assembly of AAC dimer was monitored by BN-PAGE. (**G**) The MIA substrate Cox12 was [^{35}S]-radiolabeled and imported into Tim23^{N150A}-containing mitochondria for 10, 20 or 30 min. The import reaction was stopped by addition of iodoacetamide (IAA) and subsequent PK-digest.

DOI: https://doi.org/10.7554/eLife.28324.009

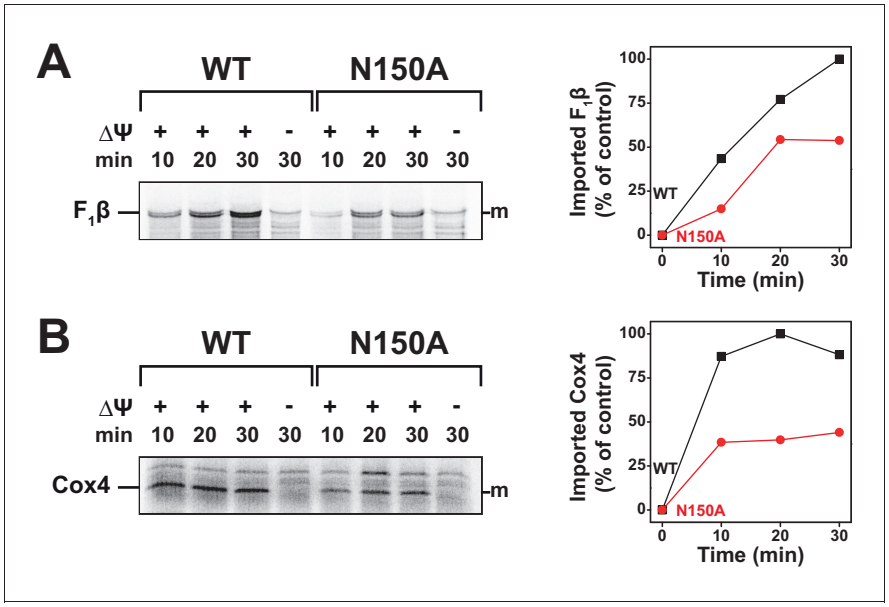

Figure 4—figure supplement 1. Import of TIM23-substrates at non-permissive temperatures. (**A** and **B**) Temperature influence on import capability of $Tim23^{N150A}$ was assessed by incubating [^{35}S]-radiolabeled $F_1\beta$ (**A**) or Cox4 (**B**) with isolated mitochondria for 10, 20 or 30 min at 37°C. Maximum import into wild type mitochondria was set to 100%.

DOI: https://doi.org/10.7554/eLife.28324.010

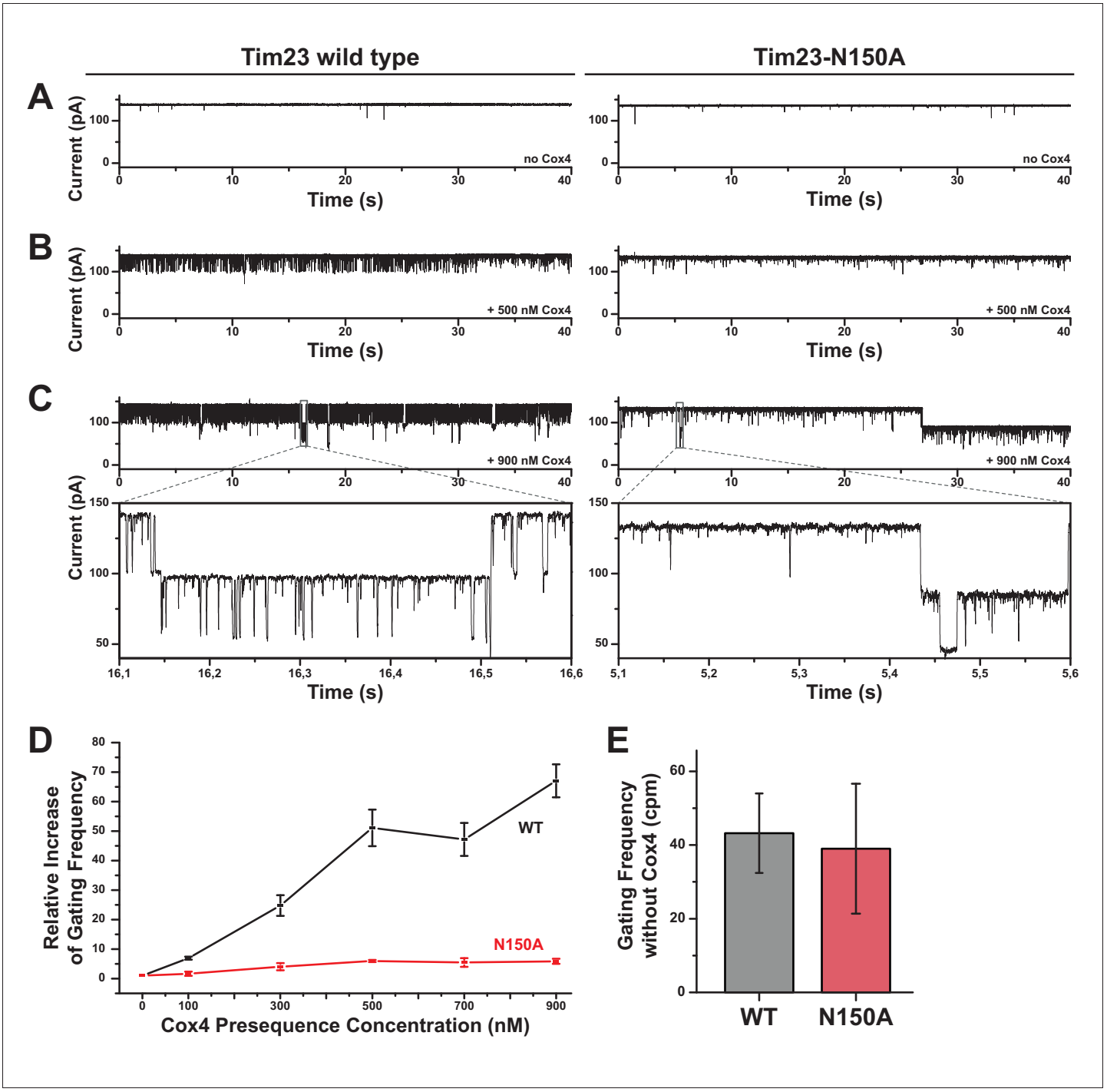

Figure 5. Increased gating frequency as a measure of channel response to presequence titration is heavily reduced for Tim23^{N150A}. (**A**) Bilayer-incorporated Tim23 (left) or Tim23^{N150A} (right) single-channel currents were recorded at +80 mV before addition of Cox4 presequence peptide. (**B**)/(**C**) Current recordings of wild type (left) and mutant (right) channels were performed after each titration step. (**D**) Channel response of Tim23 (black) and Tim23^{N150A} (red) after addition of Cox4 presequence was quantified by counting gating events and calculating the relative increase in activity compared to unstimulated channels. Error bars represent standard deviation. (**E**) Absolute gating frequency of unstimulated Tim23 and Tim23^{N150A} was determined from current recordings before presequence titration. Error bars represent standard deviation (SD, n = 3).

DOI: https://doi.org/10.7554/eLife.28324.011

3. Discussion

Since the first protein conducting translocase in mitochondria was discovered in the 1980s, the field has made great progress in identifying new import complexes and defining their subunit composition and substrate spectrum (Dudek et al., 2013; Wiedemann and Pfanner, 2017). High-end mass spectrometry has made it possible to not only delineate the core components of protein complexes, but also to pinpoint interactions between different protein import complexes, as well as with complexes that shape mitochondrial membranes, or with metabolite carriers (Horvath et al., 2015; Mehnert et al., 2014; Qiu et al., 2013). However, the basic mechanistic principals of protein transport are still not understood, mainly due to a lack of 3D structures of membrane components of the translocases and efficient reconstitution systems to study protein import in isolated systems. As a consequence, the mechanism of how proteins are translocated into mitochondria is only partially understood. The $\Delta\psi$ seems to drive import of almost all inner membrane proteins and matrix targeted proteins and is believed to act on the positive charges in the presequence of TIM23 substrates (Martin et al., 1991; Schleyer et al., 1982). However, the influence of $\Delta\psi$ on the mature part of the protein has not been considered. Moreover, it was observed that $\Delta\psi$ modulates the gating activity of TIM23 channel, but if and how this contributes to protein translocation is not understood (Truscott et al., 2001). Likewise, it became apparent that the TOM and TIM23 channels don´t only act as passive pores that allow precursor passage, but actively contribute to protein translocation by interaction with the precursor (Esaki et al., 2003; Melin et al., 2014). In this study, I extended our understanding of the role of $\Delta\psi$ in presequence protein import by showing that $\Delta\psi$ also acts on the mature part of the protein. In contrast to previous reports, I showed that Pam17 is not a motor component but only binds to the motor free version of TIM23, where it supports import of strongly $\Delta\psi$ dependent precursors. Pam17 association with the translocase is mediated by Tim50 and takes place in an early step of protein import (1st manuscript). Moreover, I analyzed pore-lining, highly conserved amino acids in the second TM of Tim23 and showed that mutation of these residues leads to reduced cation selectivity of the Tim23 channel. For one of these mutations (N150A), $\Delta\psi$, protein stability and TIM23 independent import pathways remained unaffected in

yeast, while presequence substrate translocation is diminished. This highlights an active contribution of the channel to protein translocation (2nd manuscript).

3.1 The role of membrane potential in presequence import

3.1.1 Matrix-destined precursor proteins display differential dependencies on Tim50

Tim50 is the major presequence receptor in the inner mitochondrial membrane and binds to presequences once they emerge from the TOM complex. Most likely, Tim50 receives the preprotein from $Tom22^{IMS}$, probably with the help of Tim21. Binding of a substrate to Tim50 triggers Tim21 release and the opening of the Tim23 channel. The substrate is then handed over from Tim50 to Tim23 and enters the channel formed by Tim23 and Tim17. Current concepts state that for all TIM23 substrates that are either targeted to the inner membrane or to the matrix the mechanism is the same up to this point. Consequently, one would expect motor dependent and independent substrates to require Tim50 function to the same extend. However, a surprising observation is that motor dependent substrates display a strong dependence on Tim50 for import, while inner membrane proteins that are motor independent are much less affected when Tim50 levels are reduced (Geissler et al., 2002). In order to address this conundrum, I have extended the substrate spectrum and imported a wide variety of motor dependent substrates into mitochondria with reduced Tim50 levels. Interestingly, for the reported substrates, $F_1\beta$ and the fusion protein $b_2(167)_\Delta$-DHFR, I found the same strong reduction in import, while the inner membrane protein cytochrome c_1 was much less affected. However, import of two other soluble matrix proteins, namely $F_1\alpha$ and Tim44, was also less affected and more comparable to the import of inner membrane proteins like cytochrome c_1. Since protein levels of TIM23 components and control proteins were not altered, and $\Delta\psi$ was still intact in mitochondria with reduced amounts of Tim50, unspecific effects due to the down-regulation of Tim50 were unlikely. This was also confirmed by the use of a temperature sensitive Tim50 strain, which showed the same import defect. Tim50 acts very early in protein import across the inner membrane and based on its known

functions, the difference in Tim50 dependencies for motor dependent proteins could not be explained.

3.1.2 Tim50 is important for Pam17 recruitment

One possible explanation could be that the lack of Tim50 leads to a reduction of motor components at the translocase, either by deficiencies in their recruitment, by overall complex instability, or by an unknown mechanism.
To test this, I analyzed the TIM23 complex from mitochondria with reduced Tim50 levels and found that no subunit was affected by loss of Tim50 and the complex was still intact. Only the amount of the small membrane protein Pam17 was markedly reduced. Since steady state levels of Pam17 in the Tim50 depleted mitochondria were not affected, I concluded that the loss of Pam17 from the translocase is not an indirect effect due to impaired import of Pam17 in Tim50 lacking mitochondria. More likely, Tim50 recruits Pam17 directly or indirectly to the translocase. Interestingly, Pam17 was initially described as a motor complex protein, which is required for assembly of Pam16 and Pam18 into the complex (van der Laan et al., 2005). Therefore, loss of Pam17 from the translocase due to impairment of Tim50 could explain the selective import defect for some motor dependent substrates. Indeed, it was found that loss of Tim50 and Pam17 leads to the same import phenotype. Since Tim50 is essential and Pam17 is not, it cannot be concluded that the observed Tim50 phenotype is only a secondary effect of Pam17 loss. However, it can be speculated that in mitochondria with reduced Tim50 levels, the residual amount of Tim50 that is left is sufficient to allow for a certain level of protein import to still occur. Therefore, the additional reduction of Pam17 from the complex leads to an increased import defect for Pam17-dependent precursor proteins. In this scenario, the import defect caused by loss of Pam17 from the translocase would add to the probably more uniform defect caused by Tim50 reduction. Also, in *pam17*Δ mitochondria, the import of matrix-targeted proteins is not uniformly affected, but shows the same two classes of precursor proteins. Since Pam17 was reported to be a motor subunit, it was speculated that these proteins depend, to different extents, on motor function, probably due to a stronger fold of the precursor, which would require a stronger force to unfold prior to import.

3.1.3 Motor function is not affected by Pam17 loss

It was reported that Pam17 is required for Hsp70 co-chaperone assembly. However, in mitochondria with a reduced amount of Tim50 and concomitant loss of Pam17 from the TIM23 complex, the levels of Pam16 and Pam18 were not affected. Also, we could not reproduce the observation that Pam16 and Pam18 are lost from the TIM23 complexes in *pam17*Δ mitochondria (data not shown). This could be due to differences in buffers used for isolation of the complex or tags that were used to isolated the complex. Indeed, in the original publication, Tim23 with an N-terminal Protein A Tag expressed from plasmid was used, while I used antibodies against Tim23 to isolated endogenous Tim23 (van der Laan et al., 2005). Actually, *pam17*Δ mitochondria were not affected in motor function in our analysis. First of all, loss of Pam17 did not lead to a "pulling defect", measured by PK accessibility of a stalled precursor. In this assay, a precursor with a stably folded C-terminus, which cannot be translocated across the TOM complex, is imported into mitochondria. After dissipation of the membrane potential, backsliding of the precursor serves as an indication for motor function, which is assessed by addition of PK. Moreover, Pam17 could not be co-isolated with other motor components, like Tim44 or Pam16, and was not isolated together with a TOM-TIM23 supercomplex, which represents the active, motor engaged complex ((Popov-Celeketić et al., 2008a) and data not shown). Furthermore, if $b_2(167)_\Delta$-DHFR is expressed in cells in the presence of the folate analogue aminopterine, which leads to a stable fold of the C-terminus, a crosslink between Pam17 and Tim23 is reduced, which also indicates dissociation of Pam17 from the complex in the presence of a motor dependent preprotein (Popov-Celeketić et al., 2008a).

One should note that only one precursor was used to generate a stable translocation intermediate and that the import motor undergoes dynamic subunit exchange during precursor translocation (Schulz and Rehling, 2014). It can therefore not be excluded that Pam17 transiently associates with the active translocase at some stage during the Hsp70 cycle, which was not captured under the experimental conditions used here. Surprisingly, if a slightly longer version of the b_2 protein is used (b_2(220)-DHFR), which also contains the sorting signal, *pam17*Δ cells display a pulling defect (van der Laan et al., 2005). In this construct, the heme-binding domain is intact and able to

fold tightly, which renders the imported protein dependent on motor activity. How does this observation fit to our data indicating that Pam17 does not affect motor function? It was noticed that in *pam17*Δ mitochondria, the steady state levels of Mgr2 were significantly reduced, probably due to diminished import of Mgr2. Like *pam17*Δ mitochondria, *mgr2*Δ mitochondria do not display a general motor defect. However, Mgr2 seems to be located at or near the lateral gate of the TIM23 complex and influences lateral release kinetics. Loss of Mgr2 leads to faster release of sorted proteins, including b_2(220)-DHFR, which is then processed by Imp1 in the IMS and can slide back from the TOM complex into the cytosol. This is interpreted as a "motor-defect" in the pulling assay. I therefore concluded that Pam17 does not affect motor function and previous conclusions drawn using the b_2(220)-DHFR construct were misled by indirect effects caused by Mgr2 loss in *pam17*Δ mitochondria. It can be ruled out that the phenotype observed in a *pam17*Δ strain is caused by reduced levels of Mgr2. First of all, *pam17*Δ and *mgr2*Δ show very different phenotypes, with loss of Mgr2 leading to a faster sorting of membrane proteins, but almost no defect for matrix targeted protein import (Gebert et al., 2012; Ieva et al., 2014). Also, overexpression of Mgr2 in *pam17*Δ does not rescue the defects seen in *pam17*Δ cells (data not shown). Likewise, the import of the outer membrane protein Om45 depends on Pam17 but is unaffected in an *mgr2*Δ strain.

Finally, the precursors used in this study depend to the same extent on mtHsp70 function, ruling out a role of the motor in causing the differential dependencies on Pam17 or Tim50.

3.1.4 A second Δψ-dependent step acts an the mature part of precursor proteins

Since its discovery, different reports have suggested that Pam17 is not a classical motor protein and might act prior to motor function (Popov-Celeketić et al., 2008a; Schiller, 2009; Song et al., 2014). Not only can Pam17 not be co-isolated with other motor components, but the lack of Pam17 also has a different phenotype than other motor mutants. A point mutation in Tim44 (R180A) leads to a specific defect in the import of matrix targeted proteins (Schiller, 2009; Schiller et al., 2008). However, as expected for mutants affected in motor function, the initial Δψ dependent step of

presequence translocation is not affected in this Tim44 strain. Moreover, denaturing a precursor with urea prior to import also rescues the import defect seen in the R180A mutant. In contrast, in a *pam17*Δ strain, already the presequence translocation step is affected and urea treatment does not improve import into mitochondria (Schiller, 2009). Moreover, the outer membrane protein Om45, which depends on Tim23, Tim50 and Δψ, but not Hsp70, is also Pam17 dependent (Song et al., 2014). For Om45, it is not known if it only requires the receptor domains of the TIM23 complex, or also the channel. In any case, taken together, it is likely that Pam17 acts at a very early step of protein import. Also, Lytovchenko et al. reported that the addition of presequence peptides to isolated mitochondria leads to an increased interaction of Pam17 with the translocase (Lytovchenko et al., 2013). Moreover, I found that in mitochondria lacking Tim50, Pam17 recruitment by presequences is reduced (data not shown). Therefore, one could envision that the binding of a presequence to Tim50 triggers Pam17 binding. However, switching the presequence between $F_1\alpha$ and $F_1\beta$ did not change the dependency of these proteins on Pam17. Also, fusion of different presequences to the passenger protein DHFR did not lead to import defects in *pam17*Δ mitochondria, reflecting the import rate for the full-length protein (data not shown). Surprisingly, switching the presequence also did not change the dependency of these precursors on the receptor Tim50, indicating that Pam17 levels might be rate limiting for protein import in mitochondria with reduced Tim50 levels.

Therefore, we investigated other factors that might be responsible for the differences in import efficiency. Besides ATP-dependent motor activity, Δψ is the second driving force for protein import across the inner membrane. It had previously been observed that precursors depend, to different extents, on Δψ (Geissler et al., 2000; Huang et al., 2002; Martin et al., 1991). And indeed, precursors that depend strongly on Pam17 are also more affected by changes in Δψ than precursors for which Pam17 was dispensable. Two reasons for differences in the Δψ dependencies of precursors have been discussed. On the one hand, the amount of positive charges in a presequence seems to play a role, with more positive charges rendering a presequence (and therefore the full-length protein) less susceptible to changes in Δψ (Martin et al., 1991). On the other hand, the length of a presequence and unfolded domains that reach through the TOM and TIM23 complex before a folded domain has to be unfolded at the TOM complex is important, since Δψ can unfold proteins in cases

were the presequence is not long enough to engage with Hsp70 (Huang et al., 2002). However, for $F_1\alpha$ and $F_1\beta$, the amount of positive charges is similar and still they respond differently to a reduction of $\Delta\psi$. Also, the overall length of the proteins is almost identical. Yet, denaturing precursors does not support import into *pam17*Δ mitochondria, making it unlikely that the folding state of the precursors plays a role.

It could be also envisioned that $\Delta\psi$ does not act solely on the presequence, but also on positive charges in the mature portion of the protein. Even though there is no obvious difference in charge distribution in the primary sequence of $F_1\alpha$ and $F_1\beta$, a detailed analysis of the primary sequence of many precursors of both classes should be conducted to find potential motifs that define the differences between these classes. For this, more precursors that are either strongly or only mildly $\Delta\psi$-dependent need to be identified.

Another possibility is that $\Delta\psi$ does not act on the mature region of the protein but on the protein-conducting channel. Electrophysiology experiments, with reconstituted Tim23 or with inner membrane vesicles, show that both Tim23 alone and the TIM23 complex are activated under low $\Delta\psi$ in the presence of presequences (Martinez-Caballero et al., 2007; Meinecke, 2006; Truscott et al., 2001). However, even in the absence of signal peptides, the channel gating activity increases significantly when $\Delta\psi$ is high. Additionally, Tim23 undergoes structural rearrangements in response to changes in $\Delta\psi$, independent of signal peptides. The activity of gating could directly contribute to protein translocation and might be modulated by Pam17. Therefore, the $\Delta\psi$ hypersensitive precursor might be strongly dependent on the second, presequence independent, channel activation step. This model is supported by a genetic screen, which identified a synthetic lethality between *pam17*Δ and *crd1*Δ, which encodes the cardiolipin synthase. In *crd1*Δ yeast strains, $\Delta\psi$ is affected due to defects in cardiolipin biosynthesis and therefore, reduced respiration (Hoppins et al., 2011). In the double deletion strain, the second presequence independent activation step of Tim23, which requires high $\Delta\psi$ and probably Pam17, might be strongly impaired which blocks protein import. Also other cardiolipin biogenesis mutants, namely *ups1*Δ and *ups2*Δ, display a genetic interaction with *pam17*Δ, even though the mechanism is not clear.

As to the order of events, the Pam17-dependent step appears to occur before the motor engages with the precursor and most likely is triggered by the recognition of presequences by one of the TIM23 components, probably Tim50.

3.1.5 A refined model for protein import

How can these results be merged with the known mechanism of TIM23-dependent protein import? In the prevailing model, the $TIM23^{SORT}$ complex or $TIM23^{CORE}$ complex engages with a presequence emerging from the TOM complex. This leads to release of Tim21 from the complex and Pam17 recruitment (Lytovchenko et al., 2013) (Figure 6).

However, in contrast to previous reports, Pam17 does not recruit the import motor, priming the complex for the import of matrix targeted proteins, but more likely affects the gating activity and thereby improves protein translocation. This form will be called $TIM23^{*}$ from here on. The $TIM23^{*}$ represents a highly active form of TIM23, which is required for both the import of sorted and of matrix targeted proteins. Indeed, I found that Pam17 is also required for the import of membrane inserted, motor-independent proteins (data not shown). After the initial step in import, Pam17 dissociates again from the translocase. In the case of matrix-targeted proteins, this is most likely accompanied by binding of the motor complex, even though the order of binding events is not known.

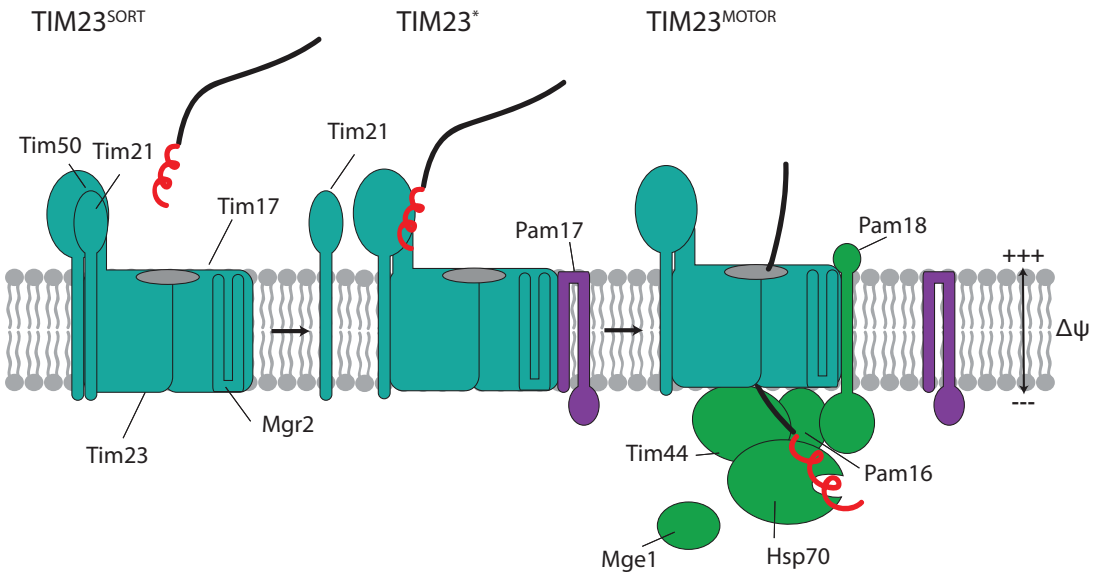

Figure 6: Function of Pam17 in protein import. The TIM23^{SORT} complex accepts substrates from the TOM complex. Recognition of a presequence by Tim50 releases Tim21 from the translocase and recruits Pam17. Pam17 supports translocation of the presequence and some portion of the mature protein through the TIM23 complex, probably by supporting the active gating form of TIM23. Once the motor engages with the substrate, Pam17 dissociates from the complex.

However, since Tim44 binds presequences and acts as a scaffold protein for both Hsp70 and the Pam16-Pam18 module, it seems likely that Tim44 is the first motor component to engage with the translocase. Tim44 then recruits all other motor components, which leads to import of the protein into the matrix. It will be interesting to test whether motor binding triggers the release of Pam17, or the other way around. In a temperature sensitive *tim44-804* strain, the amount of Pam17 bound to the translocase is increased which would argue for the first version. Based on the data at hand, it cannot be excluded that Pam17 binds to the translocase again at some point during motor cycle, however this seems unlikely.

3.2.1 Tim23 cation selectivity is crucial for presequence protein import

Tim23 is a polytopic inner mitochondrial membrane protein that was identified over 30 years ago (Dekker et al., 1993). Early studies showed that Tim23 acts as a voltage sensor that undergoes structural changes in response to altered Δψ and forms the protein conducting pore (Bauer et al., 1996; Lohret et al., 1997; Truscott et al., 2001).

Experiments with recombinant Tim23 reconstituted in lipid bilayers show that Tim23 can form a pore, independent of other TIM23 complex components, that exhibits similar characteristics to isolated TIM23 complexes, indicating that Tim23 is the main constituent of the channel (Martinez-Caballero et al., 2007; Meinecke, 2006; Truscott et al., 2001; van der Laan et al., 2007). Tim23 displays all attributes expected from a physiological channel, including high cation selectivity and a pore size that is large enough to accommodate an unfolded protein chain (Truscott et al., 2001). Due to the lack of high-resolution 3D structures, a detailed analysis of Tim23 characteristics, for example by the generation of mutants, has not been not possible. However, recent studies of Tim23 showed a clear amphipathic character of TM1 and TM2 and identified residues that face either the water filled channel or the lipid bilayer (Alder et al., 2008a; 2008b; Malhotra et al., 2013). TM2 of Tim23 undergoes structural rearrangement when $\Delta\psi$ is reduced and residues of TM2 could be crosslinked to a substrate *in transit* (Alder et al., 2008a; Malhotra et al., 2013). These advances enabled us to generate side-specific mutations of residues that face the water-filled pore and analyze their biophysical properties.

Interestingly, we found that mutations in channel-exposed residues of TM2 are essential for cation selectivity of the channel (Figure 7). Since all residues affecting ion selectivity are highly conserved in evolution, cation discrimination might be essential for presequence protein import. Of note, the channel diameter is large enough to allow passage for many ions at the same time, but still Tim23 has a high preference for cations (Meinecke, 2006; Truscott et al., 2001). However, in contrast to many ion channels, Tim23 seems not to form a defined constriction site for ions in the channel, but rather mediates selectivity by specific channel surface characteristics throughout the whole length of the pore, which has been proposed as a general model for ion selectivity (Kutzner et al., 2011).

When the cation selectivity of Tim23 was identified, it was speculated that this translates into a preference for positively charged presequences. This would imply that Tim23 not only accepts presequences with its N-terminal IMS domain, but also with parts of the channel. Indeed, mutants with a reduced cation preference were much less activated by presequence peptides. Moreover, the N150A substitution is located close to the matrix in the channel. Therefore, a precursor has to reach deep into the channel before it will engage with the N150 residue, which therefore should

be clearly different from presequence recognition by the IMS domain. However, it is likely that the other mutations that showed reduced cation selectivity in the electrophysiology experiments, and that are located more towards the IMS, would result in loss of presequence response of the channel. Presequence binding therefore would be mediated through the whole length of the channel. Unfortunately, a combination of different mutations could never be tested *in vivo* or *in organello* since all other mutations (e.g. Y159A, G156L, N60A) led to instability of the Tim23 protein.

Most of the mutants analyzed showed a growth defect at elevated temperatures in *Saccharomyces cerevisiae.* The only exception is a G153A substitution. However, the cation selectivity was reduced by 40%, whereas other mutants showed up to 70% reduction. We therefore concluded that a certain reduction of presequence binding can be compensated for *in vivo* and that presequence binding by the Tim23 channel is not rate limiting for import. After rigorously excluding all mutants that showed reduced steady-state levels or assembly defects, but reduced growth and cation selectivity, we ended up with the Tim23 N150A mutation, which indeed had the strongest selectivity loss. Importantly, other channel characteristics, like voltage-regulation by Tim50 and basal gating frequency, were not altered. Even though Tim23 N150A assembled like wild type into the complex and showed no reduction in $\Delta\psi$, import of presequence substrates was significantly affected in this mutant. Importantly, both motor dependent and independent precursors were affected, ruling out an indirect effect on the motor as seen for other point mutants in the TIM23 core complex proteins (Demishtein-Zohary et al., 2015; 2017).

In contrast to all other protein conduction channels that have been characterized so far and where the pore is made from only one protein (like TOM or SAM) or from multiple copies of the same protein (TIM22, probably MIM), the TIM23 pore likely contains more than one protein. Even though Tim23 alone can form a pore *in vitro,* Tim17 either forms a channel independent of Tim23, or together with Tim23 (Martinez-Caballero et al., 2007). Indeed, mutations in the Tim17 protein severely affect gating properties of the TIM23 complex (Ramesh et al., 2016). Mgr2 is positioned at the lateral gate where it confers quality control to the sorting process. Therefore, Mgr2 might also be part of the channel. Thus, in the intact TIM23 complex the selectivity filter might not only be established by Tim23, but also by Tim17 and/or

Mgr2. Therefore, it will be interesting in the future to analyze the electrophysiological properties of the whole complex, either by isolating it from yeast including different mutants or reconstituting the complex with all components of interest.

In mitochondria, all protein transport complexes have water-filled pores at their core that form the protein conduction channel. However, the proteins that form the channels are of different nature. For the TOM and SAM complex, each channel is formed by a single β-barrel protein, whereas the TIM23 and TIM22 channels are formed by α-helical proteins. Surprisingly, all of them show partially similar electrophysiological properties, including cation selectivity, similar channel diameters and activation by signal peptides, pointing to at least a partially conserved mechanism for protein translocation.

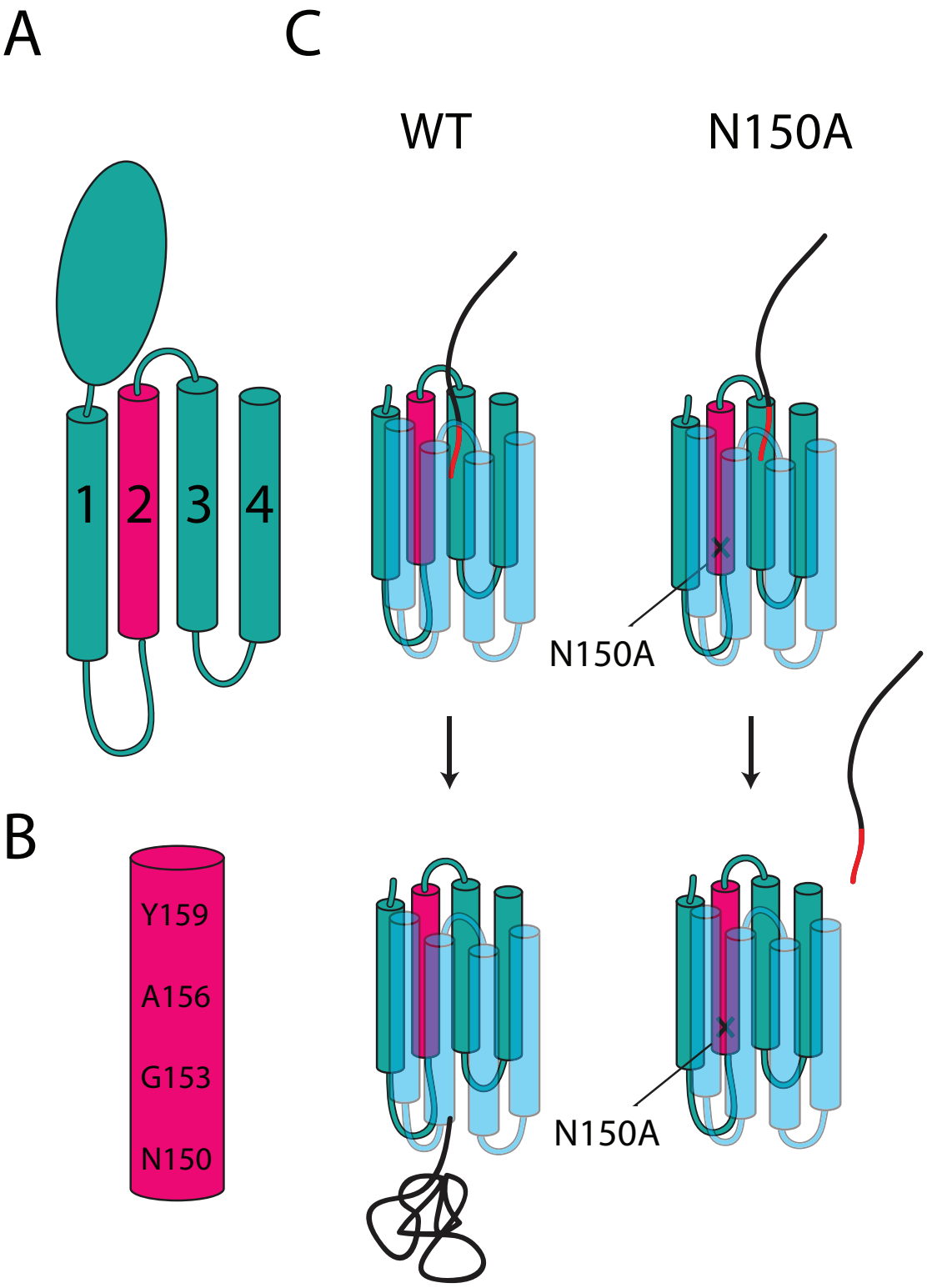

Figure 7: Tim23 cation selectivity is important for protein import. A: Topology of Tim23, transmembrane segments 1-4 are numbered. TM2, which contains the mutagenized residues, is pink. B: Selected residues in TM2 that show functional relevance for ion specificity are shown, IMS up, matrix down. C: In wild type mitochondria, Tim23 (cyan) gets activated by presequences, which involves residue N150 and leads to protein transport. In the N150A mutant, channel activation by presequences is strongly impaired which reduces import. (the intermembrane space domain of Tim23 is not shown in C for simplicity, Tim17 is shown in transparent blue).

4. Summary and future perspectives

Mitochondria perform essential roles in iron sulfur cluster biogenesis, ATP production, amino acid metabolism, β-oxidation and the urea cycle. Moreover, they are involved in cellular signaling, for example by storing Ca^{2+} ions and releasing cytochrome *c,* a key step in apoptosis. Even in non-dividing cells, mitochondria are very dynamic, undergoing constant fission and fusion in order to respond to cellular demands and to remove damaged organelles. All of this requires the constant import of proteins synthesized in the cytosol. Even though different pathways exist for protein import, the most common is the presequence pathway. Preproteins are imported through the TOM complex in the outer membrane and TIM23 complex in the inner membrane. While the driving force through the TOM complex remains largely unknown, translocation across the inner membrane requires Δψ and ATP generated by the OXPHOS system.

Here I have shown that soluble, matrix targeted proteins display different dependencies on the Δψ for import. This requirement does not depend on the presequence, since exchange of presequences between hypersensitive and less sensitive precursors does not affect their demand for Δψ. This largely changes our understanding of Δψ driven protein import, which so far was thought to only act on the presequence. Even though the concept of Δψ driven presequence translocation remains valid, the Δψ also seems to affect transport of the mature portion of the protein. Therefore, it will be interesting to analyze the mature portion of both classes of precursors to identify what defines their Δψ sensitivity. Potentially this could be the amount and/or relative distribution of charged amino acids, the hydrophobicity of unfolded regions which could lead to an import delay because these regions could be misinterpreted as "stop-transfer" signals, or small regions in the protein that tend to fold in the IMS slowing translocation down.

Interestingly, all Δψ hypersensitive proteins were also strongly Pam17 dependent. In contrast to previous reports, Pam17 does not affect Pam16-Pam18 assembly, or motor function. Instead, Pam17 recruitment requires the presequence receptor Tim50. Pam17 contains two membrane spans, an IMS loop and a small matrix domain. However, since presequence translocation is already reduced in *pam17*Δ mitochondria, and even the outer membrane protein Om45 depends on Pam17, it is

likely that not the matrix domain, but the membrane domains are essential for Pam17 function. Pam17 seems to be required especially for the import of Δψ sensitive proteins, but the molecular mechanism remains enigmatic. Pam17 could not be crosslinked to presequence peptides or precursors *in transit*. Even though a direct interaction between Pam17 and precursor cannot be completely ruled out, another attractive options is that Pam17 affects the gating activity of Tim23. Electrophysiology experiments indicate that Tim23 exists in different activity states and can be shifted towards the active state by presequences or elevated Δψ. It will be interesting to repeat these experiments, together with Pam17. Alternatively, inner membrane vesicles derived from *pam17*Δ could be used. Probably, Pam17 shifts the TIM23 complex to the active state, therefore supporting protein translocation.
Under steady state conditions, only a small portion of Pam17 seems to be associated with the translocase. In fact, is has been shown many times that Tim21 and Pam17 bind to the complex in an antagonistic manner. However, in contrast to previous reports, Pam17 is not a motor component and in fact is strictly absent in the $TIM23^{MOTOR}$ complex. Therefore, the Pam17-containing TIM23 complex seems to be another, yet undefined form of the TIM23 complex, which I termed $TIM23^{*}$. The exact mechanism recruiting Pam17 to the translocase is unknown, even though presequence recognition, probably by Tim50, seems to play a role. Also, the factor releasing Pam17 form the translocase remains to be identified. Since mutations affecting Tim44 lead to an increase in Pam17 association with the translocase, Tim44 is a possible candidate. However, if dissociation of Pam17 from the translocase is required for motor function also remains to be solved. A 3D structure of the TIM23 complex, or structural data based on crosslinking experiments with inactive and active translocase transporting a substrate, will be helpful to solve these problems.

Tim23 alone can form a pore in a lipid bilayer and can be activated by presequence peptides or high Δψ. Even though in the cell the TIM23 pore is most likely composed of more proteins, Tim23 is arguably the most important pore forming subunit. In addition to its IMS exposed presequence binding domain, we found that highly conserved pore lining residues are also crucial for channel activation by presequence peptides. Single amino acid substitution led to strongly reduced cation selectivity and a significant reduction of response to presequences. Since Δψ was not affected in

N150A mitochondria and the TIM23 complex assembled like wild type, we argue that the introduced mutation directly affects Tim23 function. Therefore, Tim23 is not only a passive channel, but directly contributes to substrate specificity, similar to the Tom40 protein, which also binds presequences and chaperones hydrophobic protein stretches. It will be interesting to figure out in the future, how the active gating of the TIM23 complex contributes to precursor translocation. Also, for Tim23, only the interaction with the presequence and hydrophobic "stop-transfer" signals have been described so far. However, interactions with the mature portion of the protein could be envisioned, either to chaperone hydrophobic stretches or to prevent backsliding of the precursor.

5. Bibliography

Abe, Y., Shodai, T., Muto, T., Mihara, K., Torii, H., Nishikawa, S., Endo, T., and Kohda, D. (2000). Structural basis of presequence recognition by the mitochondrial protein import receptor Tom20. Cell *100*, 551–560.

Albrecht, R., Rehling, P., Chacinska, A., Brix, J., Cadamuro, S.A., Volkmer, R., Guiard, B., Pfanner, N., and Zeth, K. (2006). The Tim21 binding domain connects the preprotein translocases of both mitochondrial membranes. EMBO Rep. *7*, 1233–1238.

Alder, N.N., Jensen, R.E., and Johnson, A.E. (2008a). Fluorescence mapping of mitochondrial TIM23 complex reveals a water-facing, substrate-interacting helix surface. Cell *134*, 439–450.

Alder, N.N., Sutherland, J., Buhring, A.I., Jensen, R.E., and Johnson, A.E. (2008b). Quaternary structure of the mitochondrial TIM23 complex reveals dynamic association between Tim23p and other subunits. Molecular Biology of the Cell *19*, 159–170.

Allen, S., Balabanidou, V., Sideris, D.P., Lisowsky, T., and Tokatlidis, K. (2005). Erv1 mediates the Mia40-dependent protein import pathway and provides a functional link to the respiratory chain by shuttling electrons to cytochrome c. J. Mol. Biol. *353*, 937–944.

Andrès, C., Agne, B., and Kessler, F. (2010). The TOC complex: preprotein gateway to the chloroplast. Biochim Biophys Acta *1803*, 715–723.

Bajaj, R., Jaremko, Ł., Jaremko, M., Becker, S., and Zweckstetter, M. (2014a). Molecular Basis of the Dynamic Structure of the TIM23 Complex in the Mitochondrial Intermembrane Space. Structure/Folding and Design 1–11.

Bajaj, R., Munari, F., Becker, S., and Zweckstetter, M. (2014b). Interaction of the intermembrane space domain of Tim23 with mitochondrial membranes. Journal of Biological Chemistry.

Banerjee, R., Gladkova, C., Mapa, K., Witte, G., and Mokranjac, D. (2015). Protein translocation channel of mitochondrial inner membrane and matrix-exposed import motor communicate via two-domain coupling protein. Elife *4*.

Barbot, M., Jans, D.C., Schulz, C., Denkert, N., Kroppen, B., Hoppert, M., Jakobs, S., and Meinecke, M. (2015). Mic10 oligomerizes to bend mitochondrial inner membranes at cristae junctions. Cell Metab. *21*, 756–763.

Bauer, M.F., Christian Sirrenberg, W.N., and Brunner, M. (1996). Role of Tim23 as Voltage Sensorand Presequence Receptor in Protein Import into Mitochondria. 1–9.

Bausewein, T., Mills, D.J., Langer, J.D., Nitschke, B., Nussberger, S., and Kühlbrandt, W. (2017). Cryo-EM Structure of the TOM Core Complex from Neurospora crassa. Cell *170*, 693–700.e697.

Becker, T., Guiard, B., Thornton, N., Zufall, N., Stroud, D.A., Wiedemann, N., and Pfanner, N. (2010). Assembly of the mitochondrial protein import channel: role of Tom5 in two-stage interaction of Tom40 with the SAM complex. Molecular Biology of the Cell *21*, 3106–3113.

Benz, R. (1994). Permeation of hydrophilic solutes through mitochondrial outer membranes: review on mitochondrial porins. Biochim Biophys Acta *1197*, 167–196.

Beverly, K.N., Sawaya, M.R., Schmid, E., and Koehler, C.M. (2008). The Tim8-Tim13 complex has multiple substrate binding sites and binds cooperatively to Tim23. J. Mol. Biol. *382*, 1144–1156.

Blamowska, M., Neupert, W., and Hell, K. (2012). Biogenesis of the mitochondrial Hsp70 chaperone. The Journal of Cell Biology *199*, 125–135.

Blobel, G., and Dobberstein, B. (1975). Transfer of proteins across membranes. I. Presence of proteolytically processed and unprocessed nascent immunoglobulin light chains on membrane-bound ribosomes of murine myeloma. The Journal of Cell Biology *67*, 835–851.

Bohnert, M., Rehling, P., Guiard, B., Herrmann, J.M., Pfanner, N., and van der Laan, M. (2010). Cooperation of stop-transfer and conservative sorting mechanisms in mitochondrial protein transport. Curr. Biol. *20*, 1227–1232.

Brix, J., Dietmeier, K., and Pfanner, N. (1997). Differential recognition of preproteins by the purified cytosolic domains of the mitochondrial import receptors Tom20, Tom22, and Tom70. J. Biol. Chem. *272*, 20730–20735.

Brix, J., Rüdiger, S., Bukau, B., Schneider-Mergener, J., and Pfanner, N. (1999). Distribution of binding sequences for the mitochondrial import receptors Tom20, Tom22, and Tom70 in a presequence-carrying preprotein and a non-cleavable preprotein. J. Biol. Chem. *274*, 16522–16530.

Bukau, B., and Horwich, A.L. (1998). The Hsp70 and Hsp60 chaperone machines. Cell *92*, 351–366.

Chacinska, A., Koehler, C.M., Milenkovic, D., Lithgow, T., and Pfanner, N. (2009). Importing mitochondrial proteins: machineries and mechanisms. Cell *138*, 628–644.

Chacinska, A., Lind, M., Frazier, A.E., Dudek, J., Meisinger, C., Geissler, A., Sickmann, A., Meyer, H.E., Truscott, K.N., Guiard, B., et al. (2005). Mitochondrial presequence translocase: switching between TOM tethering and motor recruitment involves Tim21 and Tim17. Cell *120*, 817–829.

Chacinska, A., Pfannschmidt, S., Wiedemann, N., Kozjak, V., Sanjuán Szklarz, L.K., Schulze-Specking, A., Truscott, K.N., Guiard, B., Meisinger, C., and Pfanner, N. (2004). Essential role of Mia40 in import and assembly of mitochondrial intermembrane space proteins. The EMBO Journal *23*, 3735–3746.

Chacinska, A., van der Laan, M., Mehnert, C.S., Guiard, B., Mick, D.U., Hutu, D.P., Truscott, K.N., Wiedemann, N., Meisinger, C., Pfanner, N., et al. (2010). Distinct forms of mitochondrial TOM-TIM supercomplexes define signal-dependent states of

preprotein sorting. Molecular and Cellular Biology *30*, 307–318.

Craig, E.A., and Marszalek, J. (2017). How Do J-Proteins Get Hsp70 to Do So Many Different Things? Trends Biochem. Sci. *42*, 355–368.

Curran, S.P., Leuenberger, D., Oppliger, W., and Koehler, C.M. (2002). The Tim9p-Tim10p complex binds to the transmembrane domains of the ADP/ATP carrier. The EMBO Journal *21*, 942–953.

D'Silva, P.D., Schilke, B., Walter, W., Andrew, A., and Craig, E.A. (2003). J protein cochaperone of the mitochondrial inner membrane required for protein import into the mitochondrial matrix. Proc. Natl. Acad. Sci. U.S.a. *100*, 13839–13844.

Daley, D.O., Adams, K.L., Clifton, R., Qualmann, S., Millar, A.H., Palmer, J.D., Pratje, E., and Whelan, J. (2002). Gene transfer from mitochondrion to nucleus: novel mechanisms for gene activation from Cox2. Plant J. *30*, 11–21.

Davis, A.J., Alder, N.N., Jensen, R.E., and Johnson, A.E. (2007). The Tim9p/10p and Tim8p/13p complexes bind to specific sites on Tim23p during mitochondrial protein import. Molecular Biology of the Cell *18*, 475–486.

de Duve, C. (2007). The origin of eukaryotes: a reappraisal. Nat. Rev. Genet. *8*, 395–403.

De Los Rios, P., Ben-Zvi, A., Slutsky, O., Azem, A., and Goloubinoff, P. (2006). Hsp70 chaperones accelerate protein translocation and the unfolding of stable protein aggregates by entropic pulling. Proc. Natl. Acad. Sci. U.S.a. *103*, 6166–6171.

Dekker, P.J., Keil, P., Rassow, J., Maarse, A.C., Pfanner, N., and Meijer, M. (1993). Identification of MIM23, a putative component of the protein import machinery of the mitochondrial inner membrane. FEBS Lett. *330*, 66–70.

Demishtein-Zohary, K., Günsel, U., Marom, M., Banerjee, R., Neupert, W., Azem, A., and Mokranjac, D. (2017). Role of Tim17 in coupling the import motor to the translocation channel of the mitochondrial presequence translocase. Elife *6*.

Demishtein-Zohary, K., Marom, M., Neupert, W., Mokranjac, D., and Azem, A. (2015). GxxxG Motifs hold the TIM23 Complex Together. Febs J. n/a–n/a.

Dietmeier, K., Hönlinger, A., Bömer, U., Dekker, P.J., Eckerskorn, C., Lottspeich, F., Kübrich, M., and Pfanner, N. (1997). Tom5 functionally links mitochondrial preprotein receptors to the general import pore. Nature *388*, 195–200.

Dimmer, K.S., Papić, D., Schumann, B., Sperl, D., Krumpe, K., Walther, D.M., and Rapaport, D. (2012). A crucial role for Mim2 in the biogenesis of mitochondrial outer membrane proteins. J Cell Sci *125*, 3464–3473.

Donzeau, M., Káldi, K., Adam, A., Paschen, S., Wanner, G., Guiard, B., Bauer, M.F., Neupert, W., and Brunner, M. (2000). Tim23 links the inner and outer mitochondrial membranes. Cell *101*, 401–412.

Dudek, J., and Maack, C. (2017). Barth syndrome cardiomyopathy. Cardiovasc. Res.

Dudek, J., Rehling, P., and van der Laan, M. (2013). Biochimica et Biophysica Acta. BBA - Molecular Cell Research *1833*, 274–285.

Ellenrieder, L., Opaliński, Ł., Becker, L., Krüger, V., Mirus, O., Straub, S.P., Ebell, K., Flinner, N., Stiller, S.B., Guiard, B., et al. (2016). Separating mitochondrial protein assembly and endoplasmic reticulum tethering by selective coupling of Mdm10. Nature Communications *7*, 13021.

Esaki, M., Kanamori, T., Nishikawa, S.-I., Shin, I., Schultz, P.G., and Endo, T. (2003). Tom40 protein import channel binds to non-native proteins and prevents their aggregation. Nat. Struct. Biol. *10*, 988–994.

Fischer, M., and Riemer, J. (2013). The mitochondrial disulfide relay system: roles in oxidative protein folding and beyond. Int J Cell Biol *2013*, 742923.

Flores-Pérez, Ú., and Jarvis, P. (2013). Molecular chaperone involvement in chloroplast protein import. Biochim Biophys Acta *1833*, 332–340.

Frazier, A.E., Dudek, J., Guiard, B., Voos, W., Li, Y., Lind, M., Meisinger, C., Geissler, A., Sickmann, A., Meyer, H.E., et al. (2004). Pam16 has an essential role in the mitochondrial protein import motor. Nat. Struct. Mol. Biol. *11*, 226–233.

Friedman, J.R., and Nunnari, J. (2014). Mitochondrial form and function. Nature *505*, 335–343.

Gebert, M., Schrempp, S.G., Mehnert, C.S., Heisswolf, A.K., Oeljeklaus, S., Ieva, R., Bohnert, M., Malsburg, von der, K., Wiese, S., Kleinschroth, T., et al. (2012). Mgr2 promotes coupling of the mitochondrial presequence translocase to partner complexes. The Journal of Cell Biology *197*, 595–604.

Gebert, N., Chacinska, A., Wagner, K., Guiard, B., Koehler, C.M., Rehling, P., Pfanner, N., and Wiedemann, N. (2008). Assembly of the three small Tim proteins precedes docking to the mitochondrial carrier translocase. EMBO Rep. *9*, 548–554.

Gebert, N., Gebert, M., Oeljeklaus, S., Malsburg, von der, K., Stroud, D.A., Kulawiak, B., Wirth, C., Zahedi, R.P., Dolezal, P., Wiese, S., et al. (2011). Dual function of Sdh3 in the respiratory chain and TIM22 protein translocase of the mitochondrial inner membrane. Molecular Cell *44*, 811–818.

Geissler, A., Krimmer, T., Bömer, U., Guiard, B., Rassow, J., and Pfanner, N. (2000). Membrane potential-driven protein import into mitochondria. The sorting sequence of cytochrome b(2) modulates the deltapsi-dependence of translocation of the matrix-targeting sequence. Molecular Biology of the Cell *11*, 3977–3991.

Geissler, A., Chacinska, A., Truscott, K.N., Wiedemann, N., Brandner, K., Sickmann, A., Meyer, H.E., Meisinger, C., Pfanner, N., and Rehling, P. (2002). The mitochondrial presequence translocase: an essential role of Tim50 in directing preproteins to the import channel. Cell *111*, 507–518.

Gilkerson, R.W., Selker, J.M.L., and Capaldi, R.A. (2003). The cristal membrane of mitochondria is the principal site of oxidative phosphorylation. FEBS Lett. *546*, 355–358.

Glick, B.S. (1995). Can Hsp70 proteins act as force-generating motors? Cell *80*, 11–14.

Glick, B.S., Brandt, A., Cunningham, K., Müller, S., Hallberg, R.L., and Schatz, G. (1992). Cytochromes c1 and b2 are sorted to the intermembrane space of yeast mitochondria by a stop-transfer mechanism. Cell *69*, 809–822.

Gold, V.A.M., Ieva, R., Walter, A., Pfanner, N., van der Laan, M., and Kühlbrandt, W. (2014). Visualizing active membrane protein complexes by electron cryotomography. Nature Communications *5*, 4129.

Gornicka, A., Bragoszewski, P., Chroscicki, P., Wenz, L.-S., Schulz, C., Rehling, P., and Chacinska, A. (2014). A discrete pathway for the transfer of intermembrane space proteins across the outer membrane of mitochondria. Molecular Biology of the Cell.

Gray, M.W., Burger, G., and Lang, B.F. (1999). Mitochondrial evolution. Science *283*, 1476–1481.

Harbauer, A.B., Opalińska, M., Gerbeth, C., Herman, J.S., Rao, S., Schönfisch, B., Guiard, B., Schmidt, O., Pfanner, N., and Meisinger, C. (2014). Cell cycle-dependent regulation of mitochondrial preprotein translocase. Science.

Hartl, F.U., Schmidt, B., Wachter, E., Weiss, H., and Neupert, W. (1986). Transport into mitochondria and intramitochondrial sorting of the Fe/S protein of ubiquinol-cytochrome c reductase. Cell *47*, 939–951.

Hawlitschek, G., Schneider, H., Schmidt, B., Tropschug, M., Hartl, F.U., and Neupert, W. (1988). Mitochondrial protein import: identification of processing peptidase and of PEP, a processing enhancing protein. Cell *53*, 795–806.

Hell, K., Neupert, W., and Stuart, R.A. (2001). Oxa1p acts as a general membrane insertion machinery for proteins encoded by mitochondrial DNA. The EMBO Journal *20*, 1281–1288.

Herrmann, J.M., Neupert, W., and Stuart, R.A. (1997). Insertion into the mitochondrial inner membrane of a polytopic protein, the nuclear-encoded Oxa1p. The EMBO Journal *16*, 2217–2226.

Hoppins, S., Collins, S.R., Cassidy-Stone, A., Hummel, E., Devay, R.M., Lackner, L.L., Westermann, B., Schuldiner, M., Weissman, J.S., and Nunnari, J. (2011). A mitochondrial-focused genetic interaction map reveals a scaffold-like complex required for inner membrane organization in mitochondria. The Journal of Cell Biology *195*, 323–340.

Horvath, S.E., Rampelt, H., Oeljeklaus, S., Warscheid, B., van der Laan, M., and Pfanner, N. (2015). Role of membrane contact sites in protein import into mitochondria. Protein Sci. *24*, 277–297.

Huang, S., Ratliff, K.S., and Matouschek, A. (2002). Protein unfolding by the mitochondrial membrane potential. Nat. Struct. Biol. *9*, 301–307.

Hulett, J.M., Lueder, F., Chan, N.C., Perry, A.J., Wolynec, P., Likic, V.A., Gooley,

P.R., and Lithgow, T. (2008). The transmembrane segment of Tom20 is recognized by Mim1 for docking to the mitochondrial TOM complex. J. Mol. Biol. *376*, 694–704.

Hulett, J.M., Walsh, P., and Lithgow, T. (2007). Domain stealing by receptors in a protein transport complex. Mol. Biol. Evol. *24*, 1909–1911.

Ieva, R., Schrempp, S.G., Opaliński, Ł., Wollweber, F., Höß, P., Heißwolf, A.K., Gebert, M., Zhang, Y., Guiard, B., Rospert, S., et al. (2014). Mgr2 Functions as Lateral Gatekeeper for Preprotein Sorting in the Mitochondrial Inner Membrane. Molecular Cell *56*, 641–652.

Ieva, R., wolf, A.K.H.S., Gebert, M., gtle, F.N.V.O., Wollweber, F., Mehnert, C.S., Oeljeklaus, S., Warscheid, B., Meisinger, C., van der Laan, M., et al. (2013). Mitochondrial inner membrane protease promotesassembly of presequence translocase by removinga carboxy-terminal targeting sequence. Nature Communications *4*, 1–11.

Ikon, N., and Ryan, R.O. (2017). Cardiolipin and mitochondrial cristae organization. Biochim Biophys Acta *1859*, 1156–1163.

Jores, T., Klinger, A., Groß, L.E., Kawano, S., Flinner, N., Duchardt-Ferner, E., Wöhnert, J., Kalbacher, H., Endo, T., Schleiff, E., et al. (2016). Characterization of the targeting signal in mitochondrial β-barrel proteins. Nature Communications *7*, 12036.

Kampinga, H.H., and Craig, E.A. (2010). The HSP70 chaperone machinery: J proteins as drivers of functional specificity. Nat Rev Mol Cell Biol *11*, 579–592.

Kang, P.J., Ostermann, J., Shilling, J., Neupert, W., Craig, E.A., and Pfanner, N. (1990). Requirement for hsp70 in the mitochondrial matrix for translocation and folding of precursor proteins. Nature *348*, 137–143.

Kerscher, O., Holder, J., Srinivasan, M., Leung, R.S., and Jensen, R.E. (1997). The Tim54p-Tim22p complex mediates insertion of proteins into the mitochondrial inner membrane. The Journal of Cell Biology *139*, 1663–1675.

Komiya, T., Rospert, S., Koehler, C., Looser, R., Schatz, G., and Mihara, K. (1998). Interaction of mitochondrial targeting signals with acidic receptor domains along the protein import pathway: evidence for the “acid chain” hypothesis. The EMBO Journal *17*, 3886–3898.

Kovács-Bogdán, E., Soll, J., and Bölter, B. (2010). Protein import into chloroplasts: the Tic complex and its regulation. Biochim Biophys Acta *1803*, 740–747.

Kozany, C., Mokranjac, D., Sichting, M., Neupert, W., and Hell, K. (2004). The J domain-related cochaperone Tim16 is a constituent of the mitochondrial TIM23 preprotein translocase. Nat. Struct. Mol. Biol. *11*, 234–241.

Kronidou, N.G., Oppliger, W., Bolliger, L., Hannavy, K., Glick, B.S., Schatz, G., and Horst, M. (1994). Dynamic interaction between Isp45 and mitochondrial hsp70 in the protein import system of the yeast mitochondrial inner membrane. Proc. Natl. Acad.

Sci. U.S.a. *91*, 12818–12822.

Kutik, S., Stojanovski, D., Becker, L., Becker, T., Meinecke, M., Krüger, V., Prinz, C., Meisinger, C., Guiard, B., Wagner, R., et al. (2008). Dissecting membrane insertion of mitochondrial beta-barrel proteins. Cell *132*, 1011–1024.

Kutzner, C., Grubmüller, H., de Groot, B.L., and Zachariae, U. (2011). Computational electrophysiology: the molecular dynamics of ion channel permeation and selectivity in atomistic detail. Biophysical Journal *101*, 809–817.

la Cruz, de, L., Bajaj, R., Becker, S., and Zweckstetter, M. (2010). The intermembrane space domain of Tim23 is intrinsically disordered with a distinct binding region for presequences. Protein Sci. *19*, 2045–2054.

Laloraya, S., Gambill, B.D., and Craig, E.A. (1994). A role for a eukaryotic GrpE-related protein, Mge1p, in protein translocation. Proc. Natl. Acad. Sci. U.S.a. *91*, 6481–6485.

Laufen, T., Mayer, M.P., Beisel, C., Klostermeier, D., Mogk, A., Reinstein, J., and Bukau, B. (1999). Mechanism of regulation of hsp70 chaperones by DnaJ cochaperones. Proc. Natl. Acad. Sci. U.S.a. *96*, 5452–5457.

Li, J., Qian, X., Hu, J., and Sha, B. (2009). Molecular chaperone Hsp70/Hsp90 prepares the mitochondrial outer membrane translocon receptor Tom71 for preprotein loading. J. Biol. Chem. *284*, 23852–23859.

Li, Y., Dudek, J., Guiard, B., Pfanner, N., Rehling, P., and Voos, W. (2004). The presequence translocase-associated protein import motor of mitochondria. Pam16 functions in an antagonistic manner to Pam18. J. Biol. Chem. *279*, 38047–38054.

Lill, R. (2009). Function and biogenesis of iron-sulphur proteins. Nature *460*, 831–838.

Lithgow, T., Junne, T., Suda, K., Gratzer, S., and Schatz, G. (1994). The mitochondrial outer membrane protein Mas22p is essential for protein import and viability of yeast. Proc. Natl. Acad. Sci. U.S.a. *91*, 11973–11977.

Liu, Q., D'Silva, P., Walter, W., Marszalek, J., and Craig, E.A. (2003). Regulated cycling of mitochondrial Hsp70 at the protein import channel. Science *300*, 139–141.

Lohret, T.A., Jensen, R.E., and Kinnally, K.W. (1997). Tim23, a protein import component of the mitochondrial inner membrane, is required for normal activity of the multiple conductance channel, MCC. The Journal of Cell Biology *137*, 377–386.

Lytovchenko, O., Melin, J., Schulz, C., Kilisch, M., Hutu, D.P., and Rehling, P. (2013). Signal recognition initiates reorganization of the presequence translocase during protein import. The EMBO Journal *32*, 886–898.

Malhotra, K., Sathappa, M., Landin, J.S., Johnson, A.E., and Alder, N.N. (2013). Structural changes in the mitochondrial Tim23 channel are coupled to the proton-motive force. Nature Publishing Group *20*, 965–972.

Mapa, K., Sikor, M., Kudryavtsev, V., Waegemann, K., Kalinin, S., Seidel, C.A.M., Neupert, W., Lamb, D.C., and Mokranjac, D. (2010). The Conformational Dynamicsof the Mitochondrial Hsp70 Chaperone. Molecular Cell *38*, 89–100.

Marom, M., Dayan, D., Demishtein-Zohary, K., Mokranjac, D., Neupert, W., and Azem, A. (2011). Direct Interaction of Mitochondrial Targeting Presequences with Purified Components of the TIM23 Protein Complex. Journal of Biological Chemistry *286*, 43809–43815.

Marom, M., Safonov, R., Amram, S., Avneon, Y., Nachliel, E., Gutman, M., Zohary, K., Azem, A., and Tsfadia, Y. (2009). Interaction of the Tim44 C-Terminal Domain with Negatively Charged Phospholipids. Biochemistry *48*, 11185–11195.

Martin, J., Mahlke, K., and Pfanner, N. (1991). Role of an energized inner membrane in mitochondrial protein import. Delta psi drives the movement of presequences. J. Biol. Chem. *266*, 18051–18057.

Martinez-Caballero, S., Grigoriev, S.M., Herrmann, J.M., Campo, M.L., and Kinnally, K.W. (2007). Tim17p regulates the twin pore structure and voltage gating of the mitochondrial protein import complex TIM23. J. Biol. Chem. *282*, 3584–3593.

Mayer, M.P. (2013). Hsp70 chaperone dynamics and molecular mechanism. Trends Biochem. Sci. *38*, 507–514.

Mehnert, C.S., Rampelt, H., Gebert, M., Oeljeklaus, S., Schrempp, S.G., Kochbeck, L., Guiard, B., Warscheid, B., and van der Laan, M. (2014). Mitochondrial ADP/ATP Carrier Associates with the Inner Membrane Presequence Translocase in a Stoichiometric Manner. Journal of Biological Chemistry.

Meier, S., Neupert, W., and Herrmann, J.M. (2005). Proline residues of transmembrane domains determine the sorting of inner membrane proteins in mitochondria. The Journal of Cell Biology *170*, 881–888.

Meinecke, M. (2006). Tim50 Maintains the Permeability Barrier of the Mitochondrial Inner Membrane. Science *312*, 1523–1526.

Melin, J., Schulz, C., Wrobel, L., Bernhard, O., Chacinska, A., Jahn, O., Schmidt, B., and Rehling, P. (2014). Presequence Recognition by the Tom40 Channel Contributes to Precursor Translocation into the Mitochondrial Matrix. Molecular and Cellular Biology *34*, 3473–3485.

Melin, J., Kilisch, M., Neumann, P., Lytovchenko, O., Gomkale, R., Schendzielorz, A., Schmidt, B., Liepold, T., Ficner, R., Jahn, O., et al. (2015). A presequence-binding groove in Tom70 supports import of Mdl1 into mitochondria. Biochim Biophys Acta *1853*, 1850–1859.

Miao, B., Davis, J.E., and Craig, E.A. (1997). Mge1 functions as a nucleotide release factor for Ssc1, a mitochondrial Hsp70 of Saccharomyces cerevisiae. J. Mol. Biol. *265*, 541–552.

Milenkovic, D., Ramming, T., Müller, J.M., Wenz, L.-S., Gebert, N., Schulze-Specking, A., Stojanovski, D., Rospert, S., and Chacinska, A. (2009). Identification of

the signal directing Tim9 and Tim10 into the intermembrane space of mitochondria. Molecular Biology of the Cell *20*, 2530–2539.

Model, K., Meisinger, C., and Kühlbrandt, W. (2008). Cryo-electron microscopy structure of a yeast mitochondrial preprotein translocase. J. Mol. Biol. *383*, 1049–1057.

Mokranjac, D., and Neupert, W. (2010). The many faces of the mitochondrial TIM23 complex. Biochim Biophys Acta *1797*, 1045–1054.

Mokranjac, D., Berg, A., Adam, A., Neupert, W., and Hell, K. (2007). Association of the Tim14.Tim16 subcomplex with the TIM23 translocase is crucial for function of the mitochondrial protein import motor. J. Biol. Chem. *282*, 18037–18045.

Mokranjac, D., Bourenkov, G., Hell, K., Neupert, W., and Groll, M. (2006). Structure and function of Tim14 and Tim16, the J and J-like components of the mitochondrial protein import motor. The EMBO Journal *25*, 4675–4685.

Mokranjac, D., Sichting, M., Neupert, W., and Hell, K. (2003). Tim14, a novel key component of the import motor of the TIM23 protein translocase of mitochondria. The EMBO Journal *22*, 4945–4956.

Müller, M., Lu, K., and Reichert, A.S. (2015). Mitophagy and mitochondrial dynamics in Saccharomyces cerevisiae. Biochim Biophys Acta *1853*, 2766–2774.

Neupert, W., and Brunner, M. (2002). The protein import motor of mitochondria. Nat Rev Mol Cell Biol *3*, 555–565.

Okamoto, K., Brinker, A., Paschen, S.A., Moarefi, I., Hayer-Hartl, M., Neupert, W., and Brunner, M. (2002). The protein import motor of mitochondria: a targeted molecular ratchet driving unfolding and translocation. The EMBO Journal *21*, 3659–3671.

Pais, J.E., Schilke, B., and Craig, E.A. (2011). Reevaluation of the role of the Pam18:Pam16 interaction in translocation of proteins by the mitochondrial Hsp70-based import motor. Molecular Biology of the Cell *22*, 4740–4749.

Palade, G.E. (1964). The Organization of Living Matter. Proc. Natl. Acad. Sci. U.S.a. *52*, 613–634.

Papić, D., Krumpe, K., Dukanovic, J., Dimmer, K.S., and Rapaport, D. (2011). Multispan mitochondrial outer membrane protein Ugo1 follows a unique Mim1-dependent import pathway. The Journal of Cell Biology *194*, 397–405.

Park, E., and Rapoport, T.A. (2012). Mechanisms of Sec61/SecY-mediated protein translocation across membranes. Annu Rev Biophys *41*, 21–40.

Park, K., Jung, S., Kim, H., and Kim, H. (2014). Mode of membrane insertion of individual transmembrane segments in Mdl1 and Mdl2, multi-spanning mitochondrial ABC transporters. FEBS Lett. 1–9.

Paschen, S.A., Waizenegger, T., Stan, T., Preuss, M., Cyrklaff, M., Hell, K.,

Rapaport, D., and Neupert, W. (2003). Evolutionary conservation of biogenesis of beta-barrel membrane proteins. Nature *426*, 862–866.

Paumard, P., Vaillier, J., Coulary, B., Schaeffer, J., Soubannier, V., Mueller, D.M., Brèthes, D., di Rago, J.-P., and Velours, J. (2002). The ATP synthase is involved in generating mitochondrial cristae morphology. The EMBO Journal *21*, 221–230.

Peleh, V., Cordat, E., and Herrmann, J.M. (2016). Mia40 is a trans-site receptor that drives protein import into the mitochondrial intermembrane space by hydrophobic substrate binding. Elife *5*.

Pfeffer, S., Woellhaf, M.W., Herrmann, J.M., and Förster, F. (2015). Organization of the mitochondrial translation machinery studied in situ by cryoelectron tomography. Nature Communications *6*, 6019.

Platta, H.W., Hagen, S., Reidick, C., and Erdmann, R. (2014). The peroxisomal receptor dislocation pathway: To the exportomer and beyond. Biochimie *98*, 16–28.

Popov-Celeketić, D., Mapa, K., Neupert, W., and Mokranjac, D. (2008a). Active remodelling of the TIM23 complex during translocation of preproteins into mitochondria. The EMBO Journal *27*, 1469–1480.

Popov-Celeketić, D., Waegemann, K., Mapa, K., Neupert, W., and Mokranjac, D. (2011). Role of the import motor in insertion of transmembrane segments by the mitochondrial TIM23 complex. EMBO Rep. *12*, 542–548.

Popov-Celeketić, J., Waizenegger, T., and Rapaport, D. (2008b). Mim1 functions in an oligomeric form to facilitate the integration of Tom20 into the mitochondrial outer membrane. J. Mol. Biol. *376*, 671–680.

Qian, X., Gebert, M., Höpker, J., Yan, M., Li, J., Wiedemann, N., van der Laan, M., Pfanner, N., and Sha, B. (2011). Structural basis for the function of Tim50 in the mitochondrial presequence translocase. J. Mol. Biol. *411*, 513–519.

Qiu, J., Wenz, L.-S., Zerbes, R.M., Oeljeklaus, S., Bohnert, M., Stroud, D.A., Wirth, C., Ellenrieder, L., Thornton, N., Kutik, S., et al. (2013). Coupling of mitochondrial import and export translocases by receptor-mediated supercomplex formation. Cell *154*, 596–608.

Rahman, B., Kawano, S., Yunoki-Esaki, K., Anzai, T., and Endo, T. (2014). NMR analyses on the interactions of the yeast Tim50 C-terminal region with the presequence and Tim50 core domain. FEBS Lett. *588*, 678–684.

Ramesh, A., Peleh, V., Martinez-Caballero, S., Wollweber, F., Sommer, F., van der Laan, M., Schroda, M., Alexander, R.T., Campo, M.L., and Herrmann, J.M. (2016). A disulfide bond in the TIM23 complex is crucial for voltage gating and mitochondrial protein import. The Journal of Cell Biology *6*, jcb.201602074.

Rehling, P., Model, K., Brandner, K., Kovermann, P., Sickmann, A., Meyer, H.E., Kühlbrandt, W., Wagner, R., Truscott, K.N., and Pfanner, N. (2003). Protein insertion into the mitochondrial inner membrane by a twin-pore translocase. Science *299*, 1747–1751.

Rowley, N., Prip-Buus, C., Westermann, B., Brown, C., Schwarz, E., Barrell, B., and Neupert, W. (1994). Mdj1p, a novel chaperone of the DnaJ family, is involved in mitochondrial biogenesis and protein folding. Cell *77*, 249–259.

Ryan, M.T., Müller, H., and Pfanner, N. (1999). Functional staging of ADP/ATP carrier translocation across the outer mitochondrial membrane. J. Biol. Chem. *274*, 20619–20627.

Schilke, B.A., Hayashi, M., and Craig, E.A. (2012). Genetic Analysis of Complex Interactions Among Components of the Mitochondrial Import Motor and Translocon in Saccharomyces cerevisiae. Genetics *190*, 1341–1353.

Schiller, D. (2009). Pam17 and Tim44 act sequentially in protein import into the mitochondrial matrix. The International Journal of Biochemistry & Cell Biology *41*, 2343–2349.

Schiller, D., Cheng, Y.C., Liu, Q., Walter, W., and Craig, E.A. (2008). Residues of Tim44 Involved in both Association with the Translocon of the Inner Mitochondrial Membrane and Regulation of Mitochondrial Hsp70 Tethering. 1–10.

Schleyer, M., Schmidt, B., and Neupert, W. (1982). Requirement of a membrane potential for the posttranslational transfer of proteins into mitochondria. Eur. J. Biochem. *125*, 109–116.

Schmidt, O., Harbauer, A.B., Rao, S., Eyrich, B., Zahedi, R.P., Stojanovski, D., Schönfisch, B., Guiard, B., Sickmann, A., Pfanner, N., et al. (2011). Regulation of mitochondrial protein import by cytosolic kinases. Cell *144*, 227–239.

Schmitt, S., Ahting, U., Eichacker, L., Granvogl, B., Go, N.E., Nargang, F.E., Neupert, W., and Nussberger, S. (2005). Role of Tom5 in maintaining the structural stability of the TOM complex of mitochondria. J. Biol. Chem. *280*, 14499–14506.

Schneider, H.C., Berthold, J., Bauer, M.F., Dietmeier, K., Guiard, B., Brunner, M., and Neupert, W. (1994). Mitochondrial Hsp70/MIM44 complex facilitates protein import. Nature *371*, 768–774.

Schulz, C., Lytovchenko, O., Melin, J., Chacinska, A., Guiard, B., Neumann, P., Ficner, R., Jahn, O., Schmidt, B., and Rehling, P. (2011). Tim50's presequence receptor domain is essential for signal driven transport across the TIM23 complex. The Journal of Cell Biology *195*, 643–656.

Schulz, C., and Rehling, P. (2014). Remodelling of the active presequence translocase drives motor-dependent mitochondrial protein translocation. Nature Communications *5*, 1–9.

Schulz, C., Schendzielorz, A., and Rehling, P. (2015). Unlocking the presequence import pathway. Trends Cell Biol *25*, 265–275.

Schülke, N., Sepuri, N.B., and Pain, D. (1997). In vivo zippering of inner and outer mitochondrial membranes by a stable translocation intermediate. Proc. Natl. Acad. Sci. U.S.a. *94*, 7314–7319.

Shiota, T., Imai, K., Qiu, J., Hewitt, V.L., Tan, K., Shen, H.-H., Sakiyama, N., Fukasawa, Y., Hayat, S., Kamiya, M., et al. (2015). Molecular architecture of the active mitochondrial protein gate. Science *349*, 1544–1548.

Shiota, T., Mabuchi, H., Tanaka-Yamano, S., Yamano, K., and Endo, T. (2011). In vivo protein-interaction mapping of a mitochondrial translocator protein Tom22 at work. Proc. Natl. Acad. Sci. U.S.a. *108*, 15179–15183.

Sichting, M., Mokranjac, D., Azem, A., Neupert, W., and Hell, K. (2005). Maintenance of structure and function of mitochondrial Hsp70 chaperones requires the chaperone Hep1. The EMBO Journal *24*, 1046–1056.

Sideris, D.P., Petrakis, N., Katrakili, N., Mikropoulou, D., Gallo, A., Ciofi-Baffoni, S., Banci, L., Bertini, I., and Tokatlidis, K. (2009). A novel intermembrane space-targeting signal docks cysteines onto Mia40 during mitochondrial oxidative folding. The Journal of Cell Biology *187*, 1007–1022.

Simbeni, R., Pon, L., Zinser, E., Paltauf, F., and Daum, G. (1991). Mitochondrial membrane contact sites of yeast. Characterization of lipid components and possible involvement in intramitochondrial translocation of phospholipids. J. Biol. Chem. *266*, 10047–10049.

Slutsky-Leiderman, O., Marom, M., Iosefson, O., Levy, R., Maoz, S., and Azem, A. (2007). The Interplay between Components of the Mitochondrial Protein Translocation Motor Studied Using Purified Components. Journal of Biological Chemistry *282*, 33935–33942.

Song, J., Tamura, Y., Yoshihisa, T., and Endo, T. (2014). A novel import route for an N-anchor mitochondrial outer membrane protein aided by the TIM23 complex. EMBO Rep. *15*, 670–677.

Söllner, T., Griffiths, G., Pfaller, R., Pfanner, N., and Neupert, W. (1989). MOM19, an import receptor for mitochondrial precursor proteins. Cell *59*, 1061–1070.

Stiller, S.B., Höpker, J., Oeljeklaus, S., Schütze, C., Schrempp, S.G., Vent-Schmidt, J., Horvath, S.E., Frazier, A.E., Gebert, N., van der Laan, M., et al. (2016). Mitochondrial OXA Translocase Plays a Major Role in Biogenesis of Inner-Membrane Proteins. Cell Metab. *23*, 901–908.

Sun, F., Huo, X., Zhai, Y., Wang, A., Xu, J., Su, D., Bartlam, M., and Rao, Z. (2005). Crystal structure of mitochondrial respiratory membrane protein complex II. Cell *121*, 1043–1057.

Takeda, S., and McKay, D.B. (1996) Kinetics of Peptide Binding to the Bovine 70 kDa Heat Shock Cognate Protein, aMolecular Chaperone. Biochemistry *35,* 4636-4644

Ting, S.Y., Schilke, B.A., Hayashi, M., and Craig, E.A. (2014). Architecture of the TIM23 Inner Mitochondrial Translocon and Interactions with the Matrix Import Motor. Journal of Biological Chemistry *289*, 28689–28696.

Ting, S.-Y., Yan, N.L., Schilke, B.A., and Craig, E.A. (2017). Dual interaction of

scaffold protein Tim44 of mitochondrial import motor with channel-forming translocase subunit Tim23. Elife *6*.

Truscott, K.N., Kovermann, P., Geissler, A., Merlin, A., Meijer, M., Driessen, A.J., Rassow, J., Pfanner, N., and Wagner, R. (2001). A presequence- and voltage-sensitive channel of the mitochondrial preprotein translocase formed by Tim23. Nat. Struct. Biol. *8*, 1074–1082.

Truscott, K.N., Voos, W., Frazier, A.E., Lind, M., Li, Y., Geissler, A., Dudek, J., Müller, H., Sickmann, A., Meyer, H.E., et al. (2003). A J-protein is an essential subunit of the presequence translocase-associated protein import motor of mitochondria. The Journal of Cell Biology *163*, 707–713.

van der Laan, M., Chacinska, A., Lind, M., Perschil, I., Sickmann, A., Meyer, H.E., Guiard, B., Meisinger, C., Pfanner, N., and Rehling, P. (2005). Pam17 Is Required for Architecture and Translocation Activity of the Mitochondrial Protein Import Motor. Molecular and Cellular Biology *25*, 7449–7458.

van der Laan, M., Bohnert, M., Wiedemann, N., and Pfanner, N. (2012). Role of MINOS in mitochondrial membrane architecture and biogenesis. Trends Cell Biol *22*, 185–192.

van der Laan, M., Meinecke, M., Dudek, J., Hutu, D.P., Lind, M., Perschil, I., Guiard, B., Wagner, R., Pfanner, N., and Rehling, P. (2007). Motor-free mitochondrial presequence translocase drives membrane integration of preproteins. Nat. Cell Biol. *9*, 1152–1159.

van der Laan, M., Wiedemann, N., Mick, D.U., Guiard, B., Rehling, P., and Pfanner, N. (2006). A role for Tim21 in membrane-potential-dependent preprotein sorting in mitochondria. Curr. Biol. *16*, 2271–2276.

van Wilpe, S., Ryan, M.T., Hill, K., Maarse, A.C., Meisinger, C., Brix, J., Dekker, P.J., Moczko, M., Wagner, R., Meijer, M., et al. (1999). Tom22 is a multifunctional organizer of the mitochondrial preprotein translocase. Nature *401*, 485–489.

Vogel, F., Bornhoevd, C., Neupert, W., and Reichert, A.S. (2006). Dynamic subcompartmentalization of the mitochondrial inner membrane. The Journal of Cell Biology *175*, 237–247.

Voisine, C., Craig, E.A., Zufall, N., Ahsen, von, O., Pfanner, N., and Voos, W. (1999). The protein import motor of mitochondria: unfolding and trapping of preproteins are distinct and separable functions of matrix Hsp70. Cell *97*, 565–574.

Vögtle, F.-N., Wortelkamp, S., Zahedi, R.P., Becker, D., Leidhold, C., Gevaert, K., Kellermann, J., Voos, W., Sickmann, A., Pfanner, N., et al. (2009). Global analysis of the mitochondrial N-proteome identifies a processing peptidase critical for protein stability. Cell *139*, 428–439.

Waegemann, K., Popov-Celeketić, D., Neupert, W., Azem, A., and Mokranjac, D. (2014). Cooperation of TOM and TIM23 Complexes during Translocation of Proteinsinto Mitochondria. J. Mol. Biol. 1–10.

Wang, C., and Youle, R.J. (2009). The role of mitochondria in apoptosis*. Annu. Rev. Genet. *43*, 95–118.

Weiss, C., Oppliger, W., Vergères, G., Demel, R., Jenö, P., Horst, M., de Kruijff, B., Schatz, G., and Azem, A. (1999). Domain structure and lipid interaction of recombinant yeast Tim44. 1–5.

Wenz, L.-S., Ellenrieder, L., Qiu, J., Bohnert, M., Zufall, N., van der Laan, M., Pfanner, N., Wiedemann, N., and Becker, T. (2015). Sam37 is crucial for formation of the mitochondrial TOM-SAM supercomplex, thereby promoting β-barrel biogenesis. The Journal of Cell Biology *210*, 1047–1054.

Wenz, L.-S., Opalinski, L., Schuler, M.-H., Ellenrieder, L., Ieva, R., Böttinger, L., Qiu, J., van der Laan, M., Wiedemann, N., Guiard, B., et al. (2014). The presequence pathway is involved in protein sorting to the mitochondrial outer membrane. EMBO Rep. *15*, 678–685.

Wiedemann, N., Pfanner, N., and Ryan, M.T. (2001). The three modules of ADP/ATP carrier cooperate in receptor recruitment and translocation into mitochondria. The EMBO Journal *20*, 951–960.

Wiedemann, N., and Pfanner, N. (2017). Mitochondrial Machineries for Protein Import and Assembly. Annu. Rev. Biochem.

Wiedemann, N., Truscott, K.N., Pfannschmidt, S., Guiard, B., Meisinger, C., and Pfanner, N. (2004). Biogenesis of the protein import channel Tom40 of the mitochondrial outer membrane: intermembrane space components are involved in an early stage of the assembly pathway. J. Biol. Chem. *279*, 18188–18194.

Wrobel, L., Topf, U., Bragoszewski, P., Wiese, S., Sztolsztener, M.E., Oeljeklaus, S., Varabyova, A., Lirski, M., Chroscicki, P., Mroczek, S., et al. (2015). Mistargeted mitochondrial proteins activate a proteostatic response in the cytosol. Nature.

Wrobel, L., Trojanowska, A., Sztolsztener, M.E., and Chacinska, A. (2013). Mitochondrial protein import: Mia40 facilitates Tim22 translocation into the inner membrane of mitochondria. Molecular Biology of the Cell *24*, 543–554.

Wu, Y., and Sha, B. (2006). Crystal structure of yeast mitochondrial outer membrane translocon member Tom70p. Nat. Struct. Mol. Biol. *13*, 589–593.

Yamamoto, H., Esaki, M., Kanamori, T., Tamura, Y., Nishikawa, S.-I., and Endo, T. (2002). Tim50 is a subunit of the TIM23 complex that links protein translocation across the outer and inner mitochondrial membranes. Cell *111*, 519–528.

Yamano, K., Kuroyanagi-Hasegawa, M., Esaki, M., Yokota, M., and Endo, T. (2008a). Step-size analyses of the mitochondrial Hsp70 import motor reveal the Brownian ratchet in operation. J. Biol. Chem. *283*, 27325–27332.

Yamano, K., Yatsukawa, Y.-I., Esaki, M., Hobbs, A.E.A., Jensen, R.E., and Endo, T. (2008b). Tom20 and Tom22 share the common signal recognition pathway in mitochondrial protein import. J. Biol. Chem. *283*, 3799–3807.

Young, J.C., Hoogenraad, N.J., and Hartl, F.U. (2003). Molecular chaperones Hsp90 and Hsp70 deliver preproteins to the mitochondrial import receptor Tom70. Cell *112*, 41–50.